Inexpensive methods of catalytic hydrophosphination utilising iron and simple metal salts

Gallagher, Kimberley

Award date:
2019

Awarding institution:
University of Bath

Inexpensive methods of catalytic hydrophosphination utilising iron and simple metal salts

Kimberley Jane Gallagher

UNIVERSITY OF BATH

Department of Chemistry

Thesis submitted for the degree of Doctor of Philosophy

March 2019

Publications arising from this work

K. J. Gallagher and R. L. Webster, Chem. Commun., 2014, 50, 12109–11.

K. J. Gallagher, M. Espinal-Viguri, M. F. Mahon and R. L. Webster, Adv. Synth. Catal., 2016, 358, 2460–2468.

Acknowledgements

It’s difficult to express the value of the people who surround me in my life, not least their contribution towards my PhD (my life for the past few years, >10% of my life so far).

During the course of this work Ruth has been there to temper my fragile ego, listen to my victories and downfalls and offer unwavering support in the face of the seemingly insurmountable task that lay before me as a keen but anxious first year. I thank her for taking a chance on me as her first PhD student while she believed me to be taking a chance on her.

Thank you to my family and particularly my husband for his support, his love and his continued assertion that I am actually quite good at chemistry.

Thank you to Maia for her shoddy Spanish lessons and the endless font of joy that she provided.

Thank you to Andrew for his teachings in rock and football and for the inspiration needed for the inception of the blue roll challenge.

Thank you to Nathan for his Happy Safari and #captivatingcolourchanges.

Thank you to Cei for making me appear saner.

Finally, thank you to Ruth for bestowing that much coveted hug.

Working together has been super awesome.

Abstract

This thesis details the development of iron-based catalysts for the hydrophosphination of unsaturated compounds. Conditions were optimised for each process and the substrate scope was established. Experimental and spectroscopic studies were used to investigate the mechanism of the hydrophosphination of styrene.

Chapter 1 gives an overview of hydrophosphination, both stoichiometric and catalytic, focusing on the reactions of iron. The value of these hydrophosphination products is discussed.

Chapter 2 details the catalytic hydrophosphination to form unusual terminally substituted phosphines using both $Fe(HMDS)_2THF$ and KHMDS respectively.

Chapter 3 Shows that by introduction of a simple salen ligand to an iron catalysed system gave room temperature reactivity at very low catalyst loadings. Only 0.5 mol% pre-catalyst was required for the room temperature synthesis of a variety of phosphines through hydrophosphination. Further, this work explored the use of an iron-porphyrin μ-oxo catalyst for a range of similar products. Hyrophosphination with phenylphosphine is outlined, wherein a single addition is seen to take place thermally.

Chapter 4 outlines kinetic and mechanistic aspects of catalytic hydrophosphination with iron(salen)-μ-oxo. A Hammett study was conducted for a variety of functional groups on the alkene substrate concluding that there was a change in the rate determining step moving from electron withdrawing to electron donating groups.

This work culminated in the publication of two papers in impactful peer reviewed journals.[1,2]

Contents

Abbreviations

acac	acetylacetonate
Ad	adamantyl
AIBN	azobisisobutyronitrile
AM	Anti-Markovnikov
BHT	3,5-di(tert-butyl)-4-hydroxy-toluene
Bn	benzyl
^{n}Bu	n-butyl-
^{t}Bu	tert-butyl-
Cy	cyclohexyl
Cp	cyclopentadienyl
DBU	1,8-diazabicyclo-[5.4.0]undec-7-ene
DCE	1,2-dichloroethane
DHP	double hydrophosphination
dppe	bis(diphenylphosphino)ethane
dppm	bis(diphenylphosphino)methane
dpbz	bis(diphenylphosphino)benzene
ee	enantiomeric excess
Et	ethyl
EWG	electron withdrawing group
EDG	electron donating group
eq	equivalent
h	hours
Hex	n-Hexyl
HMDS	hexamethyldisilazane
HP	Hydrophosphination

IMes	1,3-bis(2,4,6-trimethylphenyl)-imidazol-2-ylidine
IR	Infra-red
^{i}Pr	isopropyl
JL	Jacobsen's ligand
L	ligand
LHS	Left-hand side
M	Markovnikov
Me	methyl
Mes	mesityl
Np	naphthyl
Nu	nucleophile
PGM(s)	platinum group metal(s)
Ph	phenyl
RHS	Right-hand side
rt	room temperature
SHP	single hydrophosphination
TEA	triethylamine
TEMPO	2,2,6,6-tetramethylpiperidine-1-oxy
OTf	triflate, $[OSO_2CF_3]^-$
TMB	1,3,5-trimethoxybenzene
Trip	triisopropyl
Ts	tosyl

1 Introduction

1.1 Overview

It is unsurprising, perhaps, that iron-mediated reactions are currently at the centre of a drive towards sustainable chemistry. As an abundant, low cost and environmentally benign metal, iron is an ideal alternative to traditional precious metals both in catalysis and in stoichiometric studies; it is of lower toxicity, can display a range of oxidation states and is amenable to ligation with a range of oxygen, nitrogen and phosphorus-based ligands. Numerous synthetic procedures and reaction systems have been developed since the first iron mediated reaction was reported in 1953 by Reppe.[3–7]

Iron-mediated reactions are gradually moving towards the use of asymmetric systems with finely tuned chiral systems with sterically and electronically optimised ligand-sets.[8,9] This is an important step forward as with inexpensive and readily available iron sources the development of better ligand sets will enable access to molecular space currently dominated by methods utilising expensive and rare metals such as platinum and palladium. Furthermore, high value products such as pharmaceuticals, which require carefully tuned and oftentimes chiral products, are more readily accessed.

A counterbalance to the low cost of iron is the extreme cost of the pro-ligands that are often used to facilitate catalysis. Ligands such as 2,6-bis[1-(2,6-di-isopropylphenylimino)ethyl]pyridine (DIP family of ligands) and bis(diphenylphosphino)benzene (dpbz) are prohibitively expensive.[10] Clearly there is a need to develop better and cheaper alternatives.

The ubiquity of phosphorus in synthetic chemistry cannot be underestimated: phosphorus compounds are used routinely as ligands in catalysis, as organocatalysts, as reagents in synthesis (for example in Wittig chemistry), they are ever present in biological systems and are used in antibiotics and anti-tumour compounds.[11–14] New methods to make phosphorus-containing motifs proffer an alternative route to classic structures and more importantly give us the potential to access new areas of molecular space, either through the synthesis of new phosphorus architectures or the generation of new organic compounds when using novel phosphorus compounds as ligands in catalysis.[15,16] An efficient methodology for the generation of P–C bonds therefore plays a pivotal and widespread role in synthesis. Compared to the classical methods of phosphine synthesis, a more environmentally benign approach would be to employ a catalytic process. Traditional P–C bond forming reactions are well documented but result in stoichiometric

quantities of salt by-product and tend to show low functional group tolerance (see section 1.3).[17]

Although iron catalysed systems have, of late, received a great deal of attention, there has been relatively little focus on iron systems for catalytic hydrophosphination (HP). Along with our scientific contributions, and those of other key groups, the use of iron in catalytic HP would seem to be an area of growing interest.[1,2,18–22]

As the high activity of designed iron catalysts is uncovered this area will only achieve further investment. To achieve a full understanding of the importance of the C-P bonding chemistry discussed, it is first essential to look at the general utility of phosphines, their role as ligands and the choice of iron as a catalyst for hydrophosphination.

1.2 Phosphines

Phosphines are an extremely important class of ligands in coordination chemistry. The architecture of the PR_3 system offers an extremely versatile platform which, through judicious selection of R groups, can be tuned in several ways. This allows the chemist to select a phosphine ligand which is highly suited to any number of specific purposes *via* the tuning of electronic and steric environments at the P donor. Phosphines and the related phosphite esters, $P(OR)_3$, are dominated by their nucleophilicity and reducing character.

The classic picture of a phosphine ligand, PR_3, is that of a two-electron σ-donor with π-acceptor properties. The strength of σ-donation is modulated by the electron withdrawing/donating properties of the three R groups bound to the P atom.

The electronic properties of the phosphine can be tuned, giving a strong σ-donor by selecting R groups with strong electron donating effects (*e.g.* alkyl groups such as Cy, Et, Me). Alternatively, the electronic properties can be tuned to have a greater π-accepting character by selecting R groups that are able to withdraw or delocalise electron density (e.g. Ph, CF_3, C_6F_5). It is entirely possible to further fine-tune these electronic properties by generating phosphines with mixed R groups, e.g. PR_2R'. These effects can be quantified with the Tolman electronic parameter, where the vibrational frequency of the bonds may be measured, and a lower vibrational frequency corresponds to a weaker bond.[23]

It was originally thought that the π-accepting properties of phosphines in M-P complexes arose from the interaction between the d orbitals of the metal and 'low-lying' empty 3d orbitals on the phosphorus atom (**Figure 1**, LHS). It is now accepted,

however, that the π-backbonding interactions arise from the overlap of metal d orbitals with the LUMO of the phosphine moiety (**Figure 1**, RHS).[24]

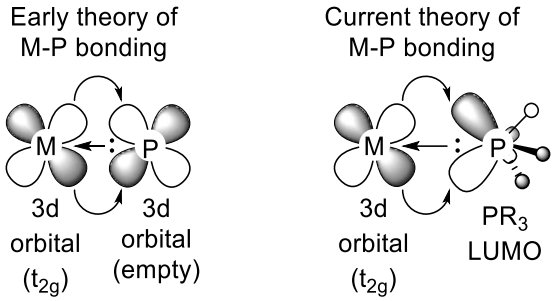

Figure 1. M-P bonding

In addition to the electronic properties of phosphines, the steric properties are also easily tuned by modulation of the steric demand of the R groups. In 1977 Tolman published a review which categorised the steric demand of phosphine ligands according to the angle they made with a hypothetical nickel atom 2.28 Å away from the P atom of the phosphine (the length of an idealised M-P bond).[23] The angle, θ, at the apex of the cone is referred to as the Tolman angle and will be greater for phosphines with more sterically demanding R groups *e.g.* the Tolman angle of PPh_3 (145˚) is greater than that of PMe_3 (109˚). As is the case with the modulation of electronic properties, the steric properties can also be fine-tuned with mixed R groups, *e.g.* $PMePh_2$ has a Tolman angle of 136˚ which lies between that of PMe_3 and PPh_3.

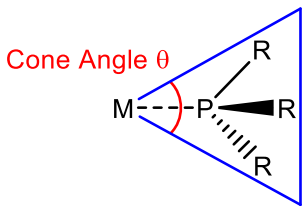

Figure 2. Phosphine cone angle

Replacing an R group of a simple tertiary phosphine, PR_3, with an alkyl bridge allows for the generation of more complex bridging or multi-dentate phosphines with a variety of properties. Taking PPh_3 as a foundation, the simplest multi-phosphine containing ligand can be formed by replacing one Ph group with a methylene bridging unit, $-CH_2-$, between two PPh_2 moieties to give dppm, $Ph_2PCH_2PPh_2$. The alkyl bridge of dppm is short and so this ligand often acts as a bridging ligand between two metal centres, forming bimetallic complexes.[25–27] Increasing the length of the alkyl bridging unit by one carbon atom gives dppe, $Ph_2PCH_2CH_2PPh_2$, the backbone of which is suitably long to allow it to chelate to a metal atom in a bidentate mode.

1.3 Synthesis of simple phosphines

1.3.1 Synthesis of primary and secondary phosphines

Much of the difficulty in the synthesis of primary or secondary phosphines from either elemental phosphorus or commodity P(III) reagents (*e.g.* PCl_3 and PH_3) is the potential for over-functionalisation, whereby rather than reacting cleanly with one equivalent of reagent, the phosphorus source reacts two or three times with the reagent leading to undesired reaction products and low yield. However, it is possible to generate monoalkyl phosphines through deprotonation of phosphine ($PH_{3(g)}$) with a strong base followed by alkylation, however, this is ill advised due to its price, low solubility in solvents and the danger associated with handling this pyrophoric gas. Primary and secondary phosphines are generally prepared in situ from the reaction of elemental phosphorus or phosphorus trichloride via reaction with sodium metal in the presence of solvent. Addition of two equivalents of a protonating agent e.g. ^{t}BuOH followed by an alkyl halide gives good conversion to monoalkylated phosphines. It should be noted that the use of more acidic reagents for this first step can lead to the irreversible formation of $PH_{3(g)}$. Methylphosphine (CH_3PH_2) and other simple alkyl derivatives are prepared in this way using a variety of alkali metal derivatives MPH_2 (M = Li, Na, K) (**Scheme 1**). Primary phosphines may then undergo *in situ* conversion to a secondary dialkyl phosphine by metalation with BuLi or with successive addition of sodium metal and alkylation.[28]

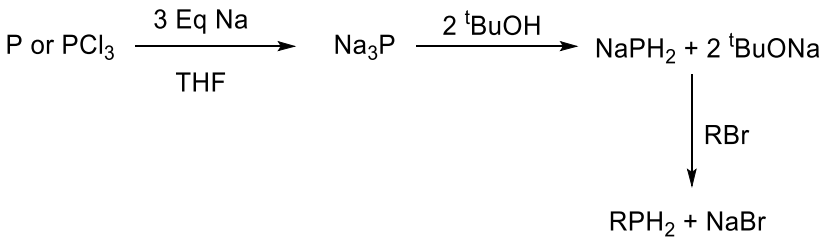

Scheme 1. General synthesis of primary phosphines

Another synthetic route begins with corresponding chlorophosphines and their reaction with a hydride reagent. For example, reduction of dichlorophenylphosphine with lithium aluminium hydride affords phenylphosphine ($PhPH_2$).

Secondary phosphines may also be obtained by alkali-metal reductive cleavage of triarylphosphines followed by hydrolysis of the resulting phosphide salt. A frequently employed phosphine, diphenylphosphine (Ph_2PH), may be prepared via this method.

There are also indirect methods for synthesis of secondary phosphines in which a dichlorophosphine is synthesised and converted into the desired phosphine by

reduction with $LiAlH_4$, sodium tetrahydroborate or sodium metal. Diorganophosphinic acids, $R_2P(O)OH$, can also be reduced with diisobutylaluminium hydride. Unfortunately, only a few mono- and dichlorophosphines are readily available by reaction of PCl_3 with Grignard reagents. Typically these are of the form R_2PCl or $RPCl_2$, where R = branched primary, secondary or tertiary alkyl group.[29] For the synthesis of tributylphosphine, a moderate yield of 53% is obtained using PCl_3 and the Grignard reagent ^tBuMgBr for low temperature alkylation under optimised conditions. Similarly, a large-scale synthesis of diisopropylchlorophosphine, ditertbutylchlorophosphine or alkyldichlorophosphines - depending on reaction stoichiometry - may be carried out via the reaction of the appropriate Grignard reagent with PCl_3 in an ethereal solvent at 40°C.

1.3.2 Synthesis of tertiary phosphines

Not only do tertiary phosphines play an important role as ligands in homogeneous catalysis, but they can also make vital building blocks for the polymer industry and as such there are a wide variety of routes to prepare functionalised tertiary phosphines. These products can be used in their current form as ligands or as intermediates in further syntheses. Tertiary phosphines are generally obtained by treatment of phosphorus trichloride or triphenylphosphite with organolithium reagents or Grignard reagents (**Scheme 2**). Although the yields are only moderate, this is a widely-utilised method – used both industrially and in the research laboratory (perhaps in part due to the ready availability of Grignard reagents for other purposes). These lower yields are due to the formation of stable diphosphine side products through P-P coupling.[30]

Di-*tert*-butylchlorophosphine or *tert*-butyldichlorophosphine may be reduced with lithium aluminium hydride giving di-*tert*-butylphosphine (82% yield), *tert*-butylphosphine (83% yield) and other tertiary phosphines. A variety of flame-retardant tertiary phosphines are accessible *via* the reaction of halophosphines and organomagnesium compounds in the presence of copper(I) iodide. Perdeuterated triisopropylphosphine is readily obtained from the reaction of isopropyl magnesium bromide and phosphorus trichloride in diethyl ether in 42% yield which may be used for kinetic studies. In a similar manner, triallylphosphine (75% yield) and trivinylphosphine (40% yield) are obtained from the reaction of allylmagnesium chloride or vinylmagnesium bromide (respectively) and phosphorus trichloride in THF.

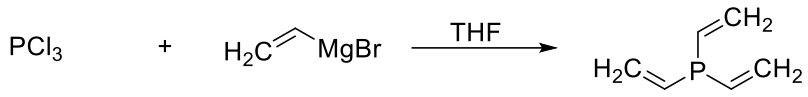

Scheme 2. Synthesis of trivinylphosphine from PCl_3 and vinylmagnesium bromide

A wider variety of trialkyl and triaryl phosphines may be accessed and through the reaction of phosphites with Grignard reagents. The undesired P-P coupling products seen in previous reactions are decreased by using phosphites – these are also far easier to handle in a laboratory environment than PCl_3.

Triphenyl phosphite reacts with perdeuterated ethylmagnesium bromide in Et_2O to give perdeuterated triethylphosphine (**Scheme 3**, 59% yield), and with vinylmagnesium chloride to give trivinylphosphine (THF, 30% yield).

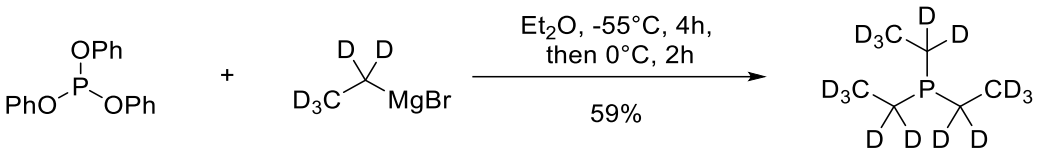

Scheme 3. Synthesis of perdeuterated triethylphosphine from triethylphosphite

Trivinylphosphine can also be prepared from vinylmagnesium bromide and trimethyl phosphite (THF, 30% yield) and may be used for the synthesis of polyphosphine ligands. In the case of the more volatile Trimethylphosphine (bp 38 °C), Et_2O (bp 35 °C), should be avoided and instead dibutyl ether used.

More complex phosphines require more complex syntheses – in some cases the use of extremely powerful reducing agents such as sodium will not be compatible with the highly tuned substituents and functionality required of more complex phosphine ligands.

Trivalent phosphorus compounds have a nucleophilicity which renders them facile precursors to phosphonium salts upon treatment with alkyl halides. Triphenylphosphine, for example, undergoes rapid, exothermic reactions to give phosphonium salts while the corresponding nitrogen compound, triphenylamine, is relatively unreactive in S_N2 reactions due to the delocalisation of the nitrogen lone pair through resonance. Phosphonium salts formed from phosphite esters, however, are often unstable and yield dialkyl phosphonate esters upon heating by way of a second S_N2 reaction.

One straightforward P–C bond forming reaction is the generation of phosphonium ylids by nucleophilic addition to an α-halo carbonyl compound (**Scheme 4**).[13,17]

Addition of NaOEt or another base would then convert this ylid to an equivalent phosphorane.

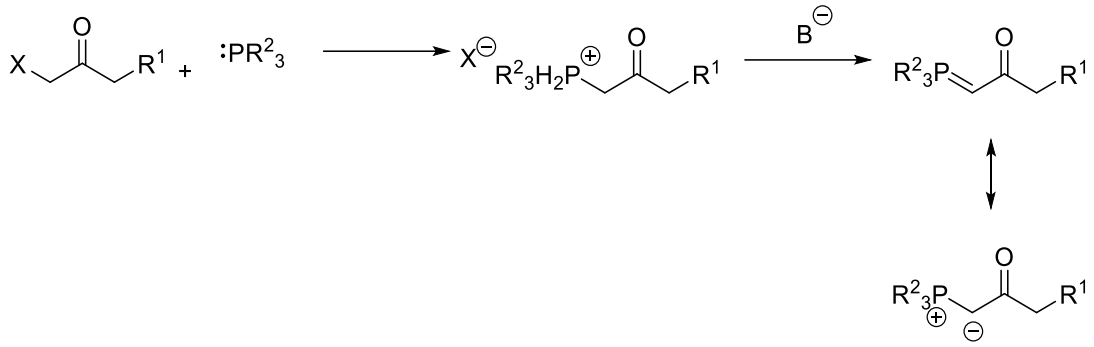

Scheme 4. General synthesis of a phosphorene from a phosphonium ylid

In comparison to synthesis utilising ^{n}BuLi for example, this synthetic route is relatively mild and can produce desired products on a large scale. The ylids generated may also act as a precursor in the Wittig synthesis of alkenes.

1.4 Synthesis of phosphines via hydrophosphination

Hydrophosphination is described by the addition of a P-C bond across an unsaturated bond (**Scheme 5**).[31] Hydrophosphination (HP) provides a viable entryway to phosphines, it is an advantageous method for the synthesis of these compounds often displaying greater functional group tolerance than traditional methods and, as a catalytic process, it allows lower temperatures, shorter reaction times and thus gives access to a wider variety of phosphines (**Scheme 5**).

Other methods of synthesis outlined lack the key benefit of hydrophosphination: the potential for 100% atom efficiency. In comparison to the simple phosphines prepared using traditional methods of synthesis this process offers the ability to tune the steric and electronic environment around the central phosphorus atom which as discussed in section 1 is vital in the field of ligand design.

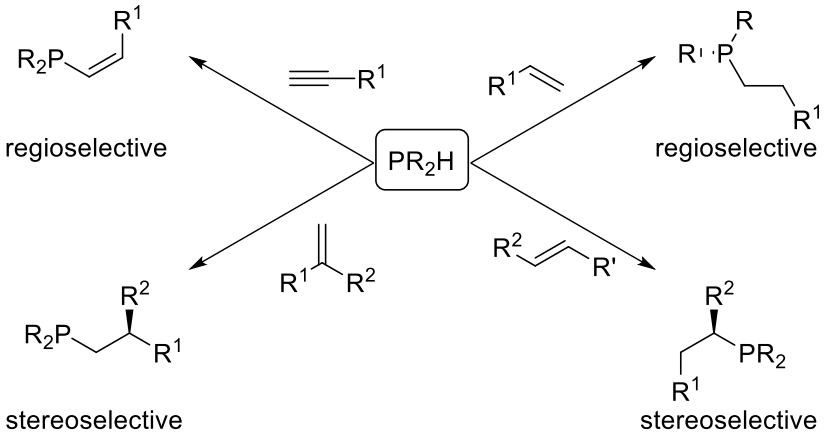

Scheme 5. Potential products of hydrophosphination with a secondary phosphine

Several simple hydrophosphination products have already found use in the literature. **Scheme 5** outlines potential products of hydrophosphination with a secondary phosphine including regio- and stereoselective products. In the reaction of an alkene with diphenyl phosphine, the ethyl-substitued phosphines yielded were demonstrated to be an appropriate ligand choice for methylcarboxylation catalysis as well as useful reagents in chemical biology.[32,33] In these cases the ethyl-substituted phosphines were synthesised according to classical methods outlined previously (**Section 1.3**), however, there is strong argument for using HP in preference, in this case, due to the relative ease of synthesis of these compounds and the high atom economy of HP. Our research has shown that these products may be prepared catalytically using 0.5 mol% of a simple iron catalyst at room temperature and indeed, the work of Gaumont shows that $FeCl_2$ may be used in a 30 mol% loading (see **Section 1.13**).[1,34] The products synthesised via hydrophosphination were shown to be convenient ligands in iron catalysed Negishi cross-coupling (see **Section 1.16**).[19] The enantiopure cyclometallated phosphines synthesised by Leung using palladium catalysed HP have also shown promise in cancer treatment (see **Section 1.20**).[35] Further, they were found to be active for enantioselective hydrophosphination (see **Section 1.20**).[36]

For the utility of hydrophosphination to be maximised, it would have to compete with, or be complementary to, the products formed through the methodologies previously outlined. It seems that the complementary reactivity through hydrophosphination is already proving valuable, and the utility of hydrophosphination products is discussed in more detail in the sections that follow (**1.16** – **1.20**).

1.4.1 Metal-Free Hydrophosphination

Alonso and co-workers demonstrated several hydrophosphination reactions that may be carried out in the absence of a catalyst (**Scheme 6**).[37] These reactions are carried

out neat, with no solvent. This transformation is presumably limited to activated substrates as it relies on a Michael addition pathway (through the nucleophilic attack on a δ^+ C atom by P).

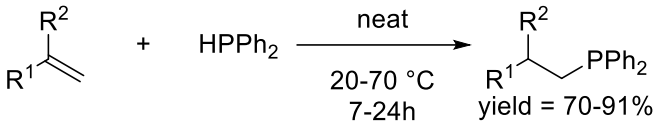

R^1 = H, Ph, 4-Cl-C_6H_4, 4-Br-C_6H_4, 4-MeO-C_6H_4, 4-MeC(O)O-C_6H_4, 2-Py, 4-Py, Np, 4-Ph-C_6H_4, $C_8H_4O_2N$, C_4H_6ON, Ph-S, MeC(O), EtOC(O), NC
R^2 = H, Me

Scheme 6. Metal-free hydrophosphination of alkenes

A screening for radical mediated processes was carried out. Trapping experiments with cumene, 2,6-di-tert-butylphenol and TEMPO showed that these additives did not reduce the yields of hydrophosphination products. Furthermore, no detectable products derived from their reaction with diphenylphosphanyl radicals were present (note that no method of detection is described in the supplementary material, nor is the concentration of radical trap mentioned, both of which would seem pertinent details in ruling out radical mediated reactions). A comparison of reaction rate in the presence and absence of radical traps would likely have provided more compelling evidence against a radical mediated mechanism. No cyclisation product was formed upon the addition of diphenylphosphine to hepta-1,6-diene (**Scheme 7**). The author infers from this result that phosphine centred radicals are unlikely to be present in these hydrophosphination reactions. It is unclear why the reaction itself was not performed in the presence of hepta-1,6-diene. This method would provide more conclusive physical evidence with which to discount a radical mediated mechanism. Regardless, the anticipated, radically-derived product was not detected. Phosphine centred radicals are therefore unlikely to take part in these hydrophosphination reactions.

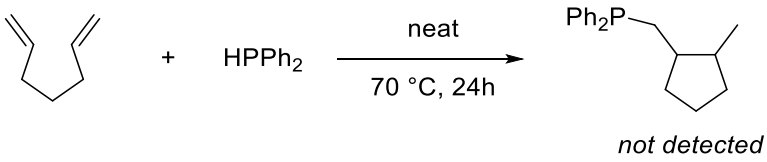

Scheme 7. Radical reaction of hepta-1,6-diene

Alonso recently furthered this work with a report which extended their substrate scope by addition of a wider variety of alkenes, alkynes and also included multicomponent hydrothiophosphination (**Scheme 8**).[38]

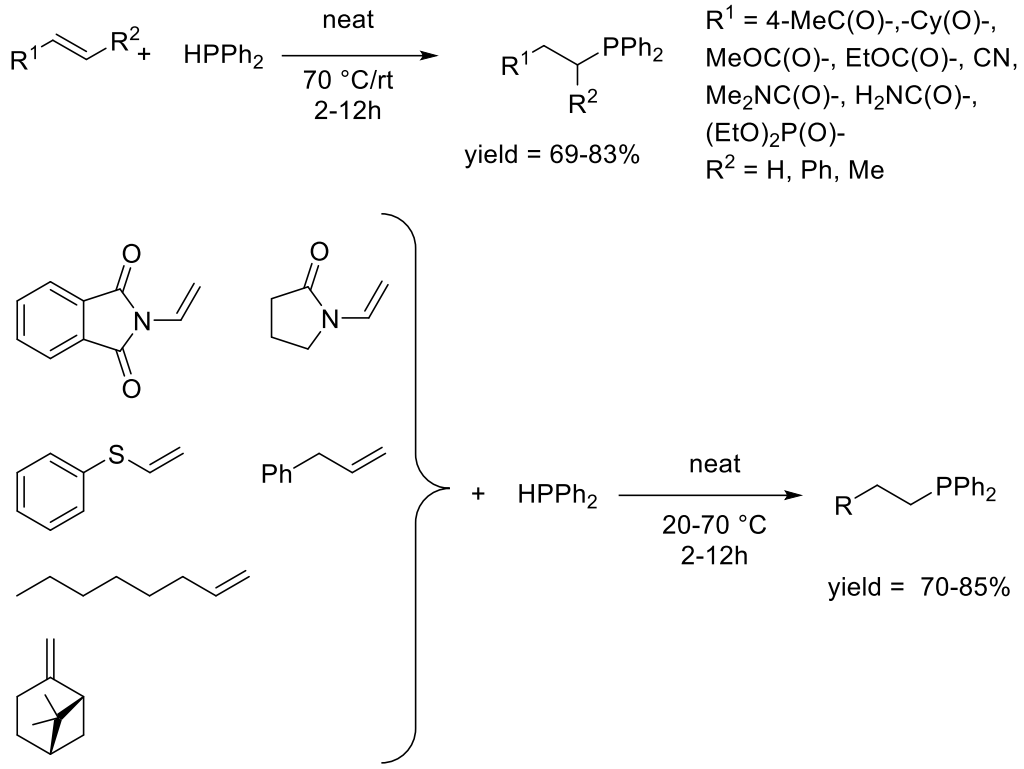

Scheme 8. Metal free hydrophosphination of activated and unactivated alkenes

These new, challenging substrates were explored utilising the same methods as in their previous publication. Alkyne hydrophosphination was shown to take place in a regio- and stereoselective manner (**Scheme 9**).

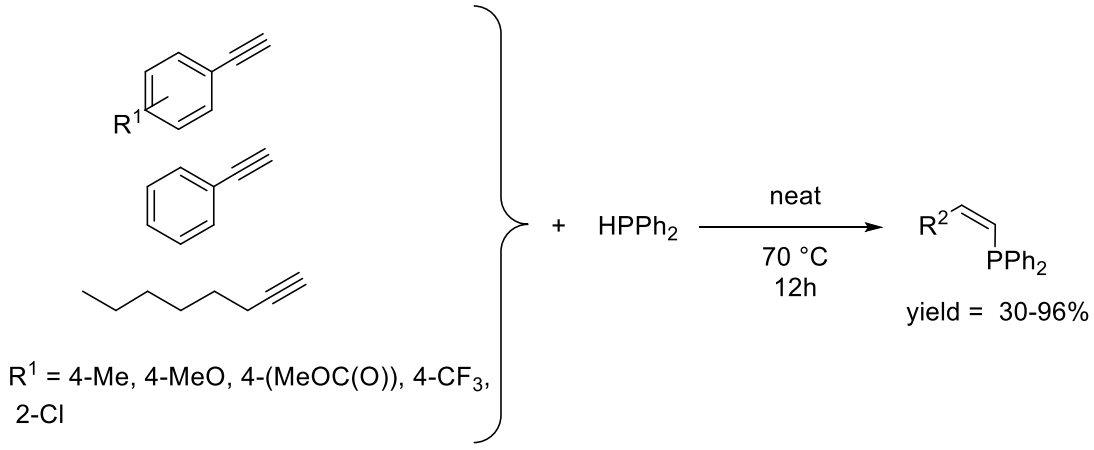

Scheme 9. Metal free hydrophosphination of activated and unactivated alkynes

A more satisfying mechanistic study was performed with further discussion attempting to rule out a radical mechanism. The new alkene products formed were exclusively (aside from methylphenylacetylene) the *Z* products, where *E* products would likely be the primary products formed in the case of a radical driven mechanism (as found in a radical promoted reaction with AIBN, **Section 1.5**).[39] Further *E/Z* equilibration does

not occur upon heating of the phosphine products providing further evidence against a radical catalysed mechanism.

The use of deuterated cyclohexylacetylene resulted in the formation of primarily (80%) the *Z* hydrophosphination product – with some H/D scrambling observed – in agreement with an anti-addition of the P-H across the C-C triple bond (**Scheme 10**). The rate of addition to styrene when using $HPPh_2$ versus $DPPh_2$ was also examined revealing a long induction period of 50 minutes for $DPPh_2$. A more thorough examination of rates would include smaller time intervals between measurements of concentration allowing a more accurate measurement of initial rate of these two reactions (including a much earlier initial measurement for accuracy of initial rate). Ideally the R^2 values would be reported for KIE measurements to make reasonable conjectures about their differences.

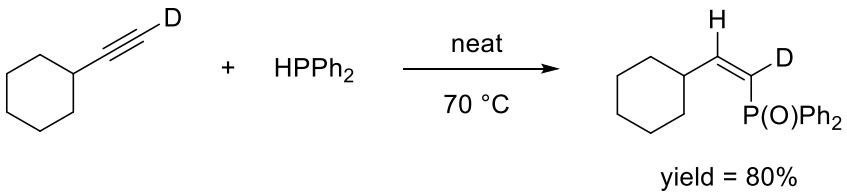

Scheme 10. Deuteration study for cyclohexylacetylene

By doubling the amount of phosphine, the rate of product formation in the reaction with styrene was seen to increase by greater than 5-fold whereas the addition of excess styrene had a negligible effect on the rate of product formation. Larger excesses of phosphine were relatively ineffective after a 1:2 ratio of styrene to phosphine.

The inclusion of alkene hydrothiophosphination is lacklustre at best. Phosohine sulphides were formed *in situ* by addition of sulphur to the authors' already established protocol, in much the same manner as phosphine oxides might form. It does, however, form a logical progression towards discussion of the alkyne hydrothiophoshination reactions performed.

1.5 Synthesis of Phosphines via Radical Addition

Radical addition was one of the earliest syntheses used to access P–C bonds and was first outlined by Stiles and co-workers.[40] They demonstrated that organophosphorus compounds could be synthesised *via* the generation of radicals by light or via peroxides. This required the use of phosphine gas and very careful handling. These reactions allowed for the functionalization of unactivated alkenes to produce terminal phosphines. Another example of radical addition to alkynes using

AIBN gave primarily the *E*-alkene product (**Scheme 11**).[41] These reactions took place over several hours to several days.

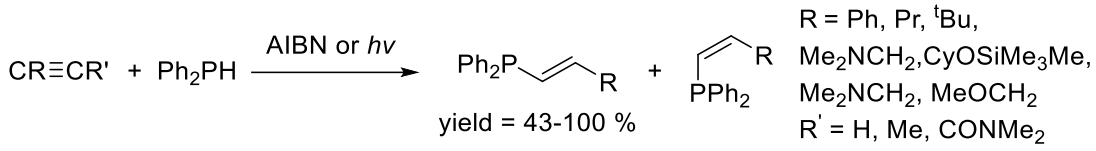

Scheme 11. Hydrophosphination by radical addition pathway

In the case of internal alkynes, there are too few examples to make a reasonable postulation as to the resulting regiochemistry, the *Z* isomer is, however, still the most readily accessed product. Stiles and co-workers also explored the use of allenes. Again, these give mixed *E/Z* isomers with *E* products being predominantly formed (type **A**, **Figure 3**), as characterised via ^{31}P NMR for a similar range of functional groups as the alkynes.

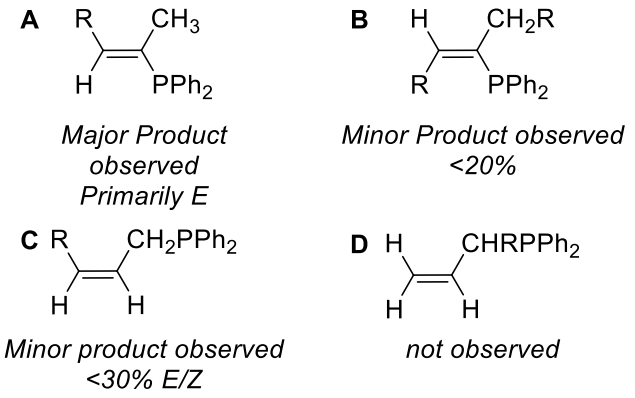

Figure 3. Products of radical addition to allenes

1.6 Base Catalysed Hydrophosphination

Several elegant examples exist using simple base-catalysed chemistry. For example, the ^{t}BuOK catalysed hydrophosphination of alkenes was reported in 2002 by Bunlaksananusorn and Knochel (**Scheme 12**).[42]

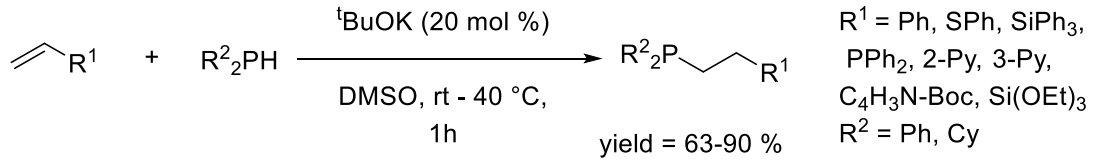

Scheme 12. ^{t}BuOK catalysed hydrophosphination

The problem of functional group tolerance is raised using ^{t}BuOK, and only modest changes in functionality of the starting material may be made. For example, the use of halogenated substrates will be limited. The difficulty in using this system is

compounded by the need for DMSO as the solvent - unfortunately, due to its high polarity, it is readily soluble and its boiling point will limit the variety of products which may be isolated either through extraction or evaporation. In addition, where R^2 = Cy only the corresponding phosphine oxide is isolable due to oxidation by DMSO. This is an effective method for producing a phosphine oxide in a shorter time interval than seen with ^{n}BuLi (*vide infra,* **Scheme 11**) and generally takes place at room temperature. However, for most applications the oxidised product must be reduced to P(III) to be of value as a ligand. The method may be used to prepare phosphorus and P,N- ligands.[18,19]

The ^{n}BuLi mediated hydrophosphination of dienes was reported by Le Gendre and co-workers (**Scheme 13**).[43] These reactions were highly regioselective giving **1** as the major product and **2** as the minor product with the phosphine moiety adding to the least hindered double bond. **2** was formed on isomerisation of the starting diene (resulting in 1,4-addition). However, **2** becomes the major product in the case of 2,3-dimethyl-1,3-butadiene where R^2 = R^3 = Me. The regioselectivity observed was therefore primarily dependent on sterics, where this trend is not observed when R^2 and R^3 are more sterically bulky.

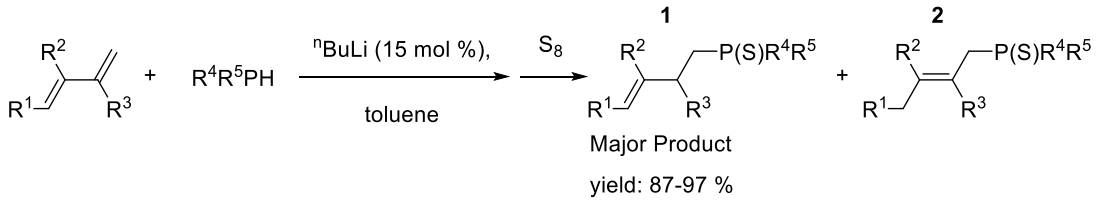

Where R includes:
R^1 = H, cyclic nonadiene, cyclic cyclohexadiene; R^2 = Me, C_6H_{11}, cyclic nonadiene;
R^3 = H, Me; R^4 = Ph, Cy; R^5 = Ph, Me, Cy

Scheme 13. ^{n}BuLi catalysed hydrophosphination.

This method was extended to include functionalisation of styrenes and several challenging substrates including alkynes in generally excellent yields. In these cases, longer reaction times (>16 h) and temperatures of 70 °C were required. However, the use of ^{n}BuLi is a drawback; not only is it pyrophoric, requiring careful handling, but the use of such a strong base can be detrimental to sensitive functionality elsewhere in a molecule and thus functional group tolerance in such a transformation is low. Indeed, no halogenated products were reported for this system. Products reported here were straightforward to isolate *via* evaporation of the solvent and starting diene, and the resulting alkenylphosphine products have the potential to be used as bidentate ligands. A significant advantage of these alkenylphosphine systems is then

the difference in binding of the phosphine and alkene moieties. The lability of the double bond upon binding to a metal may result in highly active catalytic systems.

1.7 Generic-metal-catalysed hydrophosphination

There are many examples of hydrophosphination reactions utilising a variety of transition metals - particularly those from the platinum group metals.[15,44] There are also examples of lanthanide catalysed hydrophosphination as well as main group catalysed reactions.[45–48] By far the most well developed understanding of the mechanism of hydrophosphination comes from systems utilising a platinum catalyst (which will be discussed briefly in section **1.8**).

The regioselective addition of phosphines to unsaturated C–C bonds represents a key challenge in this area. There are very few examples of this reactivity from which to construct an informed and predictable route to Markovnikov versus anti-Markovnikov products through catalyst choice and ligand design. There are two principal mechanisms of intermolecular hydrophosphination of alkenes: 1,2-insertion and Michael addition.[31,39] In 1,2-insertion (**Scheme 14**), both phosphine and olefin coordinate to the metal centre (complex **3** followed by **4**) - this is followed by migratory insertion of the phosphine moiety into the double bond of the alkene (**5**). The HP product is liberated by protonolysis yielding once again the catalytic metal complex (**3**).

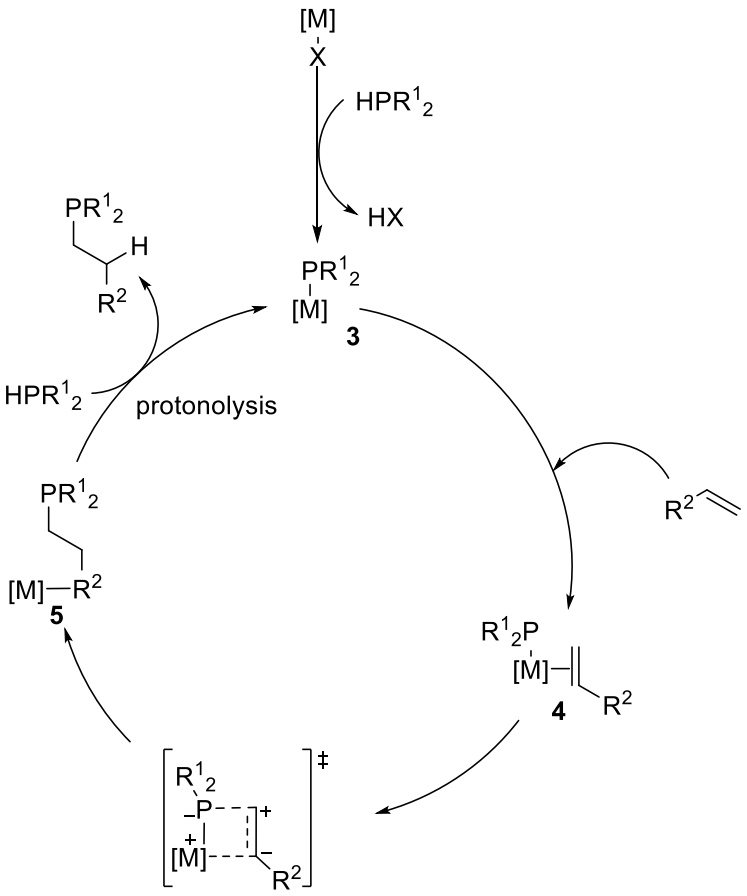

Scheme 14. Generic intermolecular hydrophosphination of alkenes by 1,2-insertion

In Michael addition (**Scheme 15**), coordination (or alternatively oxidative addition) of the phosphide moiety to the metal centre (**7**) enables attack by the phosphine on the double bond of the alkene.[49,50] This results in the formation of a zwitterionic intermediary species (**8**) which may then undergo protonolysis (or reductive elimination) to give the HP product and regenerate the metal catalyst (**6**).

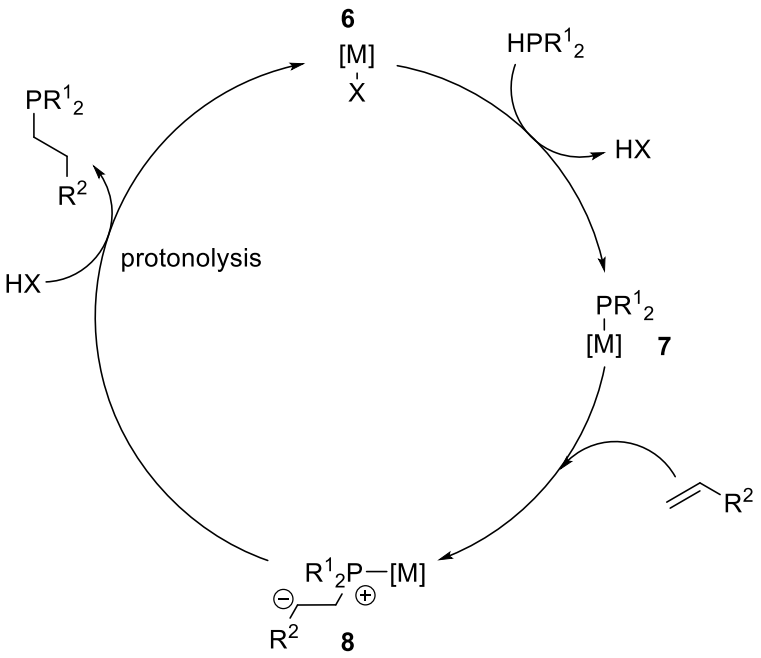

Scheme 15. Generic intermolecular hydrophosphination of alkenes *via* Michael addition

1.8 Mechanistic aspects of platinum catalysed hydrophosphination

The work of Pringle and co-workers into the hydrophosphination of acrylonitrile provided the first example of metal complex catalysed addition of a phosphine to an alkene *via* HP.[51] The group had previously shown the addition of PH_3 to formaldehyde (**Scheme 16**) was catalysed by a Pt(0) complex of $HP(CH_2OH)_2$ and thus concluded that Pt(0) complexes of $HP(CH_2CH_2CN)_2$ might be similarly effective in the hydrophosphination of acrylonitrile.

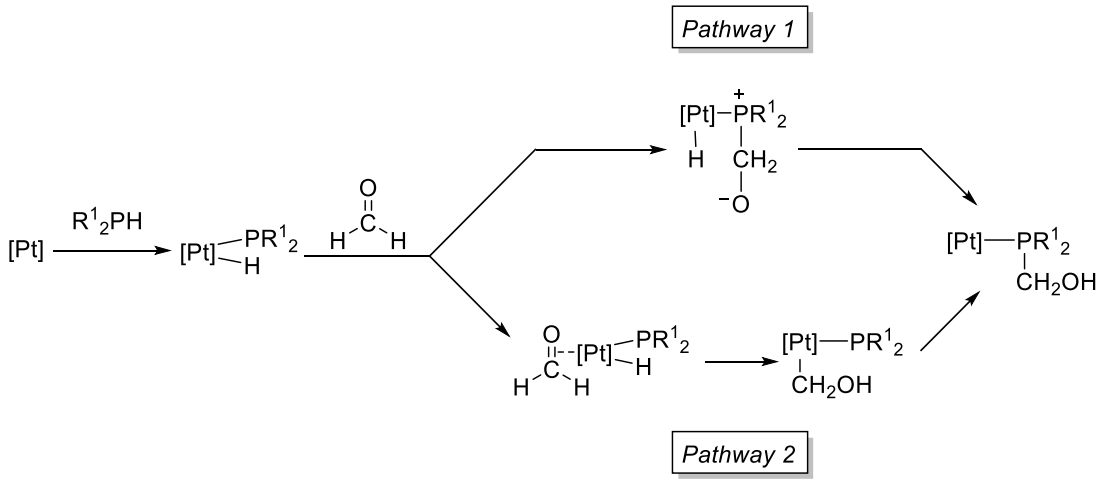

Scheme 16. Mechanism for hydrophosphination of formaldehyde

Phosphine gas was bubbled through a solution containing acrylonitrile with a platinum phosphine catalyst, giving hydrophosphination products within one hour. The mechanism proposed is similar to that of hydrosilylation by platinum phosphines. For simplicity, the authors chose to study only the final step of the hydrophosphination reaction – addition of a secondary phosphine to acrylonitrile (**Scheme 17**). The group supports their proposed mechanism through the observation that the initial coordination of acrylonitrile to their platinum complex is strongly favoured, uninhibited by the addition of a large excess of free phosphine.

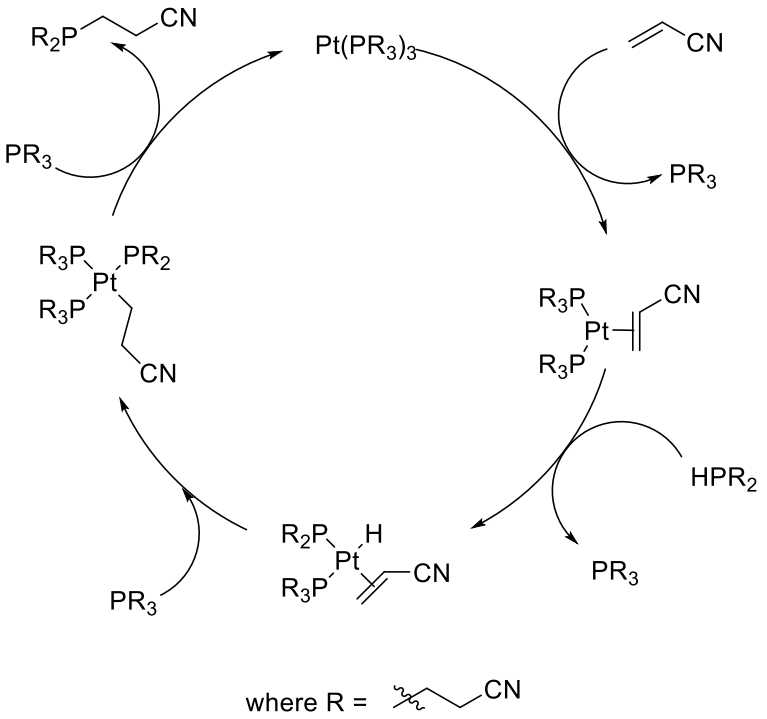

simplified to exclude bimetallic complexes

Scheme 17. Proposed mechanism for hydrophosphination of acrylonitrile

Hydrophosphination using a platinum catalyst was extensively studied by Glueck and co-workers. They also demonstrate several reactions of platinum phosphide complexes with activated alkenes which provide a useful basis from which to understand the role of platinum in their catalytic cycle.

With this series of stochiometric reactions they were able to prove that their catalytic reaction operated through a Michael addition mechanism (**Scheme 18**).[44,52]

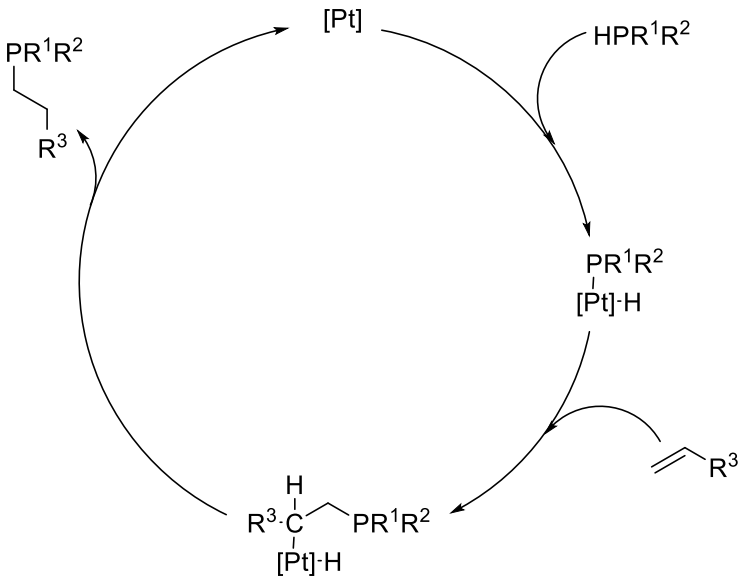

Scheme 18. Pt-catalysed hydrophosphination of alkenes via Michael addition

In determining a Michael addition pathway, first they set out to prove whether the P-C bond formation proceeds *via* insertion into the M-H bond or *via* insertion into the M-P bond (see **Scheme 16**). In the hydrophosphination of acrylonitrile, for their platinum catalysed reaction, they report evidence against the M-P bond formation pathway (*pathway 1*, **Scheme 19**) as intermediate **9** fails to undergo reductive elimination. Further, they isolate intermediates consistent with *pathway 2* in model systems. One potential intermediate complex in HP of acrylonitrile, **9**, was independently synthesised and found to be unreactive in this system. Treatment of the metal hydride with stoichiometric amounts of acrylonitrile afforded the appropriate phosphine product (as in *pathway 2*, **Scheme 19**).

This is in contrast to the work of Pringle and co-workers presented above where they present a Michael addition pathway believed to take place *via* (an analogous route to) *pathway 1*.

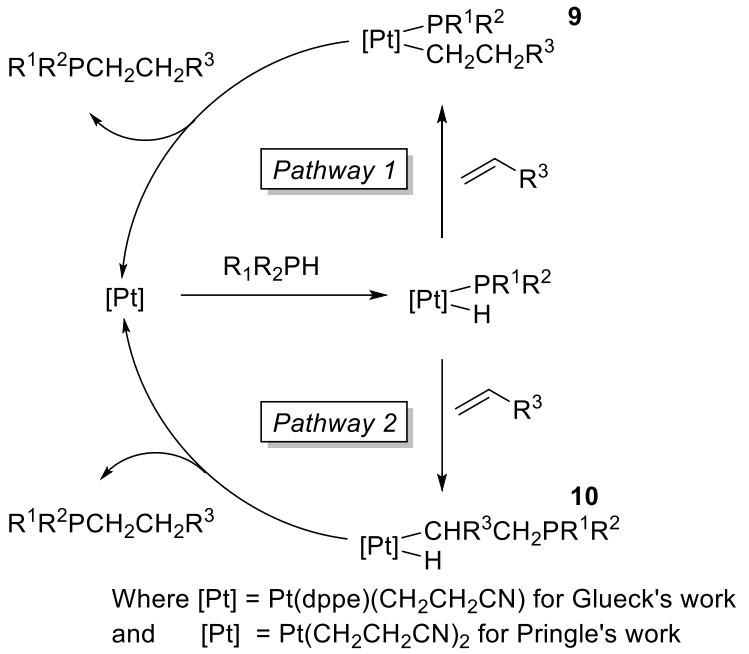

Scheme 19. Potential mechanisms of Pt-catalysed hydrophosphination of alkenes *via* Michael addition

A more recent publication by Glueck and co-workers details their proposal of a potential zwitterionic species during their Pt-catalysed hydrophosphination reactions.[44] In order to obtain evidence for the existence of this intermediate, they utilise a modified form of the Morita-Baylis-Hillman (MBH) reaction. In the typical MBH reaction, a nucleophile (*e.g.* phosphine) adds to an activated alkene forming a stabilised carbanion which in turn adds to an aldehyde with the ejection of the initiating nucleophile (**Scheme 20**).

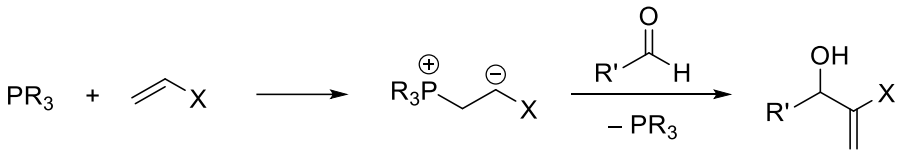

Scheme 20. Morita-Baylis-Hillman reaction with a phosphine nucleophile

Glueck and co-workers posit that their zwitterionic intermediate should behave in much the same manner as the stabilised carbanion in the standard MBH reaction. Thus, addition of benzaldehyde results in a reaction between the carbanionic species and the aldehyde (**Scheme 21**). In this modified MBH regime the phosphine is not ejected and is instead incorporated into the final product. Clearly there is competition between the standard hydrophosphination (HP) reaction and the modified MBH reaction, resulting in a mixture of the two possible products. The modified MBH route requires a bimolecular reaction which relies on the persistence of the zwitterion during the catalytic process. If this species is short-lived the HP

route will dominate, as according to Glueck and coworkers, it is a unimolecular process. The authors note that the ratio of MBH product to HP product increases with increasing concentration of benzaldehyde.

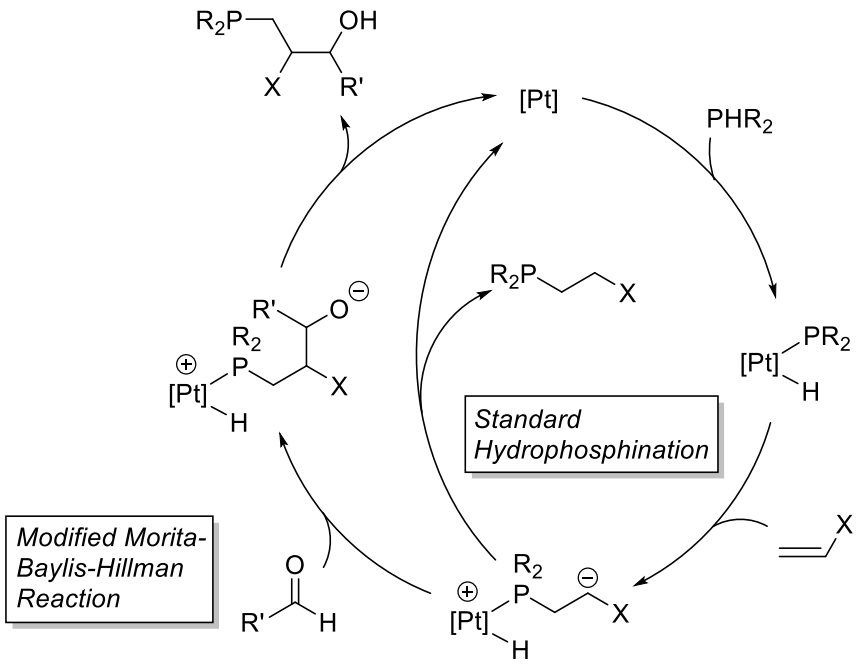

Scheme 21. Adapted Morita-Baylis-Hillman reaction during hydrophosphination for trapping zwitterionic intermediates

1.9 Catalytic phosphonylation with iron salts

Taking insight from the mechanistic understanding developed from platinum systems, turning to the focus of this investigation, in using iron for catalytic P-C bond forming processes.

Utilising a range of iron salts, Han and Ofial were able to demonstrate the catalytic α-phosphonylation of tertiary amines utilising C-H bond activation for subsequent C-P bond formation (**Scheme 22**).[53] After an initial screening of iron salts, it was found that $FeCl_2$ gave the highest yields of product with a *tert*-butyl-hydroperoxide oxidant. It is worthy of note that with the use of O_2 as an oxidant, a reasonable yield of 61% product was also achieved after an extended reaction time.

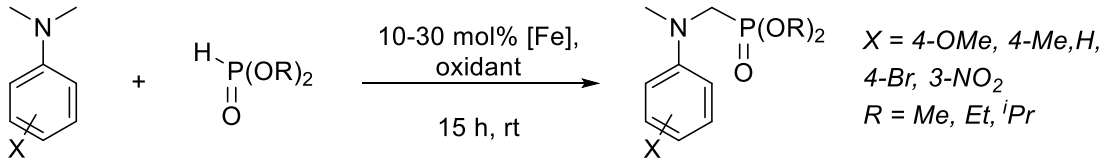

Scheme 22. Phosphonylation with Fe salts

In a follow up publication, they demonstrated the use of $FeCl_2$, once again, for the catalytic α-phosphonylation of *N,N*-dialkylanilines, and in this case they also explored the mechanistic details of the reaction.[54] A more extensive screening of substrates was carried out, although it must be said that there is little new information to be gleaned from the wider substrate scope, where in most cases there are only simple alterations made from Et groups to ^{i}Pr groups, for example (**Scheme 23**). Dimethylanilines were 'upgraded' to longer chain alkyls or cyclic groups.

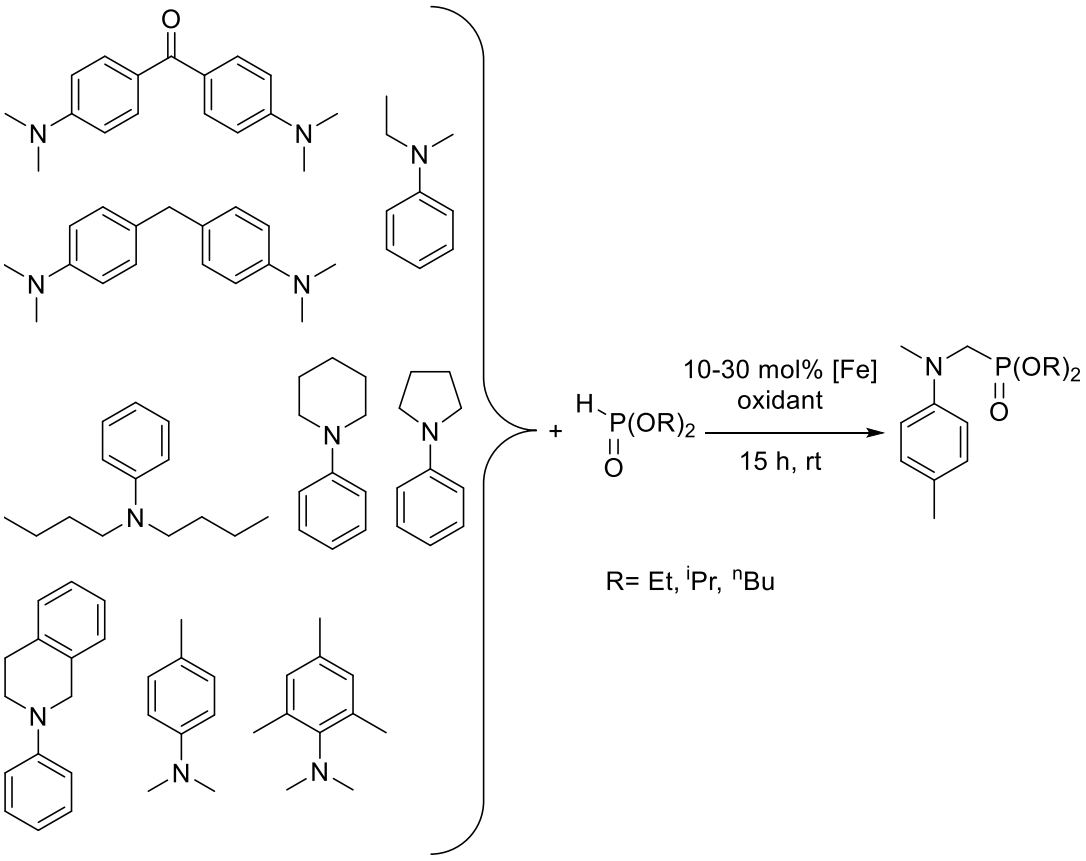

Scheme 23. Catalytic phosphonylation of tertiary amines with iron salts

An improvement on this system was the discovery of its tolerance of NO_2 functionality in the *meta* position on the aryl ring as well as an ester, carboxylic acid and alcohol functionality in the *para* position. Finally, the α,α'-bis-phosphonylation of N,N-dimethylmesidine and N,N-dimethyl-p-toluidine.

It seems unusual that, given the use of peroxides in this system that can act as radical initiators, a radical mechanism was not more thoroughly explored by the authors experimentally. Indeed, much detail of other systems was discussed but no specific conclusion drawn and with only one radical trapping experiment showing some reduction in yield versus the standard catalytic system. The authors rationalise that only a slight reduction in yield may be due to a much higher rate of reaction with the

substrate than with the radical trap, as in the case of Miura and co-workers.[55] An examination of rates for the standard and radical trap experiments may have been of value (overall reaction rate would likely be reduced in the case of a radical system). An ionic mechanism was also invoked by the authors as seen in the case of Li and co-workers, based on the similarly lowered yields seen with the radical trap BHT for their coupling reaction of an amine with a nucleophile (**Scheme 24**).[56]

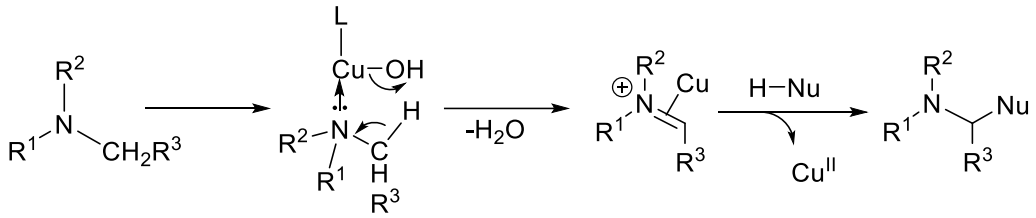

Scheme 24. Ionic mechanism for Cu-catalysed cross-dehydrogenative coupling reaction of an amine with a nucleophile

1.10 Catalytic hydrophosphorylation with iron salts and ligands

The asymmetric hydrophosphorylation of aldehydes was reported by Muthupandi and Sekar.[57] Using $Fe(OAc)_2$ in combination with a salen-type ligand, they were able to catalyse the production of optically active α-hydroxy compounds (**Scheme 25**). Using these ligand sets they hoped to extend reactivity to include hydrophosphorylation of aldehydes as an important step forward in the synthesis of α-hydroxy phosphonates – although there are a number of catalytic systems for their production, they generally require highly sensitive metal salts or rare (expensive) f-block compounds.[58–60] For example, Jingsong and co-workers utilise $Ti(O^iPr)_4$ for one such transformation.[61] This work provides the first example of an iron catalyst being used for the asymmetric hydrophosphorylation of aldehydes which would be of advantage in comparison to the costly systems mentioned previously.

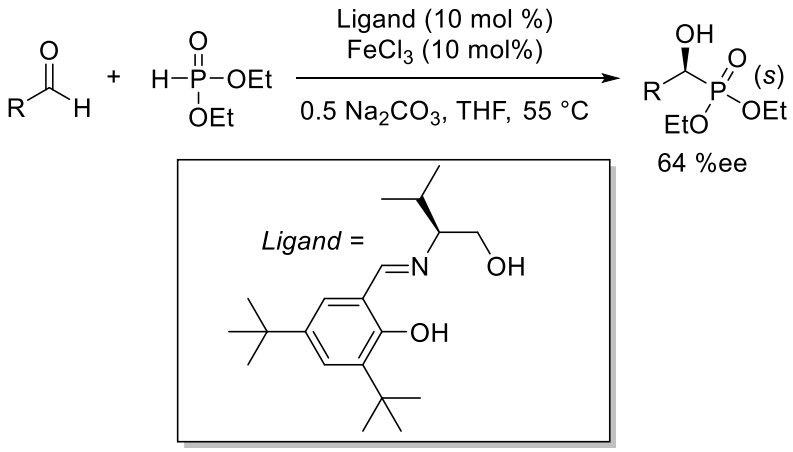

Scheme 25. Hydrophosphonylation with iron

With the highest ee presented in this research being 64%, further tuning of this system to produce larger enantiomeric excess would be desirable. Moving from Fe(II) vs Fe(III) showed a significant improvement in ee and was well rationalised by the authors (**Figure 4**).

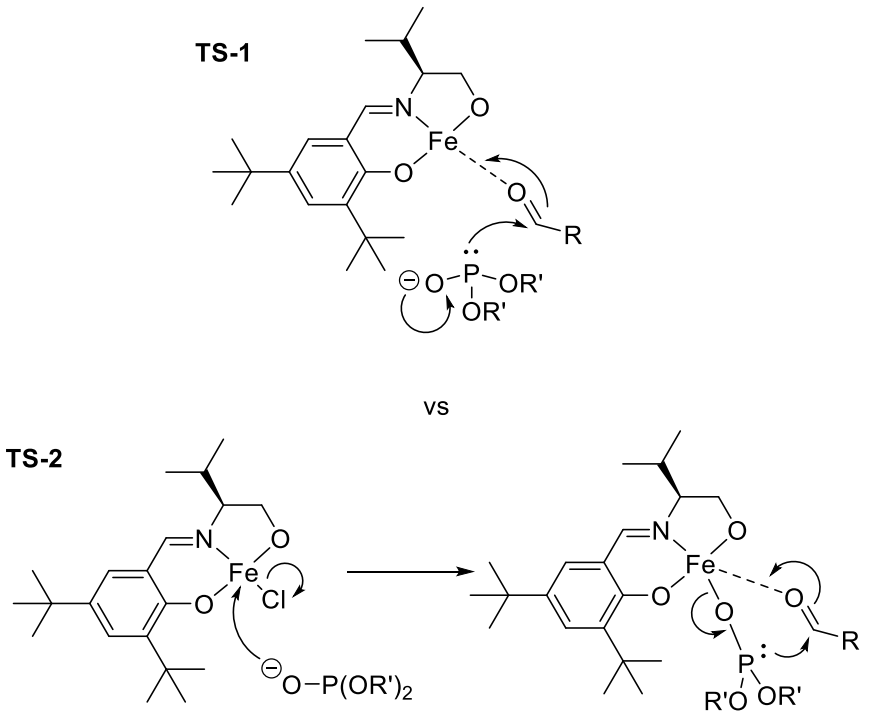

Figure 4. Simplified reaction mechanism (dimeric structure not included)

The authors screened several ligand variations with increasing bulk in various positions, substituting methyl- and isopropyl- groups for *tert*-butyl- or phenyl- groups. Only in one case did they alter the ligand structure to include further chiral groups, substituting the aromatic structure of their ligand system with an R-BINOL type functionality (**Figure 5**).

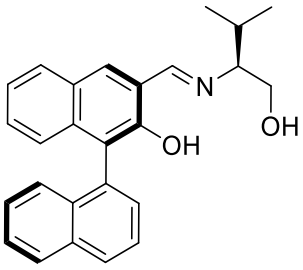

Figure 5. R-BINOL type ligand

Although screening of this ligand set was undertaken, no change in ee was observed. This disappointing finding is perhaps due to the remote location of the chiral group resulting in little influence on chirality over the course of the reaction. Perhaps with

further exploration of the ligand system (or similar ligand systems), for example alteration of the ^{i}Pr functionality, higher ee's may be possible.

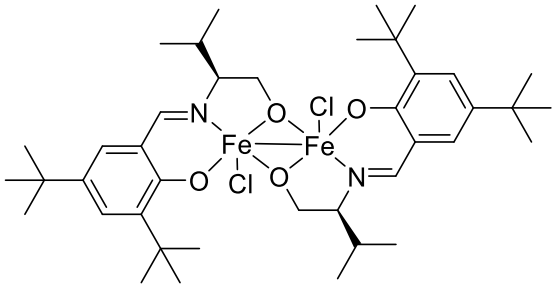

Figure 6. Dimeric iron species

In the course of their studies an unusual iron dimer was identified as a catalytically active species (**Figure 6)**. It is important to note that this was determined by isolation of the dimer followed by addition to the reaction and observation of catalysis. Comparable yields and enantioselectivity may indicate that this dimer is only a resting state able to access the catalytically active species. There was no reported attempt to gauge the rate of the reaction with respect to catalyst formed in situ from the iron salt + ligand. Confirmation of a comparable rate would provide some evidence for this as the catalytically active species, a particularly important consideration due to the focus of this publication on this iron dimer species. Wide sweep width ^{1}H NMR was also performed on the dimeric iron species, as well as mass spectrometry, but no evidence was presented for its presence in the crude catalytic reaction mixture. A simple NMR DOSY experiment could be used to identify the presence of the dimer in solution versus the monomer.

1.11 Catalytic hydrophosphorylation with [FeCl(SBAIB-d)]$_2$

It is perhaps of no surprise, shortly after the work of Muthupandi and Sekar, that a catalytic system with higher ees was developed.[62] After a thorough and extensive screening of the Camphor-based ligand motifs SBAIB (**Scheme 26**), with a variety of functionalities and under a range of conditions, it was determined that using the SBAIB-d (the Schiff base of aminoisoborneol) ligand resulted in the highest ee for the test reaction of benzaldehyde with di-n-butylphosphite in the presence of base. Indeed at 99% ee, this is the highest ee given by any chiral iron complex.

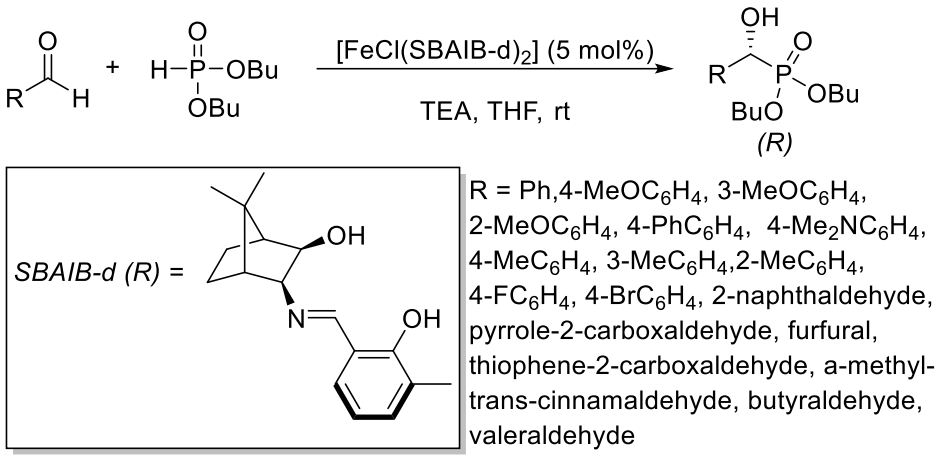

Scheme 26. Hydrophosphonylation with FCl(SBAIB-d)]$_2$

A wide range of aldehyde substrates were screened (**Scheme 26**) and all isolated in excellent yield. This includes substrates with electron donating substituents giving high ee and electron withdrawing halogens giving good, but slightly reduced ees. Enantioselectivity could then be further improved via recrystallization of the products. A variety of heterocycles were also tolerated by this system.

As with the work of Muthupandi and Sekar, a bimetallic iron species as the active catalyst was invoked (**Figure 7**). In this case, the mechanism is believed to proceed via the substitution of the chloride ion by a phosphite (generated *in situ* by the base) on to the metal centre (as seen in **Figure 4**, TS-2). Subsequent coordination of the aldehyde to the second metal centre (with an inter- or intra- molecular Cl^- shift) allows delivery of the phosphite to the *re* face of the aldehyde. Further reaction with the base-chloride salt or reaction with a phosphite anion then generates the product and regenerates the catalytically active species.

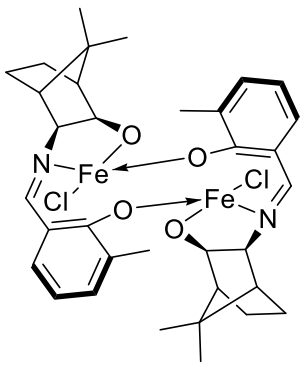

Figure 7. Dimeric iron species

1.12 Stoichiometric hydrophosphination with $Cp_2Fe_2(CO)_4$

The reaction of $Cp_2Fe_2(CO)_4$ with primary phosphines of the form PRH_2 (where R = Ph, Mes) was reported in 2005 by Ogino *et.al.*[63] The resulting product (where R =

Ph) (**11**, **Scheme 27**) can undergo further oxidation with HOTf, release of H_2 gas and coordination of CO to give a precursor (**12**, **Scheme 27**) which is capable of undergoing intermolecular hydrophosphination with an excess quantity of either alkyne or alkene (**13** and **14** respectively, **Scheme 27)** at room temperature. The transformation from **11** to **12** requires a shift in conformation from trans- to cis-geometry. Despite the high activation barrier for this rearrangement, the transformation is favoured by virtue of the lower energy state of the final product. With exclusive formation of the *E*-styryl group in **13** (or equivalently, the alkyl in **14**), it is rather unfortunate that the authors do not report isolation of the styrene product *via* further reaction of **13**, even stoichiometrically. These processes are both believed to take place through a radical mechanism due to the far reduced reaction rate in the presence of duroquinone, a radical scavenger.

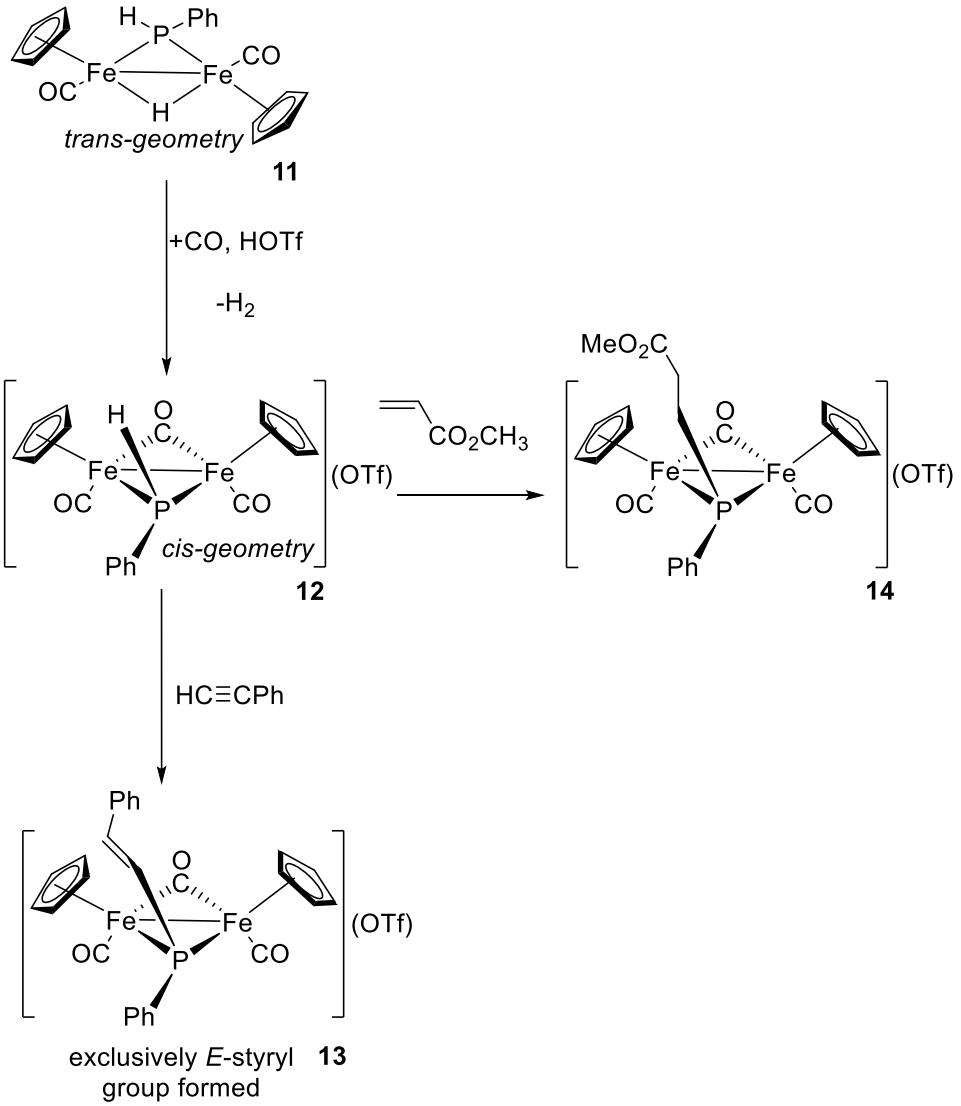

Scheme 27. Stoichiometric hydrophosphination with $Cp_2Fe_2(CO)_4$

1.13 Catalytic hydrophosphination with $CpFe(CO)_2Me$

In a publication from Nakazawa and co-workers, $CpFe(CO)_2Me$ was found to promote the double hydrophosphination of terminal alkynes (**Scheme 28**).[64] Due to the potential for a doubly phosphinated product (now acting as a bidentate ligand) to bind to the metal centre, these products are particularly challenging to access through metal catalysis. As such, this is the first non-stoichiometric (analogous to the stoichiometric reaction discussed preciously, **Section 1.13**) double hydrophosphination reported. The reaction is performed neat as the use of organic solvents was found to completely inhibit hydrophosphination and instead result in the formation of the isolable complex $CpFe(CO)(PPh_2H)\{C(O)Me\}$ (**16**, **Scheme 28**). A number of terminal alkynes were tested in this catalytic system and the doubly phosphinated products were isolated in generally good yield. It is worth noting that these yields were obtained from a lengthy reaction time of three days.

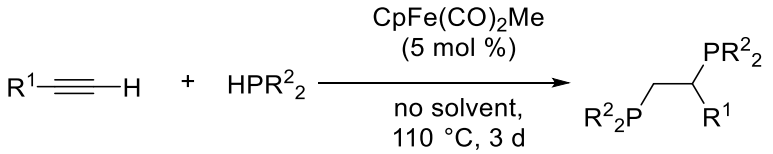

R^1 = 4-MeC_6H_4, 4-$^tBuC_6H_4$, 4-$MeOC_6H_4$, 4-$(NH_2)C_6H_4$, 4-$(CF_3)C_6H_4$, 3-pyridyl, 3-thiophenyl, 2-pyridinyl

R^2 = Ph, 4-MeC_6H_4, 4-$(MeO)C_6H_4$

Scheme 28. The catalytic double hydrophosphination of terminal alkynes using an iron complex

Isolation and use of the complex $CpFe(CO)(PPh_2H)\{C(O)Me\}$ (**16**, **Scheme 29**) under the optimised conditions for catalytic double hydrophosphination resulted in a similar level of activity. Addition of $HPPh_2$ to **15** results in the formation of **16** and elimination of HC(O)Me generates the catalytically active iron complex, **17**. Beginning with *cycle 1*, it is believed that coordination of the alkyne to the metal centre is followed by insertion of the alkyne into the Fe-P bond. This generates a singly substituted alkene which is then liberated by addition of $HPPh_2$ (in turn regenerating the catalytically active iron species). Moving to *cycle 2*, the singly substituted alkene is then free to bind to the metal centre and is thought to undergo a similar transformation resulting in the doubly substituted HP product. Single substitutions are far more common in the literature.[65–68]

This work provides the (currently) definitive catalytic cycle for double hydrophosphination with iron which has been further supported by the DFT calculations of Liu and co-workers.[69]

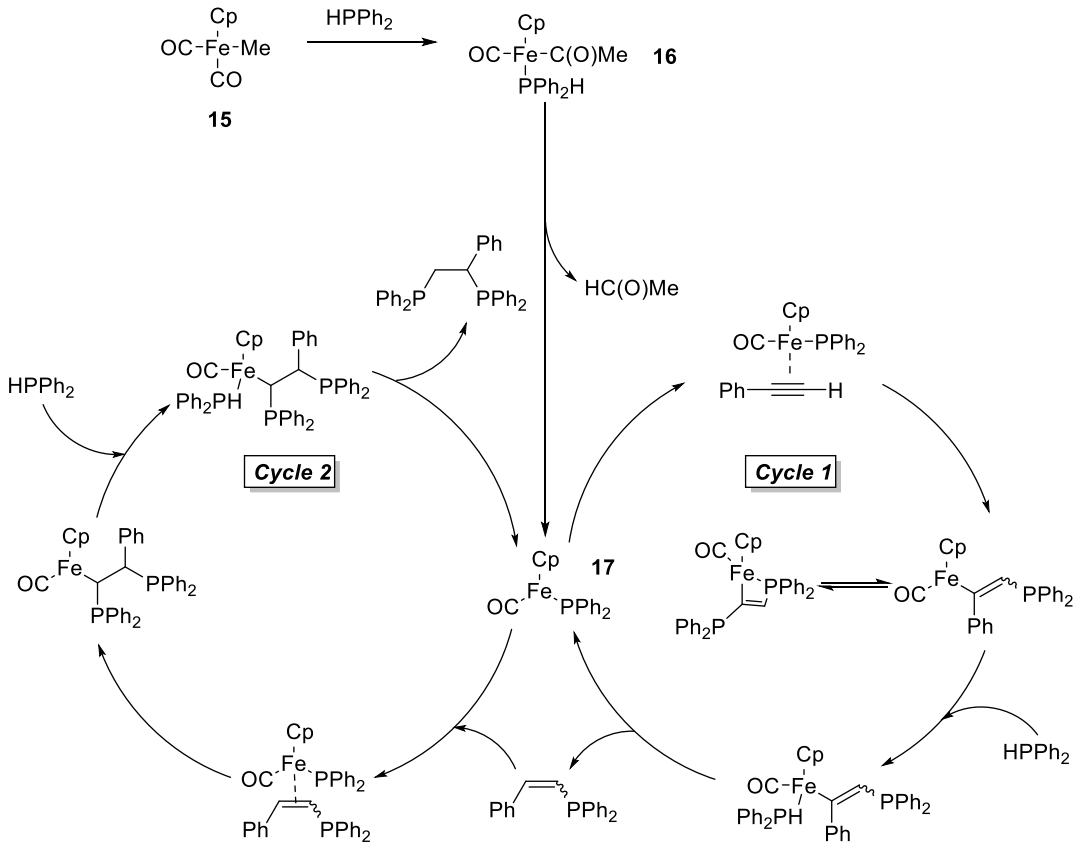

Scheme 29. CpFe(CO)(PPh_2H){C(O)Me} and mechanism

A follow-up publication by Nakazawa and co-workers details the hydrophosphination of terminal alkynes with secondary phosphines (**Scheme 30**).[70] The pre-catalyst Cp*Fe(CO)(py)(Me) (10 mol%) is used to access the catalytically active Cp*Fe(CO)PPh_2. This simple change from Cp to Cp* results in the regioselective formation of the *Z*-vinylphosphine product of hydrophosphination, *i.e*. completing *cycle 1* of **Scheme 29**. These vinylphosphines can be converted to the corresponding unsymmetrical 1,2-bis(phosphino)ethane products *via* reaction with another secondary phosphine in the presence of $CpFe(CO)_2(Me)$ (5 mol%), the authors' original pre-catalyst.

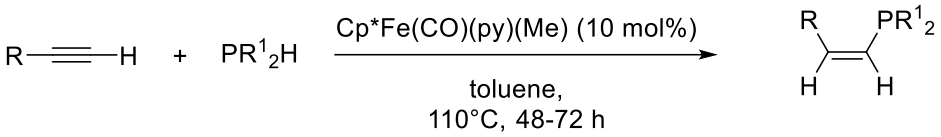

R = Ph, 4-MeC_6H_4, 4-$(MeO)C_6H_4$,4-$(NH_2)C_6H_4$, 4-FC_6H_4, 4-$^tBuC_6H_4$, 2-pyridinyl, 3-thiophenyl, ferrocenyl
R^1 = Ph, 4-MeC_6H_4, 4-$(MeO)C_6H_4$

Scheme 30. Regioselective hydrophosphination of terminal alkynes with Cp*Fe(CO)(py)(Me)

The authors report a robust functional group tolerance for the acetylenic R group, with electron withdrawing and donating aryl moieties producing similarly high yields and good E:Z ratios. Unsurprisingly, alkyl-alkynes were not reactive under the same reaction conditions, likely resulting from a lack of activation of the C–C triple bond. Substrates with challenging functional groups, *e.g*. thiophenyl and NH_2, were found to be tolerated by this system, but were unfortunately isolated in low yield. The hydrophosphination reaction was found to be unique to terminal alkynes, with internal alkynes showing no reactivity under similar reaction conditions.

Several intermediates identified in this catalytic cycle were independently synthesised, including a metallacyclophosphabutene. Each of these were shown to catalyse the hydrophosphination of terminal alkynes, supporting the validity of the proposed catalytic cycle.

1.14 Catalytic hydrophosphination with $FeCl_2$ and $FeCl_3$

It was found by Gaumont and co-workers that simple iron chloride salts promoted regioselective hydrophosphination.[34] Interestingly, use of $FeCl_2$ promoted anti-Markovnikov addition (**Scheme 31**), whilst $FeCl_3$ promoted the more challenging Markovnikov addition (**Scheme 33**). In the case of $FeCl_2$, a variety of functionalised styrenes were screened, giving generally good yields and isolated as the anti-Markovnikov BH_3 adduct.

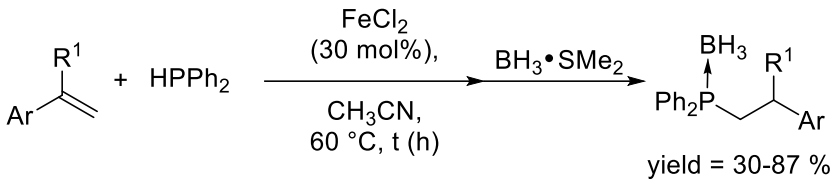

Ar = Ph, 4-(MeO)C_6H_4, 2-(MeO)C_6H_4, 3-MeOC_6H_4, 4-BrC_6H_4, 2-(CF_3)C_6H_4
R^1 = H, Me

Scheme 31. Hydrophosphination with $FeCl_2$ of styrenes to anti-Markovnikov products

Halogens are well tolerated by this Fe(II) system. A radical activation of molecular oxygen is believed to be the initiator for the primary mechanism for formation of the AM product – addition of a radical inhibitor or performing the reaction in the dark reduced yields significantly. Although the authors do not postulate beyond this statement on the effect of radical traps, it could be envisaged that initial formation of a phosphido radical attacks the styrene double bond, resulting in a stable benzylic radical which then actives $HPPh_2$, releasing the product and another phosphido radical (**Scheme 32**). In this case diphenylphosphine may be cleaved to form radical PPh_2 fragments which carry out HP.

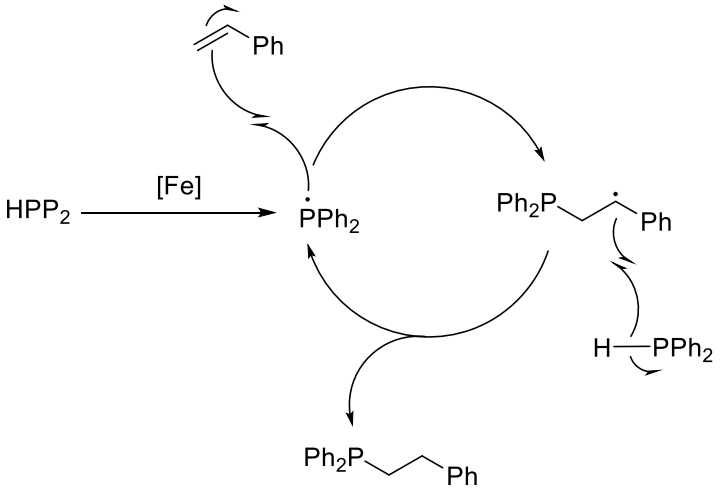

Scheme 32. Radical initiated HP mechanism

In the case of $FeCl_3$ (**Scheme 33**), EDGs are well tolerated, however EWGs such as halogens are poorly tolerated. The presence of -CF_3 and -Br on the phenyl ring results in reduction of yields to <5 %.

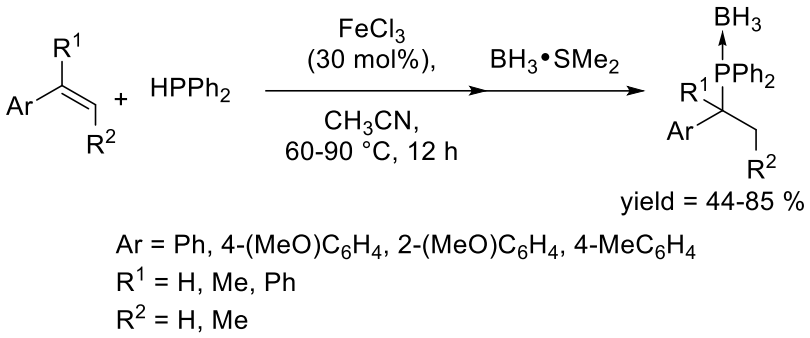

Scheme 33. Hydrophosphination of styrenes to Markovnikov product

The higher Lewis acidity of $FeCl_3$ than $FeCl_2$ is offered as a potential explanation for the selectivity of these systems (AM versus M product) – the increased ability of $FeCl_3$ to accept electron density from the alkene making the first step in the catalytic cycle more favourable (**Scheme 34**). Indeed, other iron salts ($Fe(acac)_3$ and $K_3[Fe(CN)_6]$) also led to the selective formation of the AM product. For Markovnikov addition, in the case of $FeCl_3$ π-coordination of the styrene, resulting in an umpolung charge distribution, followed by addition to the activated double bond is postulated. Phosphine is available to attack the double bond of the coordinated alkene. This forms HCl which in turn protonates the Markovnikov product and reforms the catalyst.

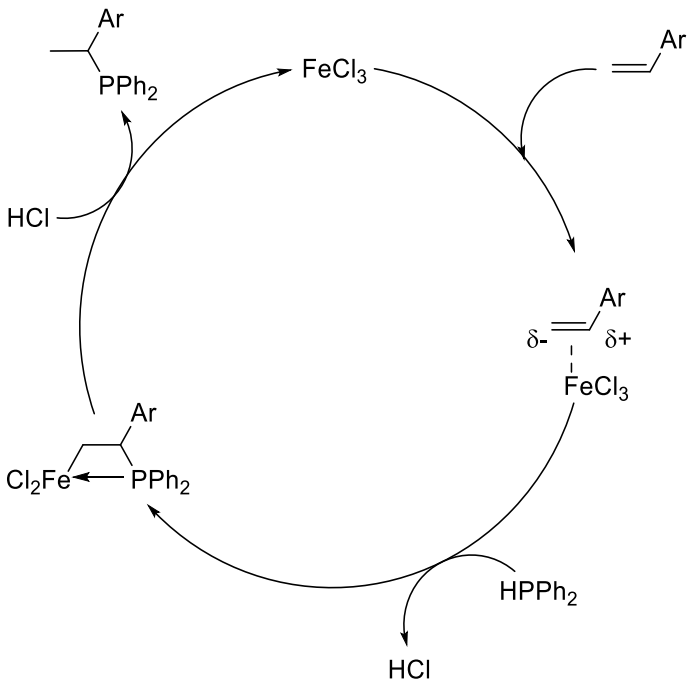

Scheme 34. Markovnikov mechanism for hydrophosphination

These simple iron salts have the advantage of being cheap and commercially available. This is of advantage in the synthesis of the much sought-after, high value Markovnikov product. However, it does mean the tunability of this system is low and improvement of tolerance of EWG for example is unfeasible. This is reflected in the observation of AM for all other iron salts studied and indeed, addition of a ligand to this system is found to switch reactivity to give solely the AM product indicating a finely balanced system (see **Chapter 3**).

1.15 Catalytic hydrophosphination of Isocyanates using iron(II)

The hydrophosphination of isocyanates was reported by the Kays group (**Scheme 35**).[22] This reaction employs low coordinate iron(II) species as pre-catalysts. An excellent substrate scope is achieved, with EWG, EDG and aliphatic groups all being well tolerated in this system.

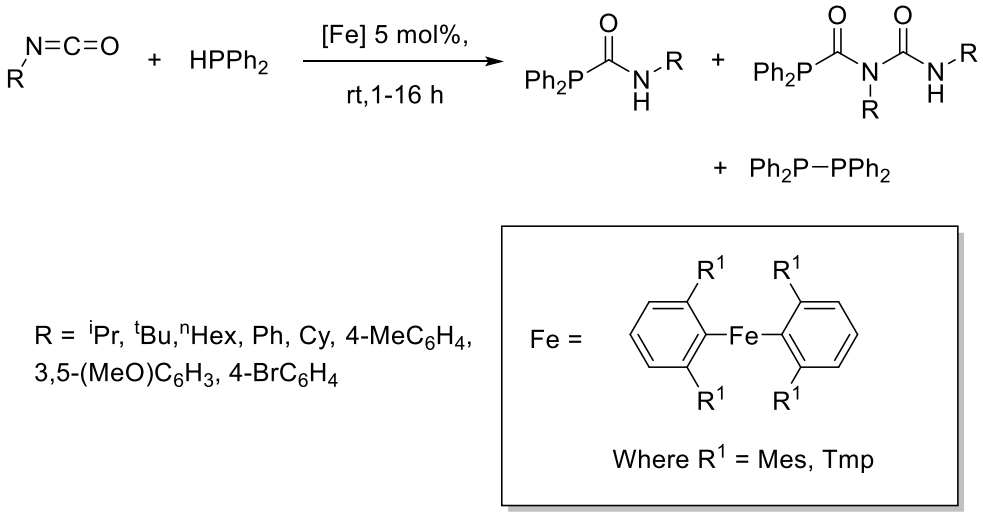

Scheme 35. Hydrophosphination of isocyanates with Fe(II)

The authors propose a catalytic cycle reminiscent of Glueck's work in Pt catalysed hydrophosphination (discussed previously, see **Section 1.8**) – with the formation of a phosphonium-amide zwitterion (**Scheme 36**). Where R^1 = Mes, only *cycle 1* takes place to form the isocyanate phosphine. In the case where R^1 = Tmp, *cycle 1* is followed by the co-ordination of the phosphine product of *cycle 1* to the metal centre, accessing *cycle 2* to then yield the phosphinodicarboxamides.

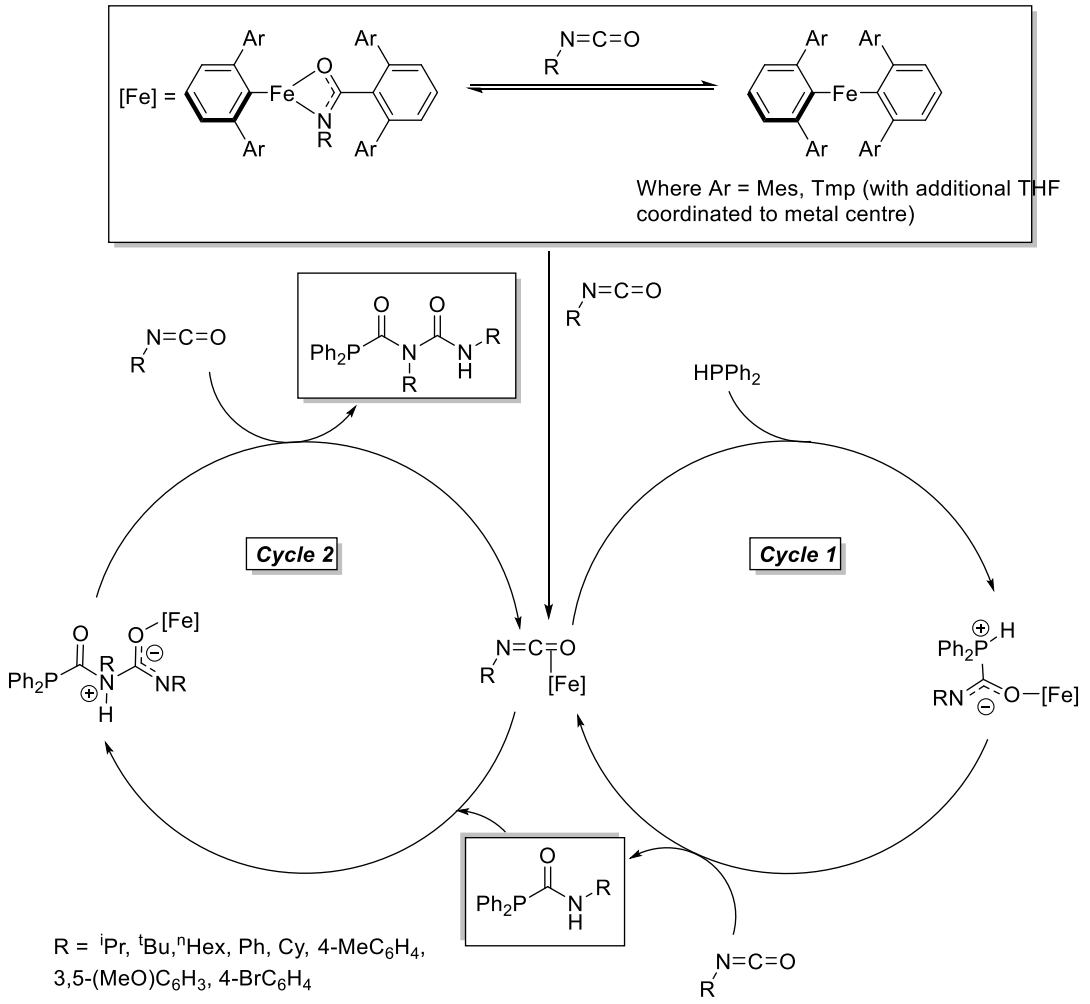

Scheme 36. Proposed catalytic cycle for the hydrophosphination of isocyanates with Fe(II)

Addition of benzaldehyde to the catalytic mixture, according to the work of Glueck, to trap a zwitterionic species in this case could have been fruitful in proving the proposed mechanism. Using a 1:1 mixture of PhNCO and CyNCO with $PHPh_2$, the authors find a mixture of four phosphinodicarboxamides: the monoinsertion products $Ph_2PC(O)NHPh$ and $Ph_2PC(O)NHCy$, a homocoupled phosphinodicarboxamide $Ph_2PC(O)N(Ph)C(O)NHPh$ and a heterocoupled phosphinodicarboxamide $Ph_2PC(O)N(Ph)C(O)NHCy$. Curiously, neither tof the two other potential products, $Ph_2PC(O)N(Cy)C(O)NHCy$ or $Ph_2PC(O)N(Cy)C(O)NHPh$, are observed. This suggests that only $Ph_2PC(O)NHPh$ is capable of acting as a nucleophilic species in *cycle 2*. A possible explanation for this observation is the presence of the phenyl group, which is able to support the positive charge on the N atom of the zwitterion due to resonance stabilisation. Cyclohexyl lacks the ability to disperse the positive charge of the zwitterion and hence its role as a nucleophile in *cycle 2* is disfavoured.

1.16 Applications of HP Phosphines

1.16.1 Negishi cross-coupling

Although the form of the products produced by hydrophosphination often diverges from the classical picture of a phosphine ligand, which are typically simple mono phosphines or symmetrical bis-phosphines, the tunability of these products means that they have found utility in several areas and clearly warrant further exploration as ligands. These phosphines have been applied as ligands to several different cross-coupling reactions. The monophosphines used have all been prepared according to our 2014 publication (See **Chapter 3**).[1,18] Negishi cross-coupling – the coupling of aryl bromides with diphenyl zinc reagents is shown to be catalysed by an iron source with a selection of these monophosphine ligands.[19] Varying the electronic properties of the ligands (**L**= **19**, **20**, **21**), it is found that the simple unsubstituted styrene-based ligand offers the optimum reactivity (**L**=**18**,**Scheme 37**).

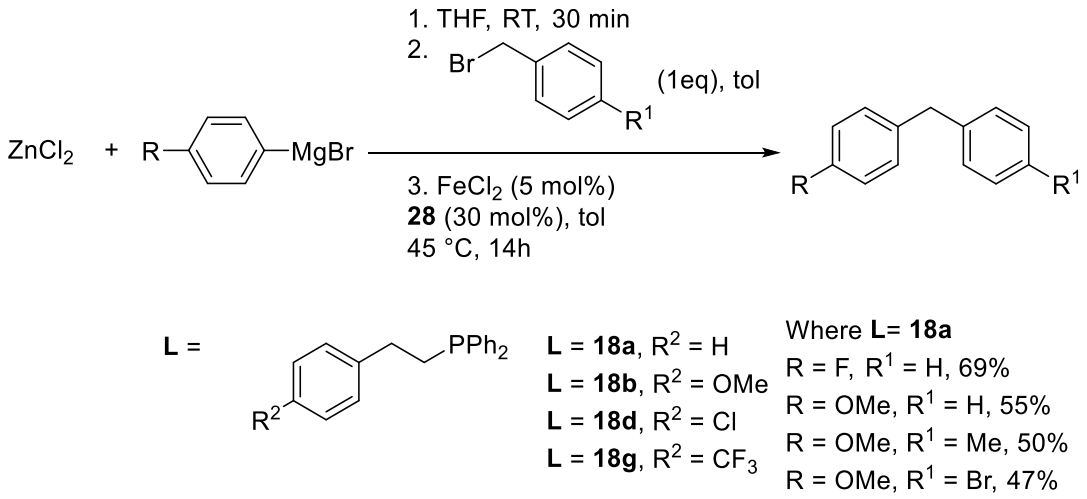

Scheme 37. Iron catalysed Negishi cross-coupling

Several R groups were screened for both the Grignard reagent and the coupling partner demonstrating a competent range of activity. Preparation of the discrete four-coordinate iron complex of the styrene-based ligand was also achieved and the iron-phosphine complex isolated and used effectively in catalysis.

1.16.2 Heck cross-coupling

The ability of ethyl phosphines to act as ligands in a range of cross-coupling reactions was recently assessed by Webster and co-workers.[18] A range of electronically and sterically challenging substrates were chosen for these reactions to assess the effectiveness of this phosphine ligand motif versus the classically used triphenylphosphine (**Scheme 38**).

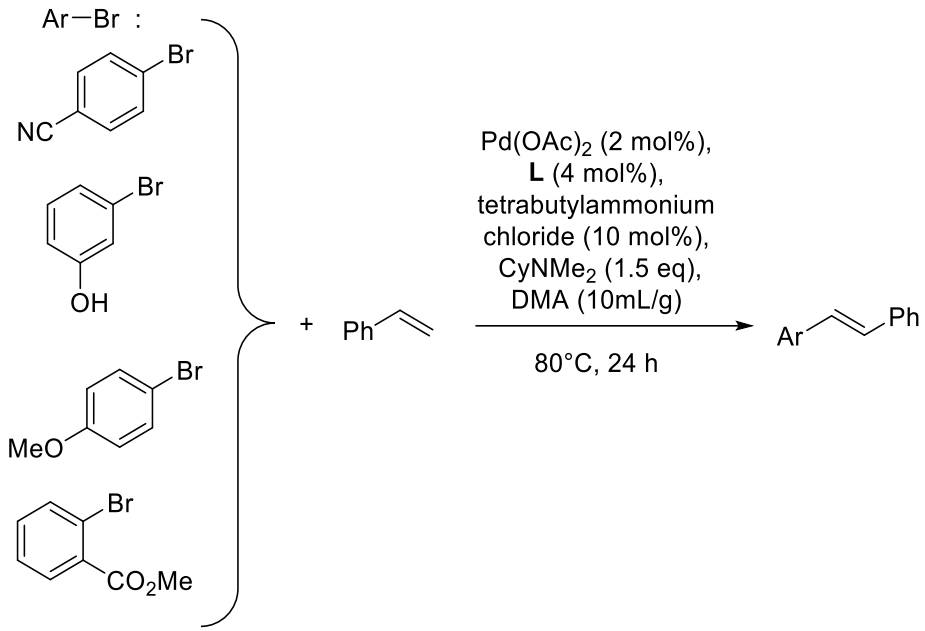

Scheme 38. Heck cross-coupling with a range of phosphines

The simple standard Heck reaction was carried out with 4-bromobenzonitrile and styrene and the range of ligands shown in **Figure 8**. **32** is clearly an excellent choice of ligand (95% yield) alongside PPh_3 (92% yield) in this case. Ligand **23** also gives a reasonable yield (64% yield) for this reaction but gives generally poor yields for other substrates, including 3-bromophenol, a more challenging substrate due to its electronic characteristics. Ligand **22** was found to be the most effective in this instance. The cross coupling of the sterically encumbered 4-bromoanisole was most effectively catalysed with ligand **24** even in comparison to PPh_3, likely due to its comparatively lower bulk than any of the ligands examined. Unsurprisingly all ligands pictured were ineffective for cross-coupling of 1-bromo-2-ethylbenzene which is both sterically and electronically demanding. Ligand **23** was also seen to perform effectively alongside PPh_3 for the bromo-aryl ester, arguably the most challenging substrate in terms of steric and electronic characteristics.

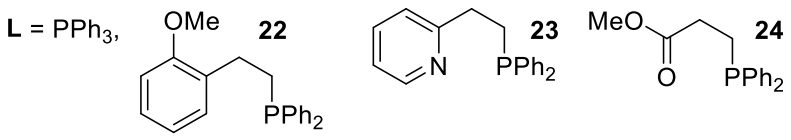

Figure 8. Ligands studied for cross-coupling reactions

The alkene substrate was then varied revealing, in general, better performance of the ethyl phosphines. Both methyl acrylate and methyl methacrylate were screened revealing that generally, ligand **22** and **24** provide complementary reactivity to triphenylphosphine. It is worthy of note that the use of $Pd(OAc)_2$ with these ligands in

many cases is competitive with or surpasses the yields reported with commercial (and expensive) Pd(0) and Pd(II) pre-catalysts.[71]

1.16.3 Suzuki-Miyaura cross-coupling

The level of reactivity of a variety of substrates was screened using the sterically and electronically demanding substrate 2-methoxyphenyl boronic acid with a range of aryl bromides in a standard Suzuki-Miyaura reaction (**Scheme 39**).[18,72]

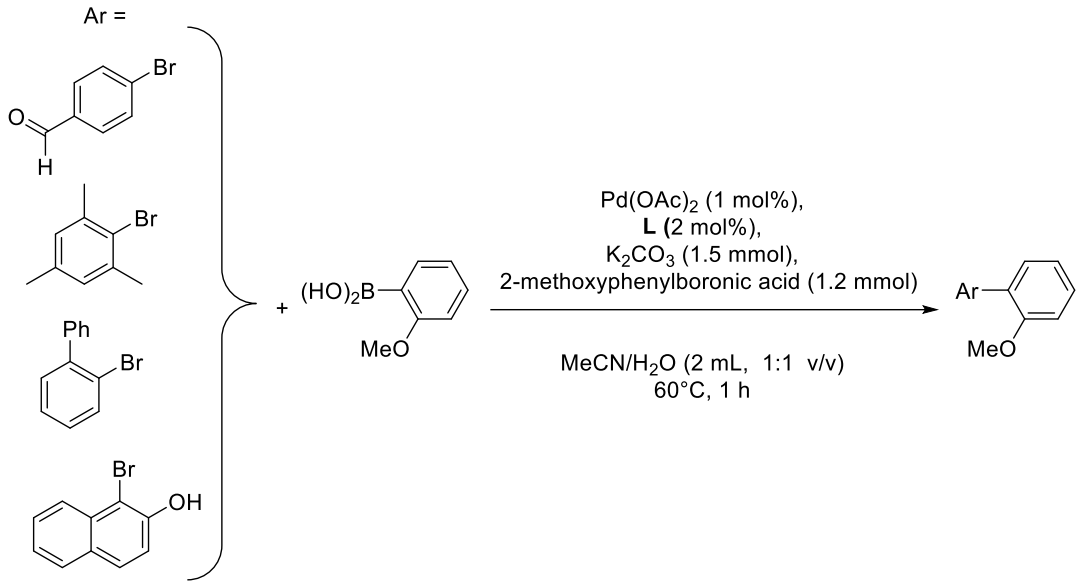

Scheme 39. Suzuki cross-coupling with a range of phosphine ligands

Here ligand **22** (**Figure 8**) was found to be the most effective for coupling aryl bromides with a range of challenging substrate functionalities including 2-phenyl (87% yield) and naphthol (50% yield) substituted reagent. Only in the case of bromobenzaldehyde does PPh_3 (94% yield) outperform **22** (76% yield).

The coupling of aryl chlorides with phenylboronic acid was also studied. The wider variety of commercially available aryl chlorides than aryl bromides makes this a more desirable (though more demanding) substrate to study for Suzuki-Miyaura coupling. Ethyl phosphines outperformed PPh_3 in all cases. Ligand **22** was found to be the most effective for these reactions, outstripping yields obtained with PPh_3 thoroughly for 2-chloropyridine (61% vs 28%) and 2-chlorothiophene (62% vs 25%).

1.16.4 Buchwald Hartwig cross-coupling

Buchwald Hartwig amination was studied under standard conditions.[18,73] The challenging synthesis of multi-heteroatom amination products works well with all ligands studied (**Scheme 40**). Once again ligand **22** was the best ligand choice for the range of substrate combinations explored. The enhanced electronic properties proffered by the electron donating methoxy group is postulated to be responsible for

the enhanced activity of this ligand across the board for cross-coupling reactions. The coordinating ability of the heteroatom may also help to stabilize reactive intermediates. 4-Chloroanisole gave a poor yield of product regardless of ligand choice and this substrate is problematic both in terms of oxidative addition of the starting material and reductive elimination of the product. Use of a stronger base does not affect the yield significantly. The use of a primary amine with an aryl bromide would have been a nice final touch for this study, to compare activity of primary and secondary amines in this system.

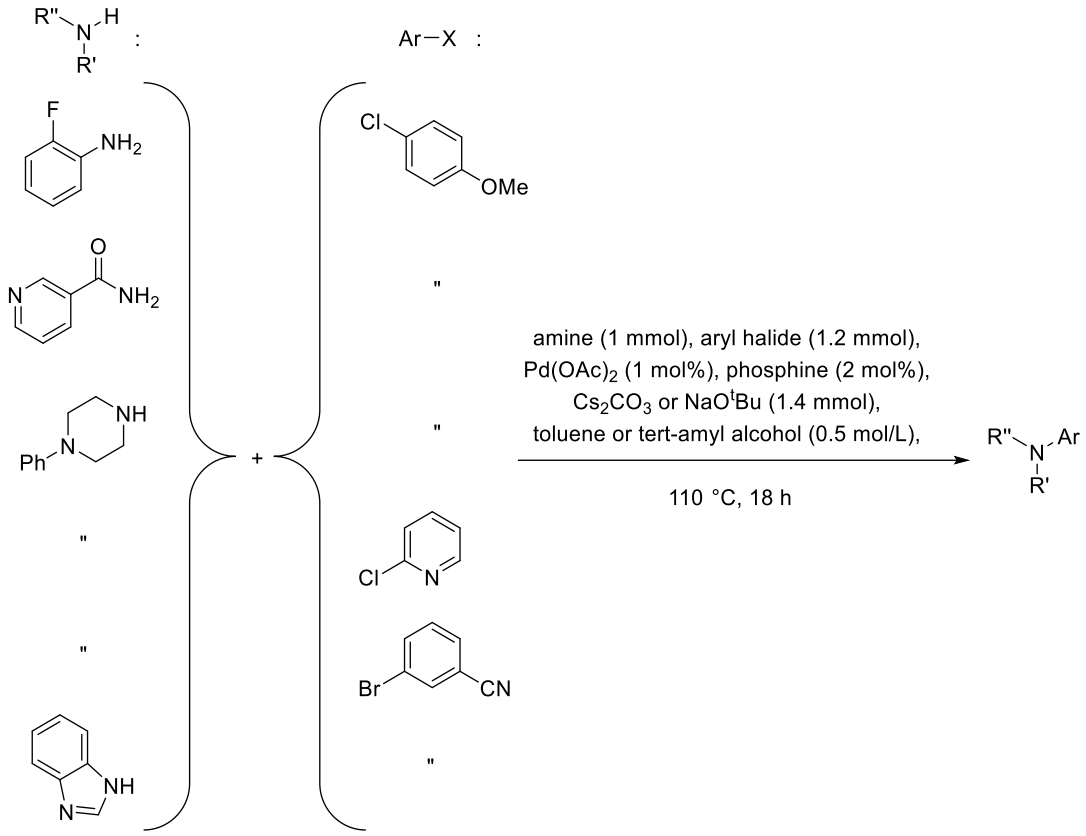

Scheme 40. Buchwald Hartwig cross-coupling with a range of phosphine ligands

1.17 Further valuable applications of hydrophosphination

1.17.1 Phosphinoester synthesis

Conversion of azides into diazo compounds was found to be facilitated through synthesis of a phosphinoester. This product was much more readily accessed through hydrophosphination than the complex organic synthesis used.[33]

Leung and co-workers have presented the hydrophosphination of N-enyolbenzotriazoles using a Pd based catalyst.[74] Under optimised conditions the process gives the selective addition of a secondary arylphosphine across a double

bond with high conversion and enantiomeric selectivity (**Scheme 41**). A range of functional groups adjacent to the reaction site were screened. These exhibited good reactivity; however, the scope of testing was largely limited to arene functionalities and did not include any alkyl groups.

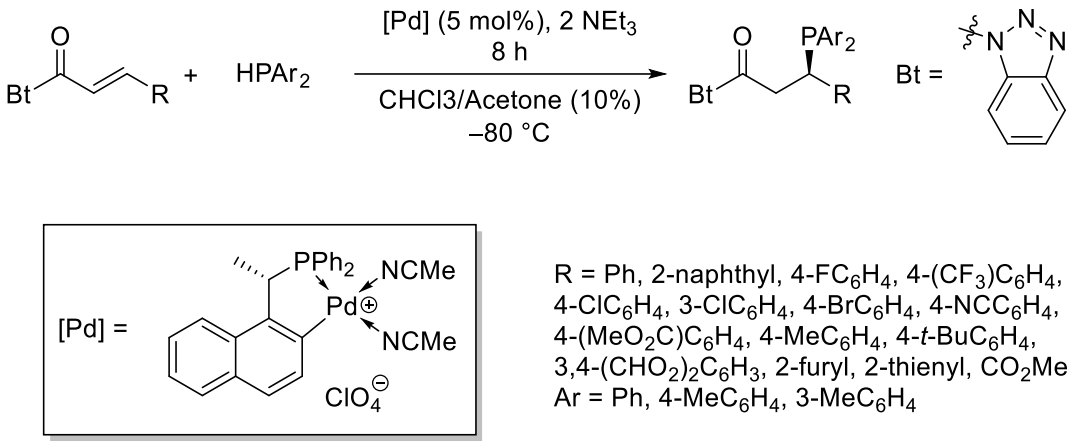

Scheme 41. Hydrophosphination of N-enoylbenzotriazoles

The enantiomeric excesses of the products were determined by analysing the $^{31}P\{^{1}H\}$ spectrum from diastereomers formed from reaction of the phosphinated products with a racemic mixture of a chiral Pd complex (**Scheme 42**). Attempted purification of one mixture of these diasteromers (R = Ph, Ar = Ph) via chromatography led to hydrolysis resulting in elimination of the benzotriazole group and formation of a neutral P,O-chelated complex .

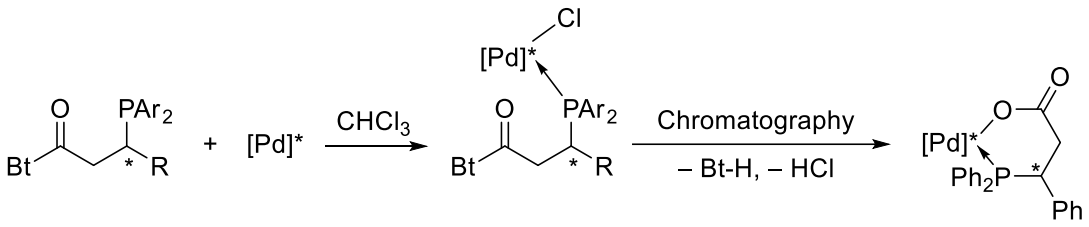

Scheme 42. Selective hydrolysis of Pd phosphine diastereomers (absolute stereochemistry omitted)

Isolation of a hydrophosphinated product (R = Ph, Ar = Ph) was achieved by treating with sodium methoxide in methanol and chloroform, followed by addition of elemental sulphur to give the phosphine sulphide ester product with no loss of optical purity (**Scheme 43**).

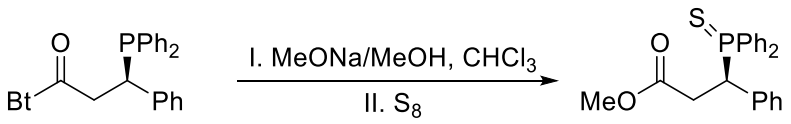

Scheme 43. Esterification and sulphonation of phosphine products

The authors employed these phosphine products as a series of ligands in Au-based complexes, which were tested for anti-cancer properties. These Au complexes exhibited moderate tumor suppression activity.

1.17.2 Synthesis of asymmetric phosphines *via* hydrophosphination

The asymmetric hydrophosphination of achiral ferrocenylenones *via* a palladium-based catalyst was reported by Pullarkat and co-workers (**Scheme 44**).[75] The reaction was shown to be high-yielding (> 99% isolated yield) under optimised conditions. The high activity of the enone substrate is perhaps unsurprising due to the strong electron donating properties of the ferrocenyl group adjacent to the reaction site. A range of functional groups adjacent to the enone moiety were tested, with high conversions (< 99%) reported in each case. The duration of the reaction however seemed to vary strongly with the choice of substrate, from 2 h for the furyl-substituted enone (the optimised system) to 4 days for a phenyl-substituted system and up to 9 days for the methyl-substituted system. In many cases the extended reaction times can be attributed to the authors performing the reaction at low temperatures (−80 °C) to attain improved selectivity. The authors note that substrates such as 2-pyrrole and (4-NO_2)C_6H_4, which have a tendency to chelate Pd and thus disrupt catalyst regeneration, often failed to reach full conversion, even after 1 week.

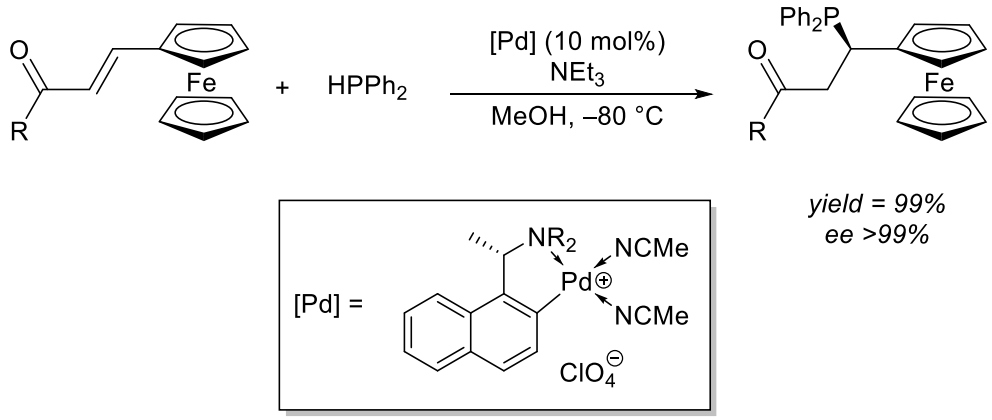

Scheme 44. Selective hydrophosphination of a ferrocenylenone with a chiral palladium catalyst

To assess the ability of the ligand to impart planar chirality, the authors affixed the phosphorus-containing ligand to a Pd centre via a cyclopalladation (**Scheme 45**). Subsequent chiral resolution with sodium prolinate gave two signals in the $^{31}P\{^{1}H\}$ spectrum with a ratio of 1:5 indicating a relatively selective reaction. The authors point out that this diastereoselectivity is the result of the C-chirality imparted by the enantioselective hydrophosphination reaction. Crystallisation of this mixture gave the enantiopure product as the S enantiomer (with respect to the planar chirality). This

was converted back to the initial Pd-containing product by reaction with LiCl and AcOH in MeOH with total retention of stereochemistry.

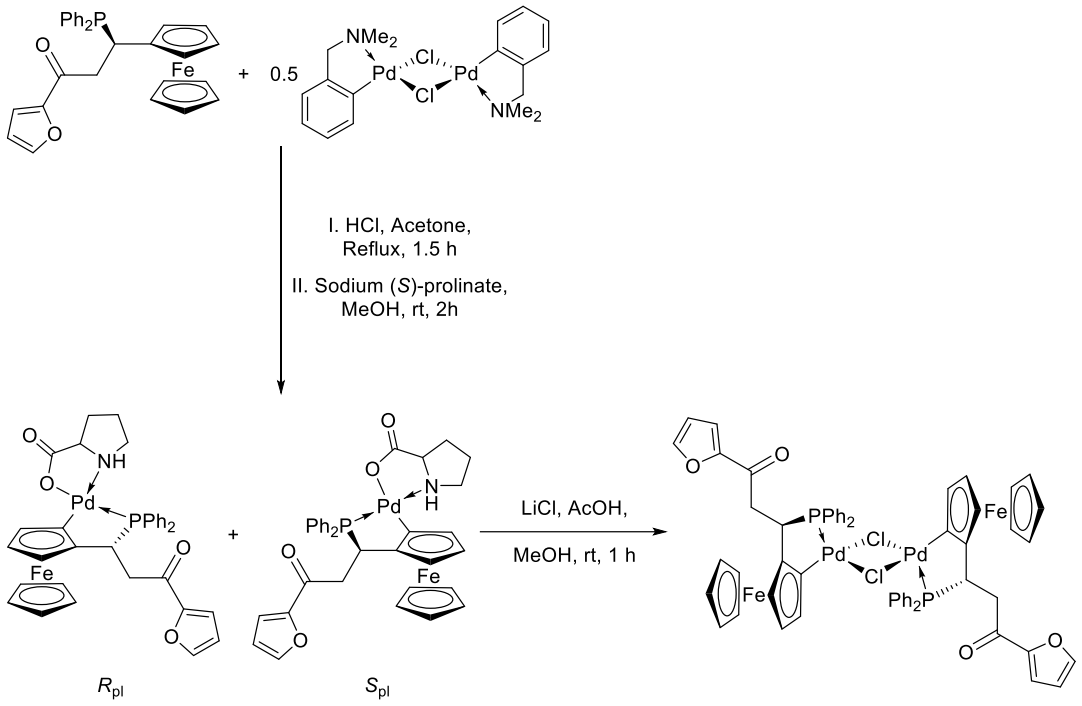

Scheme 45. Chiral resolution of phosphine products

The effort Pullarkat and co-workers put into their chiral resolution bore fruit in the form of a successful asymmetric reaction carried out with the palladacycle catalyst. Using the resulting enantiopure complex, a catalytic coupling reaction is achieved between aryl boronic acid and 2-cyclohexanone (**Scheme 46**).

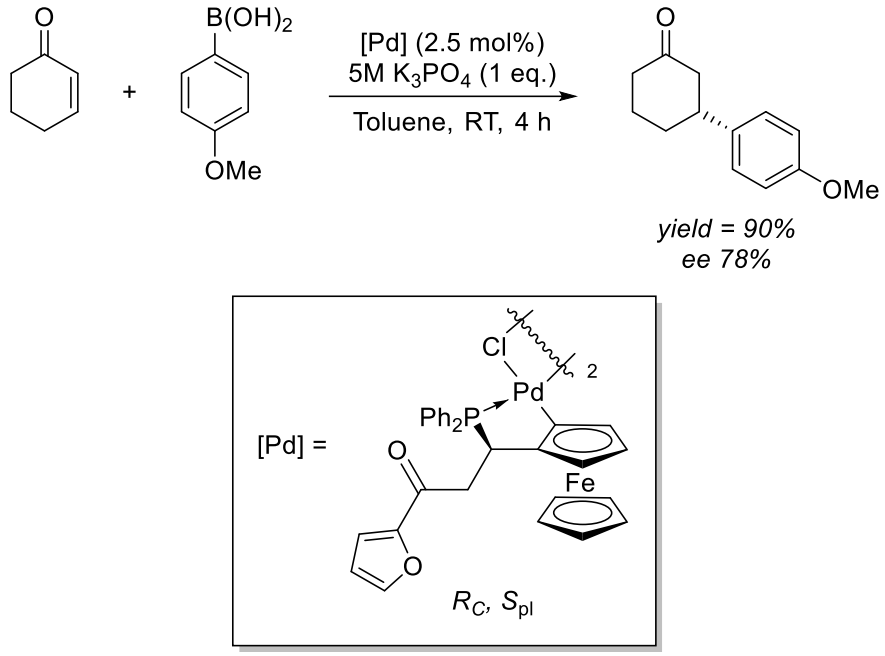

Scheme 46. Use of a chiral phosphine ligand with Pd-based catalyst to promote addition of phenylboronic acid to cyclic alkene

1.17.3 Synthesis of anti-cancer compounds

Leung and Chew recently published an extensive review of their progress in the field of chiral phosphines.[76] Many of these are produced through asymmetric syntheses utilising palladacycle catalysts. These chiral phosphines have been used by Leung and co-workers as ligands in various gold(I) complexes, which were investigated for their cytotoxic properties in anti-cancer studies.[35,77,78] The inclusion of chiral phosphine ligands allowed the effects of chirality to be investigated with respect to anti-cancer activity and selectivity. In one example, a pair of chiral gold(I) phosphine enantiomers were prepared from the enantiomerically pure phosphabicycloheptene ligands (**Figure 9**).[35] Both enantiomers showed significant anti-cancer activity against various cell-lines and extremely limited cytotoxicity in healthy cells.

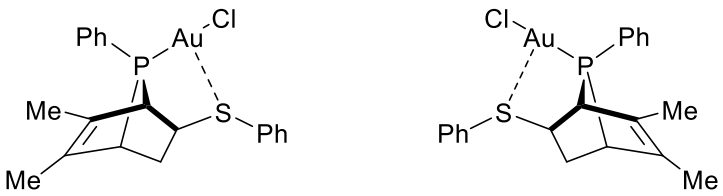

{(*S*)-L}AuCl {(*R*)-L}AuCl

Figure 9. Chiral gold(I) phosphines for anti-cancer applications

In a more recent example, although the (*RR*)-enantiomer and (*SS*)-enantiomer of a digold(I) compound showed little difference in anti-cancer cancer activity against a

breast cancer cell line, the (*RR*)-enantiomer was markedly more toxic against healthy cells than its (*SS*) counterpart(**Figure 10**).[78]

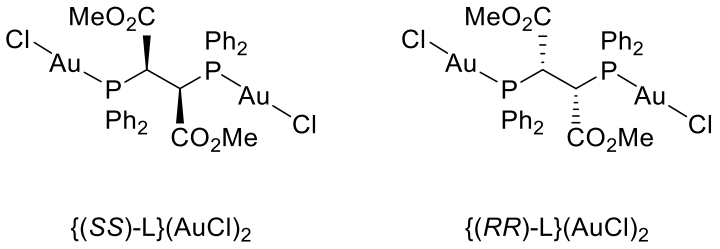

Figure 10. Chiral digold(I) phosphines for anti-cancer applications

1.17.4 Synthesis and use of phosphine pincer ligands for hydrophosphination

Leung, Pullarkat and co-workers have used their Pd-catalysed hydrophosphination approach to generate phosphine-containing pincer ligands.[79] The use of their established catalytic protocol allows the generation of optically pure diphosphine pincer ligands, which are complexed initially to a palladium chloride salt (**Scheme 47**). Testing of this complex found it to be catalytically inactive for the hydrophosphination reaction. Treatment of this complex with AgOAc generates the (L)PdOAc complex *via* a simple salt metathesis reaction (**Scheme 47**). Acetate is a much better leaving group than chloride and hence the Pd-OAc complex is able to catalyse hydrophosphination reactions.

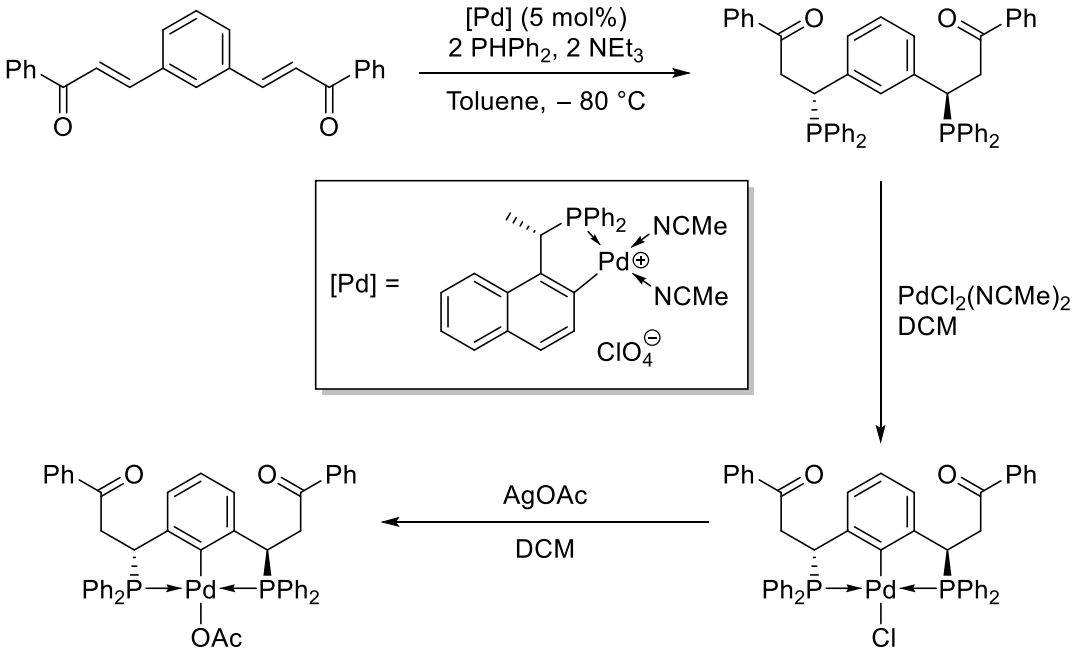

Scheme 47. Synthesis of a diphosphine pincer ligand *via* hydrophosphination and its complexation to palladium

Hydrophosphination catalysts containing pincer ligands operate *via* a different catalytic pathway than the cyclometallated complexes seen thus far. The authors

state that pincer type complexes tend to activate the P–H bond *via* initial P→Pd coordination, followed by inter-molecular P–C bond formation. This is largely irrelevant for the outcomes of reactions with α,β-unsaturated substrates but becomes important once substrates contain more than one chemically reactive site, such as α,β,γ,δ-unsaturated species. In this case a pincer-type catalyst is likely to produce the 1,6-addition product which is disfavoured for cyclopalladated catalysts due to the invocation of an unfavourable 8-membered intermediate. Hence cyclopalladated catalysts operate *via* an intra-molecular reaction involving a 6-membered intermediate which ultimately produces the 1,4-addition product.

In order to test the selectivity of their pincer-type catalyst against a standard cyclometallated-type catalyst, the authors screened reaction conditions for the hydrophosphination of diethyl-2-cinnamylidenemalonate, an α,β,γ,δ-unsaturated substrate, with both types of catalyst (**Scheme 48**).

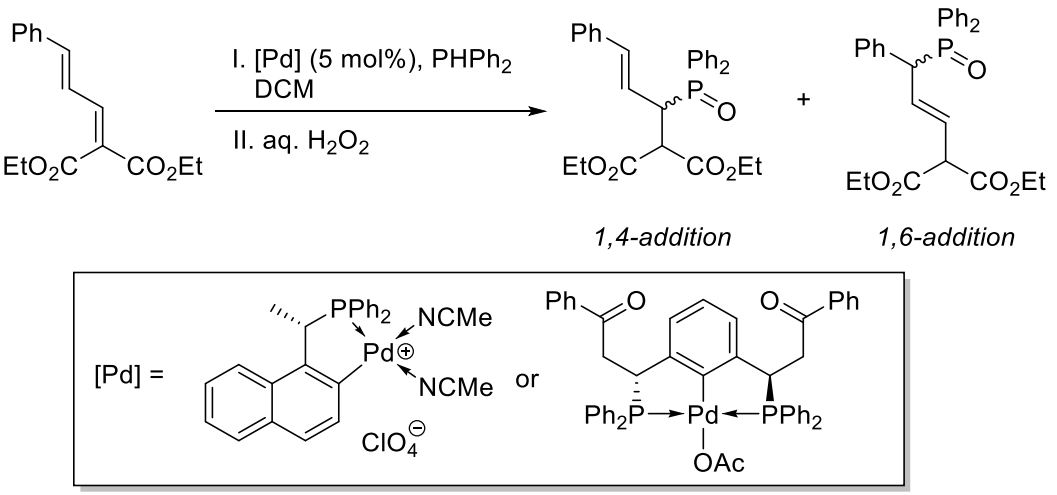

Scheme 48. Selective hydrophosphination with pincer-type and cyclometallate-type palladium catalysts

When the cyclopalladated catalyst was used at −80 °C, only the 1,4-addition product was observed with >99% ee. When the same reaction was performed at room temperature the 1,4-addition product was still the major product (97%), albeit accompanied by a small quantity of the 1,6-addition product. The enantioselectivity of the reaction also decreases with the major enantiomer of the 1,4-addition product being formed in only 55% ee. When performed at 50 °C, the selectivity of the reaction is poor with a ratio of 1,4-addition to 1,6-addition products of 62:38 and very poor enantioselectivity (<40%) for both products.

Conversely when the pincer complex was used at room temperature the 1,6-addition product was obtained as the sole product. The enantioselectivity of this process was poor, affording the major enantiomer in only 38% ee. When performed at −80 °C the

pincer complex afforded the 1,6-addition product in 60% ee, albeit with a small quantity (6%) of the 1,4-addition product, demonstrating a subtle interplay of selectivity and reactivity present in these catalytic systems.

This forms an example of the versatility of the hydrophosphination reaction; in which selection of an appropriate coordination environment on the catalyst alters the selectivity of the reaction for certain products. Pincer-type catalysts for selective hydrophosphination continue to be developed.[80,81]

1.18 Summary

This Chapter presented an overview of phosphines and the traditional methods employed in their synthesis More advanced methods of synthesis were then discussed, including catalytic and enantiospecific routes to phosphines. Applications of these phosphines as ligands in catalysis were outlined.

A gap in the scientific literature was identified for a well-defined method of catalytic hydrophosphination with abundant, cost-effective and environmentally benign metal complexes. The work detailed in this thesis sets out to explore hydrophosphination reactions with iron catalysts and provide a more robust mechanistic understanding of these processes.

2 Catalytic hydrophosphination with simple metal salts

2.1 Overview

This chapter describes the catalytic double hydrophosphination of activated terminal alkynes catalysed by $Fe(HMDS)_2THF$. The x-ray structure of the ethylpropiolate product is presented and a potential mechanism for its formation is presented. The analogous reaction is reported with KHMDS as the catalytic species.

2.2 Catalytic double hydrophosphination of activated terminal alkynes

Following on from the work of Tilley into hydrosilylation we were first interested in the exploration of the commonly used HMDS ligand.[82] In his work, Tilley outlines the use of $Fe(HMDS)_2$ for the room temperature hydrosilylation of a variety of ketones with Ph_2SiH_2 (**Scheme 49**). The HMDS ligand is prevalent across inorganic chemistry and many of their metal compounds were synthesised by Bradley and Lappert from the 1970s onwards.[83] Despite the synthesis of the iron-silyl-amide in 1988, their use for catalysis with iron is only a relatively recent affair.[84]

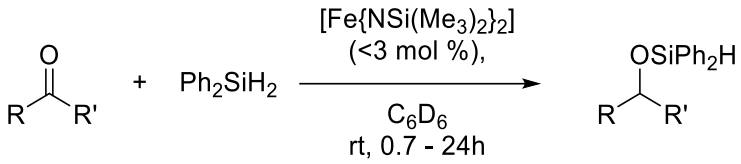

R= Ph, Et, 1-butene, 4-Br-C_6H_4, 4-(NMe_2)-C_6H_4,4-(MeO)-C_6H_4,4-(NC)-C_6H_4
R'= H, Me, Et

Scheme 49. Hydrosilylation with $Fe[N(SiMe_3)_2]_2$

The synthesis of $Fe(HMDS)_2$ was achieved via the reaction of $FeBr_2(THF)_{1.5}$ with KHMDS followed by an inert atmosphere distillation according to the procedure outlined by Power (**Scheme 50**).[83]

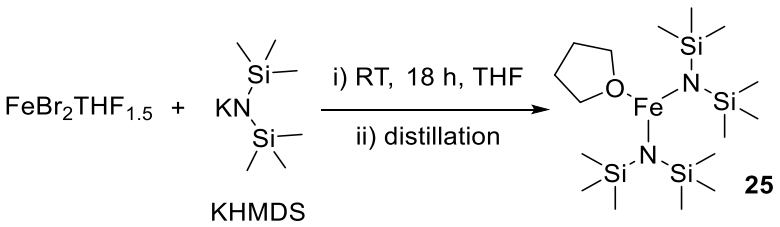

Scheme 50. Synthesis of $Fe(HMDS)_2THF$

To capitalise on the newfound catalytic reactivity discovered by Tilley and co-workers, multiple hydrophosphination reactions with $Fe(HMDS)_2THF$ were attempted (summarised in **Table 1**).

It was quickly established that whilst this compound was ineffective for the hydrophosphination of styrene, the hydrophosphination of alkynes was possible. There are several possible configurations for the final product of this system (**Scheme 51**).

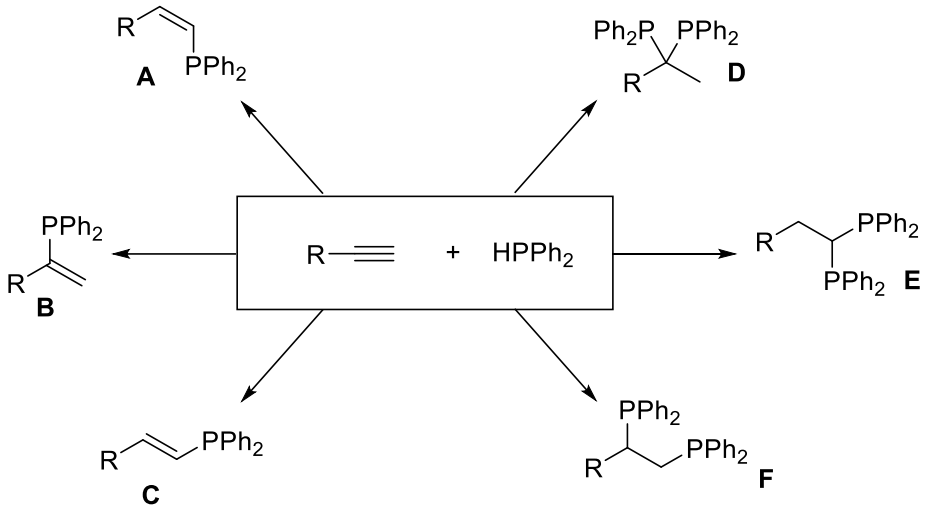

Scheme 51. Possible hydrophosphination products for alkynes

Following an optimisation procedure of temperature, catalyst loading and screening of substrates, it was found that only highly activated alkynes, such as ethyl propiolate, were active in the reactions. Not only was HP possible, but upon increasing the catalyst loading the unexpected formation of doubly terminally substituted product was observed. A solvent screen revealed that this reactivity was only seen in certain solvents.

Table 1. Solvent screening with $Fe(HMDS)_2THF$

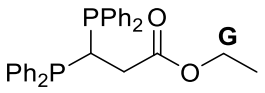

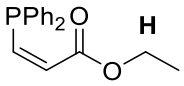

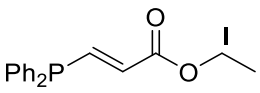

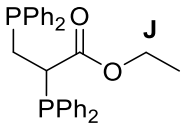

Entry	Conditions	Product
1	neat	**H**
2	DCM	**G/H**

3	THF	**H**/*multiple unidentified products*
4	MeCN	**G/H/J**
5	C_6H_6	**H**
6	neat[b]	**H/I**

Conditions: alkene (1.04 mmol, 1.82 eq), $HPPh_2$ (0.57 mmol, 1 eq), $Fe(HMDS)_2THF$ (0.5 mol%)), solvent (0.35 mL), rt, 24 h, using 1,2-DCE as a standard

The 1,1-diphos product (**E**, **Scheme 51**) could be formed exclusively under mild reaction conditions (**Table 1**).

Table 2. Substrate screening with $Fe(HMDS)_2THF$

Entry	Substrate	Conditions	Product	Spectroscopic Yield
1	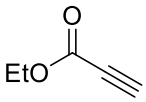	1 mol% [Fe]	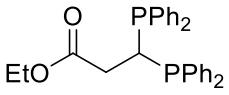	32 %
2	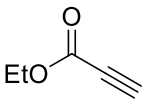	5 mol% [Fe]	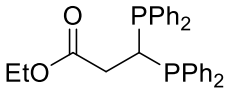	54 %
3	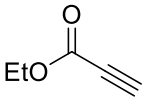	10 mol% [Fe]	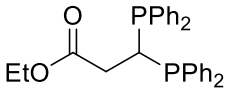	87 %
4	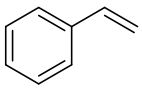	0.5 mol% [Fe]	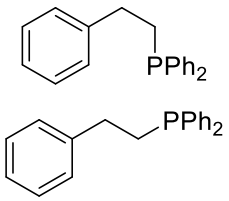	*no reaction*
5	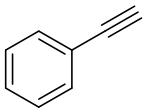	0.5 mol% [Fe]	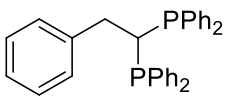	*no reaction*

Conditions: alkyne (1.04 mmol, 1.82 eq), $HPPh_2$ (0.57 mmol, 1 eq), [Fe] = $Fe(HMDS)_2THF$, MeCN (0.2 mL), rt, 24 h, using 1,2-DCE as an internal standard

Increasing the catalytic loading enabled the preferential synthesis of the terminal product in high yields (**Scheme 52**).

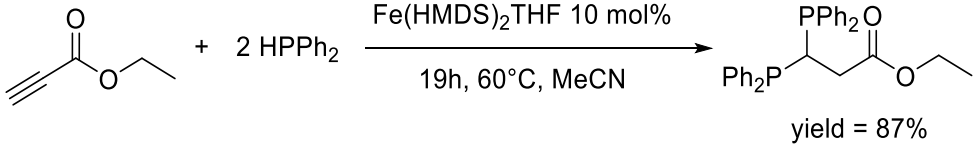

Scheme 52. Catalytic synthesis of 1,1-Diphos with $Fe(HMDS)_2THF$

The pure 1,1-diphos product of ethylpropiolate was purified and crystallised in DCM with the crystal structure revealing the PCP angle of 103.60°.

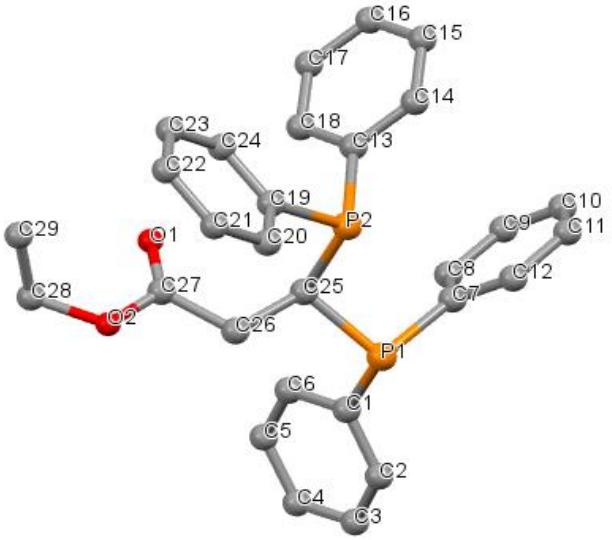

Figure 11. Crystal structure of 1,1-diphos

Higher temperatures resulted in greater yields, but with 3 Eq of propiolate required for reasonable reactivity, this also resulted in further singly substituted product. This further suggests the formation of the singly substituted product is a limiting factor in the synthesis of the doubly substituted product – indicating that the stepwise addition mechanism may be the at play in this catalytic reaction. A radical clock reaction showed no indication of radicals in the reaction solution, which proceeded as normal.

No cyclotrimerization products were present in the hydrophosphination reactions performed, indicating that hydrophosphination is favoured over cyclotrimerisation.[85] Poisoning studies performed by Wangelin and co-workers using PMe_3 indicate that $HPPh_2$ could perform a similar role in our studies. In our hands, cyclotrimerization reactions were unsuccessful under similar conditions – at present the reason for this is unclear, however, the choice of toluene as a solvent (versus MeCN) may be the key factor in the success of Wangelin.

It was found that KHMDS was also an effective catalyst for this reaction (**Scheme 53**).

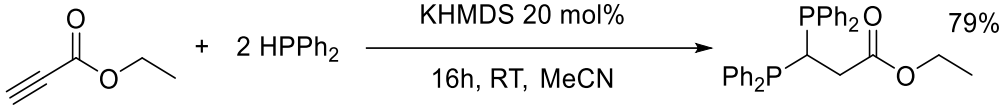

Scheme 53. Synthesis of 1,1-Diphos

A screening of substrates revealed similar levels of activity with KHMDS. Increased catalyst loading was required for KHMDS, however, this is clearly an advantageous route to these bisphosphine products as they do not require the synthesis and purification of $Fe(HMDS)_2THF$ (with challenging inert atmosphere distillation). Indeed, KHMDS is generally readily available in synthetic inorganic laboratories.

Table 3. Substrate screening with KHMDS

Entry	Alkyne	Product		Isolated Yield
1	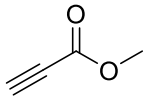	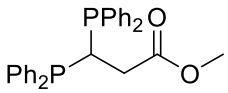	**36a**	86%
2	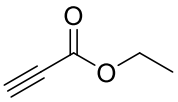	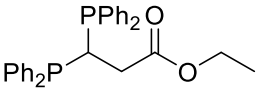	**36b**	79%
3	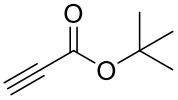	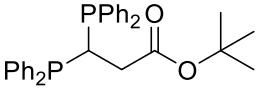	**36c**	72%
4	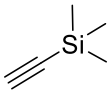	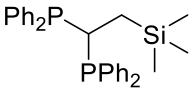		*no reaction*
5	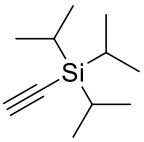	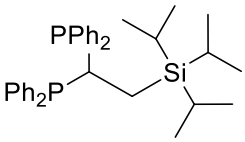		*no reaction*
6	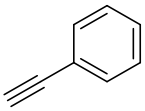	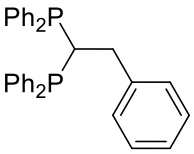		*no reaction*
7	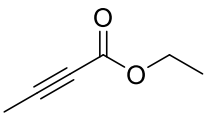	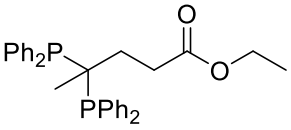		*no reaction*

General reaction conditions: substrate (0.5 mmol), $HPPh_2$ (174 µL, 1 mmol), KHMDS (20 mol%), rt, 16 h, using 1,2-DCE as a standard

The only example in the literature of using a metal complex for this kind of reactivity is seen in the templated synthesis of a ligated system.[86] The stoichiometric formation of the bisphosphine utilised a palladium template which was removed at the end of

the reaction by addition of HCl, eliminating chirality by allowing free rotation of the phosphine moiety, followed by KCN. As this is a stoichiometric method to access these phosphines, it is extremely costly when compared with the iron or base catalysed system.

The addition of NEt_3 in the templating reaction of Leung's invention must not be overlooked – a series of reactions with catalytic amounts of base were performed. In the case of NEt_3, little reactivity was observed.

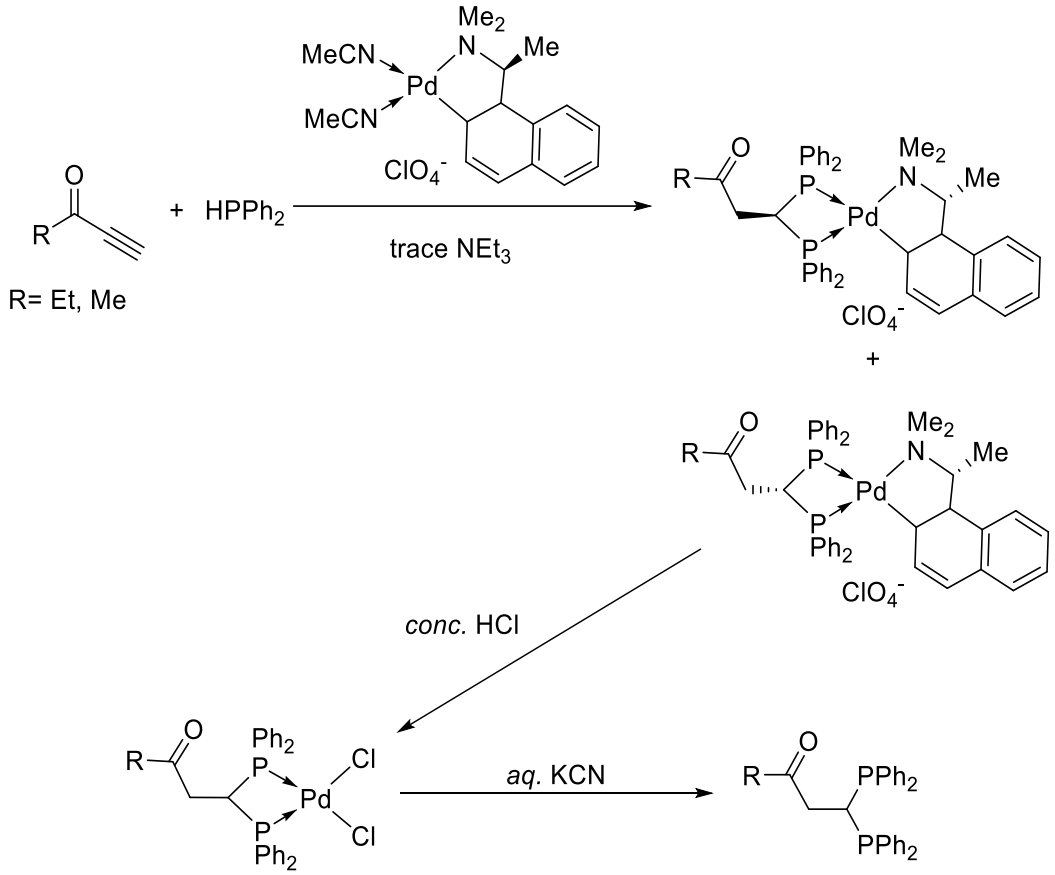

Scheme 54. Palladium-templated synthesis of a terminal bisphosphine

The narrow bite-angle phosphines formed in these reactions have huge potential as ligands for catalysis. Indeed, similar PCP ligands have already found use in a wide variety of catalytic reactions.[87–92] Utilising a catalyst for the synthesis of these narrow bite-angle phosphines opens the door to far greater tunability of these ligand systems and improved atom economy in comparison to traditional methods of synthesis.[93,94]

Several possible mechanisms may be invoked to explain the formation of the 1,1-diphosphine products.

Starting from $Fe(HMDS)_2THF$, reaction with an alkyne may take place to afford complex **26**. This may be followed by the addition of two equivalents of phosphine (in the form of two diphenyl- or one tertraphenyldi- phosphine respectively). Due to the

prevalence of tetraphenyl diphosphine formation in iron based HP systems and the formation of a small quantity of dehydrocoupling product observed in the reaction mixture in early optimisation, initially the possibility of addition of the dehydrocoupling product adding directly to the alkyne was explored (**Scheme 55**).

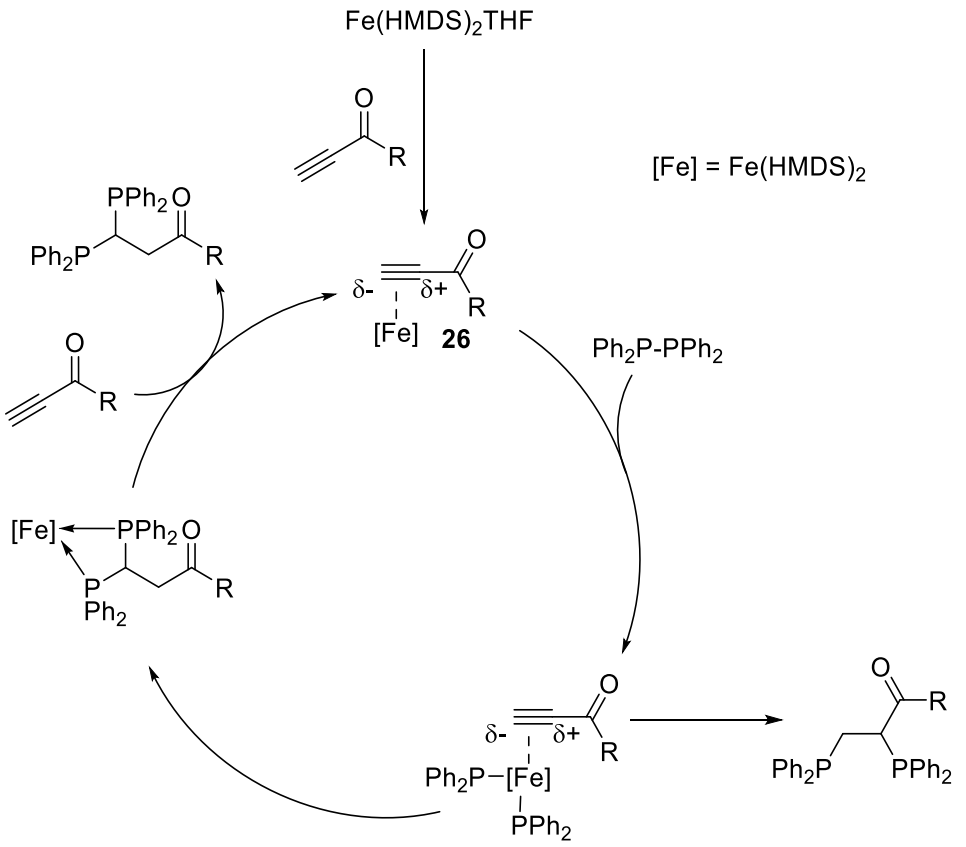

Scheme 55. Potential mechanism of tetraphenyldiphosphine mediated terminal hydrophosphination

The simplest way to determine the involvement of tetraphenyl diphosphine was by isolation of a pure sample of this compound and its addition to the reaction mixture in place of diphenylphosphine. Formation of the terminal phosphine was not observed via ^{31}P NMR, implying that this is not a part of the catalytic cycle. Interestingly though, addition of tetraphenyldiphosphine does result in the appearance of the 1,2-diphosphine – suggesting that not only is this compound not involved in the catalytic cycle, but that its addition goes via an alternative reaction pathway associated with Markovnikov alkane product.

Further to this, the standard catalytic reaction was performed under 1 atm of hydrogen as this has been seen to suppress dehydrocoupling activity.[95] No adverse effect on the catalytic production of 1,1-diphos was observed.

Via $^{31}P\{^{1}H\}$ NMR a triplet phosphine signal was observed next to the much larger singlet of $HPPh_2$ at -39 ppm. This is attributed to the formation of $DPPh_2$ in the reaction mixture – with exchange taking place with the deuterated NMR solvent.

The reaction of diphenylphosphine oxide was also attempted with ethylpropiolate, however this was deemed to be ineffectual. Further, reactivity of $HPCy_2$ was tested in this system in place of $HPPh_2$, to no avail.

Addition of the independently prepared singly substituted *Z*-alkene in place of ethylpropiolate resulted in the formation of the terminal phosphine product**.** The ability of the *Z*-alkene phosphine to enter the catalytic cycle could indicate a stepwise mechanism (**Scheme 56**), as seen previously in the works of Nakazawa and Kays (**Chapter 1**, **Section 1.13** and **1.15**, respectively).

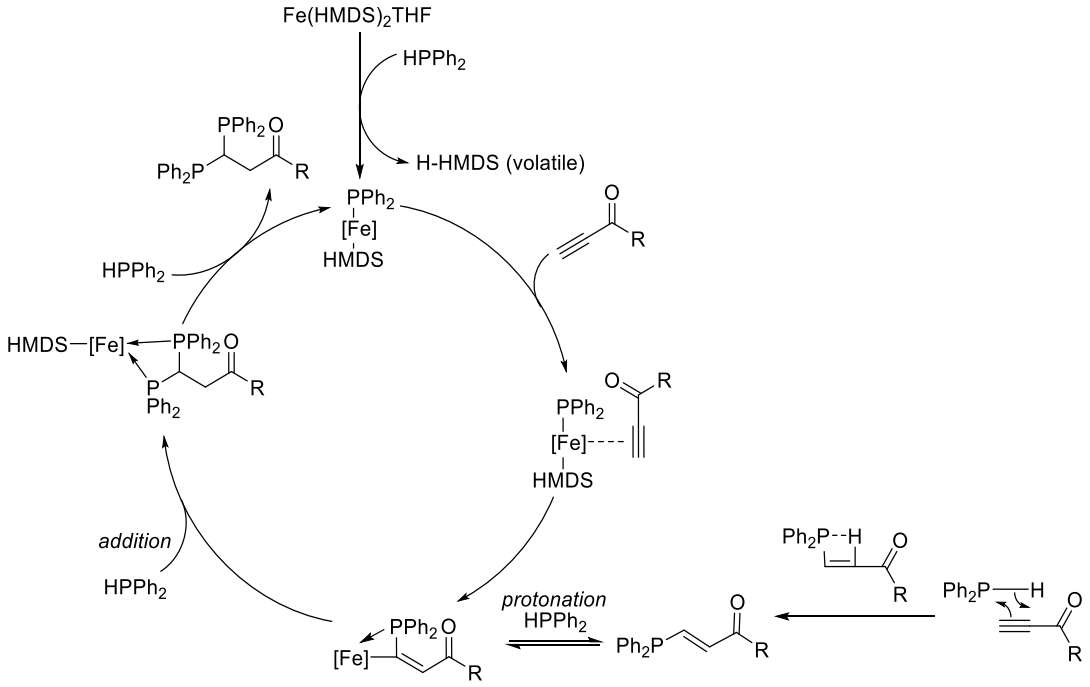

Scheme 56. Potential mechanism of hydrophosphination of ethylpropiolate

2.3 Summary

The work contained in this chapter described the catalytic double hydrophosphination of activated terminal alkynes to give doubly terminally substituted diphosphine products. The reaction was found to be successful only for activated substrates, while less activated alkynes such as phenylacetylene were shown to be unreactive. A potential mechanism for the double hydrophosphination reaction was presented, supported by experimental observations. The same reactivity was observed when KHMDS was used as the catalytic species for several alkyl propiolates.

3 Iron catalysed hydrophosphination using μ-oxo compounds

3.1 Overview

This chapter describes the synthesis of several iron complexes with simple ligand sets (salen and porphyrin) and their application in the catalytic hydrophosphination of alkenes with $PHPh_2$. Both catalytic systems are optimised and assessed for their substrate scope and functional group tolerance. Changing the phosphine used to PH_2Ph allows for thermal hydrophosphination of alkenes. Further hydrophosphination of these singly substituted phosphines was investigated using μ-oxo-bis(N,N'-ethylenebis(salicylideniminato))iron(III). The synthesis of enantiopure chiral phosphines is investigated.

3.2 Hydrophosphination with iron-salen

Salen and its derivatives are widely used as ligands in organometallic chemistry with many of these being commercially available. Synthesis of the simplest possible salen pro-ligand is a straightforward condensation reaction between salicaldehyde and ethylenediamine (**27**, **Scheme 57**) in EtOH. After two hours at reflux, the solution is cooled with ice water and **27** crashes out as a yellow crystalline solid which may then be filtered and washed with cold EtOH to purify. It is produced in good yield (77%).

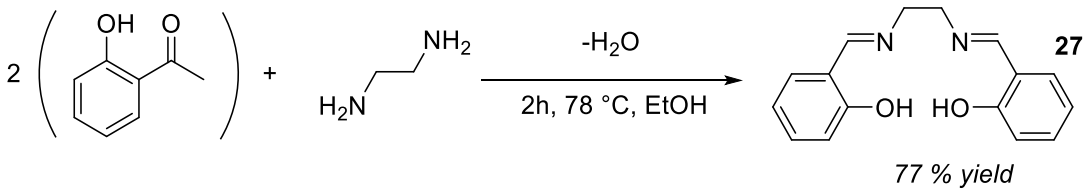

Scheme 57. Synthesis of salen ligand **27**

Reaction of **30** with $Fe(OAc)_2$ open to air produced an oxo-bridged metal complex (**28**, **Scheme 58**). Upon addition of $Fe(OAc)_2$ to **27**, there is an immediate observation of a dark red solution indicative of the formation of complex **28,** however, to ensure high yield and purity of the final complex the EtOH solution is heated to reflux for two hours before filtering and washing with cold EtOH. Complex **28** was produced in good yield (72%) and high purity. This was confirmed by IR with an oxo-bridging stretch observed at ~ 850 cm^{-1}, elemental analysis and a crystal structure. Complex **28** has previously been used for the catalytic cyclopropanation of olefins.[96]

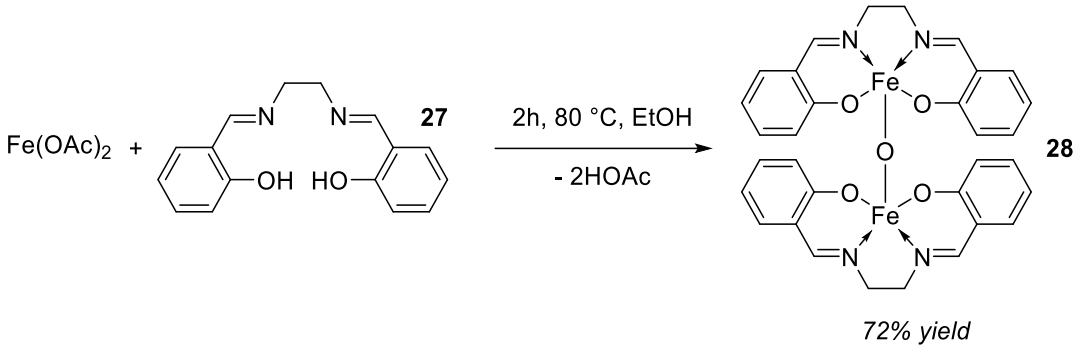

Scheme 58. Synthesis of Fe^{III}_2-μ-oxo(salen)$_2$ (**28**)

Previous syntheses of this compound have all used $FeCl_3$ as a starting point. This generally requires skilful handling as it is more likely to lead to impurities of $Fe^{III}Cl$(salen) in the final product (*e.g.* Nguyen *et al.* report the need to use methanol distilled over $Mg(OMe)_2$ to produce a clean product and also required addition of triethylamine).[96]

Synthesis of **28** also prompted the subsequent synthesis of the Fe^{II}(salen) analogue under an inert atmosphere. This compound was found to be highly air-sensitive and required careful handling, but due to its low solubility, proved easily isolable (**29**, **Scheme 59**). The compound's identity was confirmed by IR and elemental analysis. Unfortunately, due to its poor solubility, an X-ray crystal structure of **29** could not be obtained. The sensitivity of this compound is well documented, and it has been suggested that this has hampered its use in catalysis. One review suggests that it should be approached from the corresponding Fe_2Mes_4, however, this does not seem necessary.[97] There also seems to be some level of confusion in the literature as to which compound has been synthesised - in some cases the μ-oxo seems to have been used in subsequent reactions without the authors' awareness.[98]

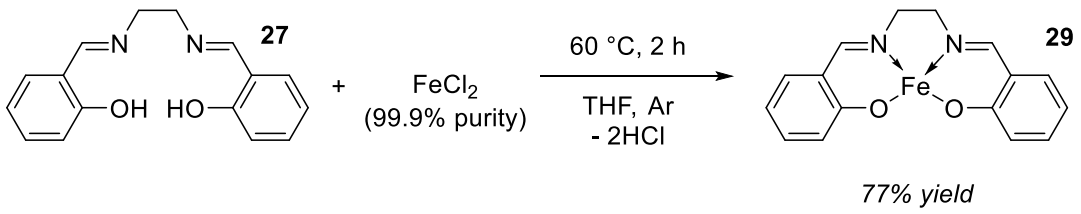

Scheme 59. Synthesis of Fe(salen) (**29**)

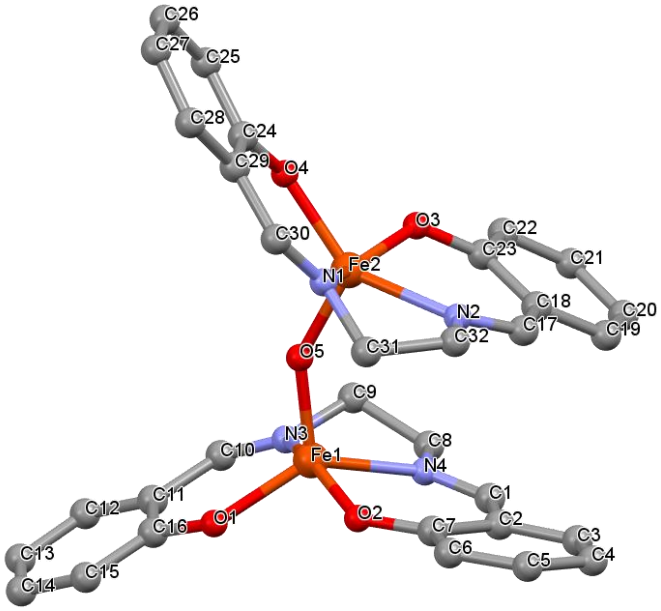

Figure 12. Crystal structure of **28**, μ-oxo-bis(N,N'-ethylenebis(salicylideniminato))iron(III)

The solid-state structure of **28** shows two inequivalent Fe centres bridged by a μ-oxo group O(5) with an angle of 146.37(1)˚. The five-coordinate Fe(1) centre is best described as having a distorted square-based pyramidal geometry with the μ-oxo ligand occupying the apical position and the two oxygen and two nitrogen atoms of the κ⁴-salen ligand occupying the basal plane (τ = 0.3375), according to the method outlined by Addison and co-workers.[99] The Fe(1) atom is displaced from the least-squares plane of the O(1)-O(2)-N(4)-N(3) plane by 0.581 Å. Fe(2) has a similar five-coordinate geometry and analogous connectivity to Fe(1) but shows significantly less distortion and is closer in structure to a true square-based pyramidal geometry (τ =0.1542). The Fe(2) atom is displaced from the least-squares plane of the O(3)-O(4)-N(1)-N(2) plane by 0.602 Å.

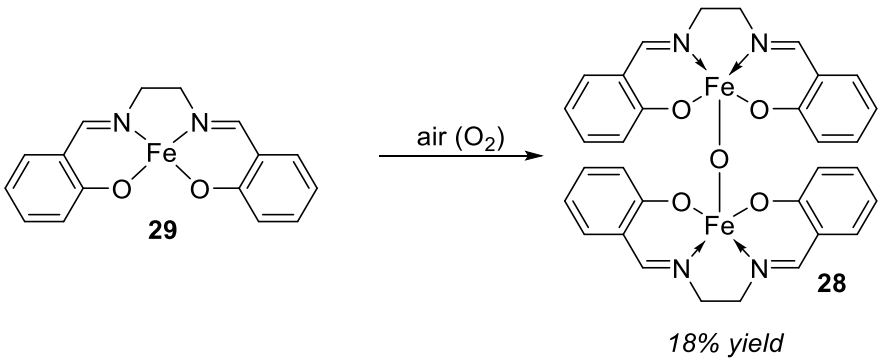

Scheme 60. Oxygen activation by Fe^{II}(salen) (**29**) to Fe^{III}_2-μ-oxo(salen)$_2$ (**28**)

The activation of O_2 was observed for **29** to give **28** (**Scheme 60**). This is a common motif in early transition metal complexes and is observed commonly in salen-type

metal complexes. The potential implications of this observation, which has not been explored with such a simple ligated iron complex, will be discussed in the future work section. However, some relevant examples do exist in the field of small molecule activation.[100,101] For example, Houser *et al.* have reported the synthesis of an N_3O_2 pentadentate ligand and its coordination to an Fe(II) centre.[102] They demonstrate the reactivity of this complex with molecular O_2 which affords the oxo-bridged diiron(III) complex.

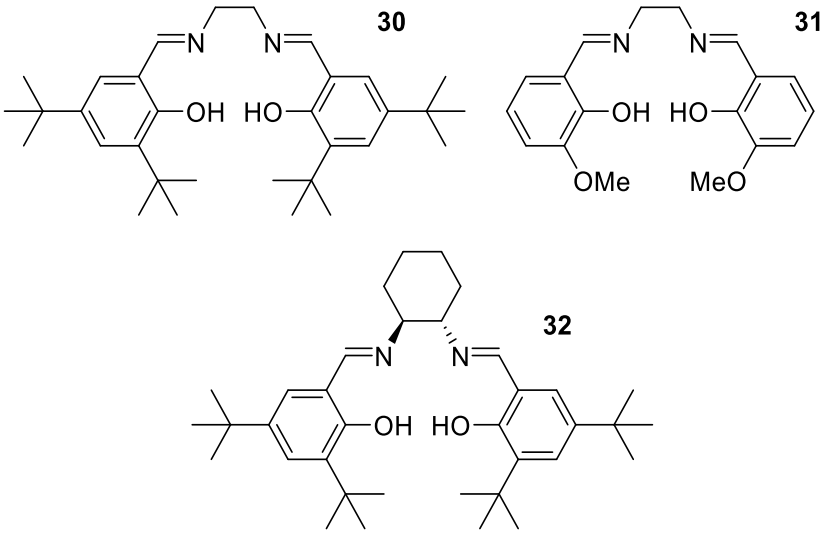

Figure 13. Salen ligand derivatives

Following the same procedure as for the synthesis of salen (**27**), ^{t}Bu-salen (**30**) and MeO-salen (**31**) may be synthesised. Along with **27**, Jacobsen's ligand is a frequently invoked ligand motif (**32**, **Figure 13**). Jacobsen's ligand is commonly used in a manganese system for the asymmetric epoxidation of alkenes.[103] The synthesis is slightly more complex than the simpler salen derivatives, requiring the use of K_2CO_3 and gradual addition of the benzaldehyde for the condensation to take place, as well as a more involved post-synthetic work up. Pure Jacobsen's pro-ligand was obtained as a yellow powder in good yield (76 %) (**Scheme 61**).

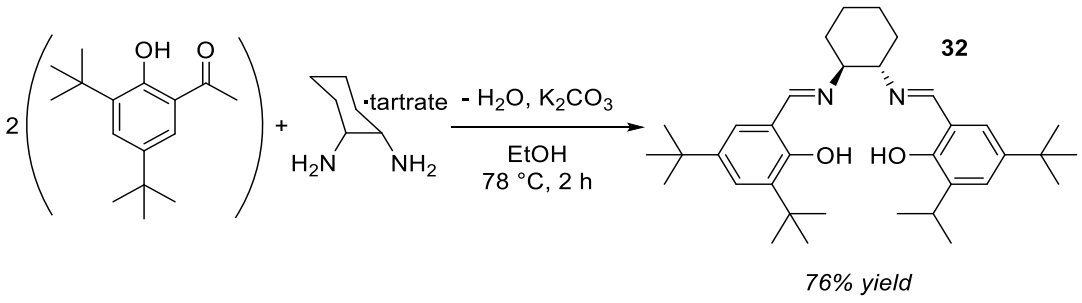

Scheme 61. Synthesis of Jacobsen's ligand (**32**)

Reaction of salen derivatives **30** and **32** with $Fe(OAc)_2$ gave the corresponding μ-oxo complexes (**Scheme 61 and 62**). In the case of **31**, the reaction did not proceed cleanly and was therefore discarded.

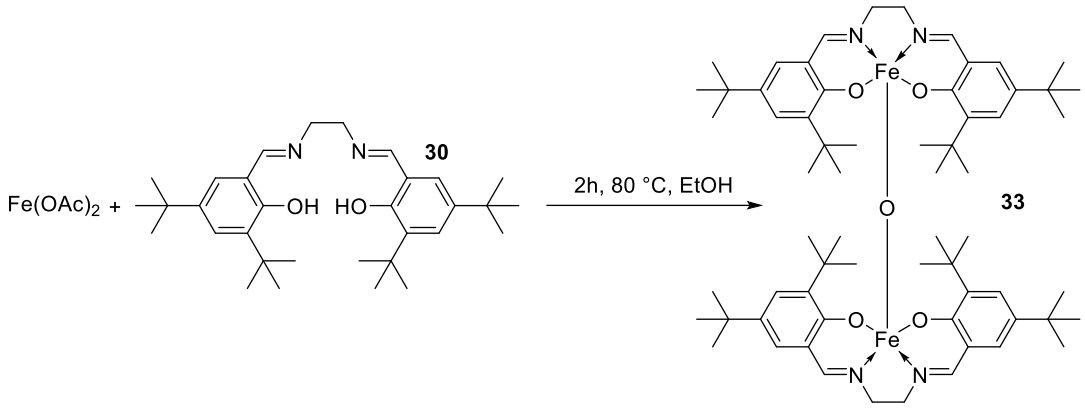

Scheme 62. Reaction of **30** with $Fe(OAc)_2$

An IR spectrum revealed an oxo-bridging stretch similar to that of **28** at ~ 850 cm^{-1}, for both **33** and **34** (*vide infra*).

The use of a chiral ligand system may allow access to a variety of highly valued chiral products. Evidence from Gaumont and co-workers showed that Fe(III) produced the Markovnikov product from the HP of styrenes and diphenylphosphine, therefore complex **34** (**Scheme 63**) was prepared with the hope of accessing unprecedented enantiopure Markovnikov HP selectivity with iron.

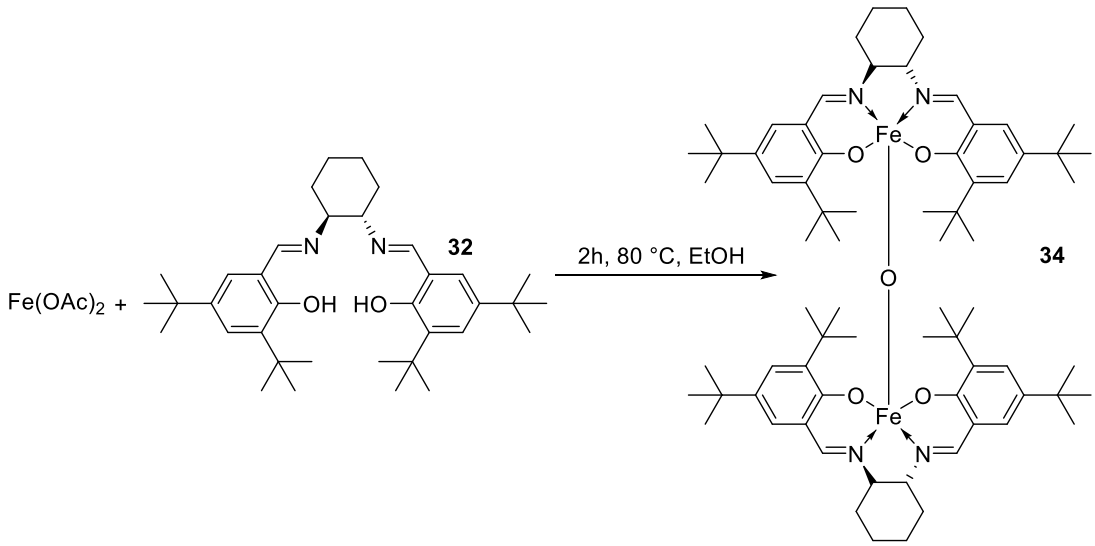

Scheme 63. Reaction of **32** with $Fe(OAc)_2$

Table 4. Ligand screening with iron

Entry	Complex	Conditions	Spectroscopic Yield, **18** (%)
1	**33**	60˚C, 18h	67 %[a]
2	**34**	60˚C, 18h	66 %[a]
3	**31** + $FeCl_3$	rt, 16h	82 %[b]

Conditions: styrene (1.04 mmol, 1.82 eq), $HPPh_2$ (0.57 mmol, 1 eq), Solvent (0.35 mL), spectroscopic yield only. 1,3,5-trimethoxybenzene used as standard.[a] **37** (54 mg, 15 mol%), Carried out at 60˚C, 18h. [b] **37** (18 mg, 5 mol%), rt, 16h.

Although synthesis of an Fe (**30**) metal-ligand complex was unsuccessful, it was found that *in situ* addition of ligand with $FeCl_3$ resulted in the formation of anti-Markovnikov product – essentially switching off the Markovnikov selectivity observed by Gaumont and co-workers with unligated $FeCl_3$. In any event, screening of these salen-metal complexes in the simple AM hydrophosphination of styrene to generate **18** (**Scheme 64**) with diphenylphosphine revealed positive results in the formation of the anti-Markovnikov product for all complexes

It was determined that due to the relative ease of synthesis of **28** and equivalently high yields for hydrophosphination in all cases, that screening of only **28** for functional group tolerance was necessary.

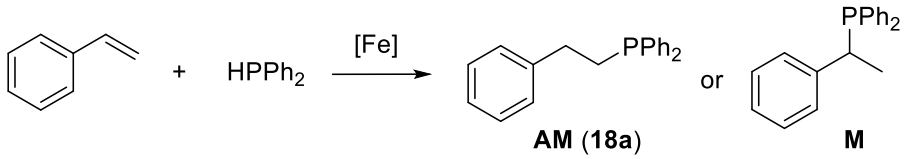

Scheme 64. Generalised HP transformation with possible products

Variations in solvent for this system revealed high tolerance towards a variety of solvents (**Table 5**) and in fact that the reaction may be performed neat. In the interest of ease of study, MeCN was used as the reaction solvent.

Table 5. Solvent screening with Fe^{III}_2-μ-oxo(salen)$_2$

Entry	Solvent	Spectroscopic Yield[a], (%)
1	toluene	76 %
2	dichloromethane	98 %
3	tetrahydrofuran	84 %
4	acetonitrile	89 %
5	methanol	92 %

6	neat	98 %

General reaction conditions: styrene (120 mL, 1.04 mmol, 1.82 equiv.), $HPPh_2$ (100 mL, 0.57 mmol), cat. (0.0029 mmol, 0.5 mol%), 24 h, rt, inert atmosphere.

[a] Yield determined by ^1H NMR spectroscopy using 1,2-DCE as a standard.

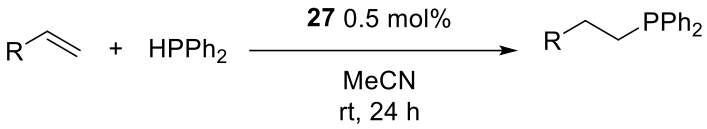

Scheme 65. General hydrophosphination reaction.

Table 6. Substrate screening with Fe^{III}_2-μ-oxo(salen)$_2$

Entry	Alkene	Product		Spectroscopic Yield[a] [Yield][b]
1	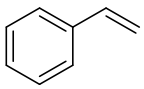	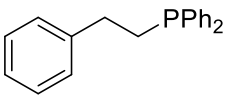	**18a**	100 [89]
2	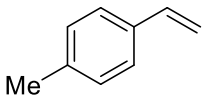	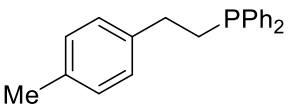	**18b**	96 [79]
3	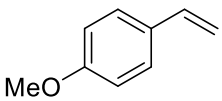	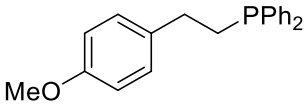	**18c**	97 [89]
4	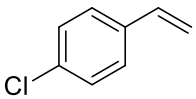	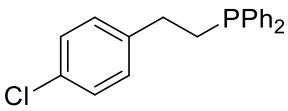	**18d**	100 [74][c]
5	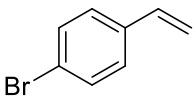	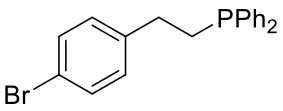	**18e**	82 [65]
6	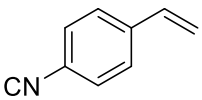	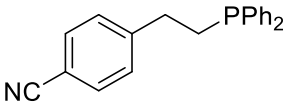	**18f**	93 [43]
7	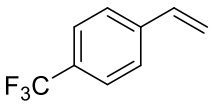	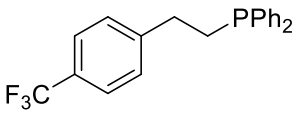	**18g**	85 [83]

8	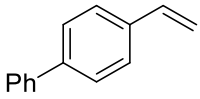	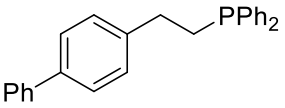	**18h**	85 [58][d]
9	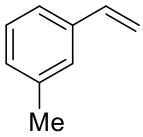	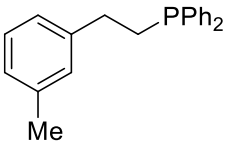	**18i**	100 [95]
10	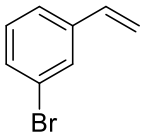	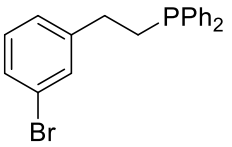	**18j**	98 [98]
11	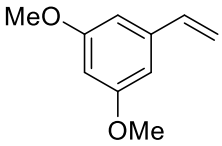	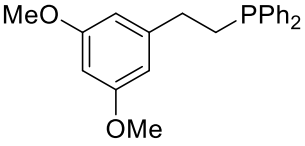	**18k**	[89]
12	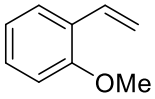	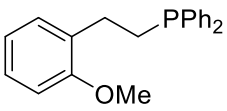	**18l**	87 [62]
13	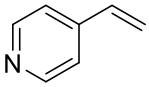	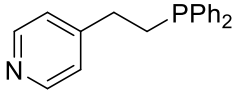	**18m**	80 [75][e]
14	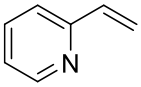	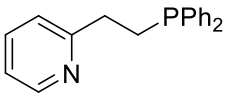	**18n**	92 [86][e]
15	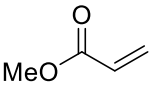	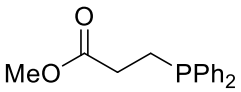	**18o**	80 [69]
16	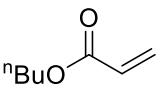	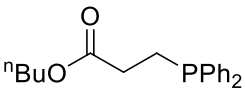	**18p**	93 [76]

General reaction conditions: alkene (1.04 mmol,1.82 equiv), $HPPh_2$ (100 mL, 0.57 mmol), cat. (0.0029 mmol, 0.5 mol%), neat or MeCN(0.35 mL), 24 h, room temperature,under argon.

[a] Reaction performed in MeCN (350 mL). Spec.Yield = spectroscopic yield, determined using ^{1}H NMR spectroscopy with 1,2-DCE as a standard.

[b] Isolated yield [%] given in square brackets.

[c] Reaction performed neat, spectroscopic yield determined using ^{1}H NMR spectroscopy with 1,2-DCE as a standard. Isolated yield [%] given in square brackets.

[d] At 114 h.

[e] At 60°C.

[f] For 72h.

Variation of functional groups on the phenyl ring shows the wide substrate scope of this reaction. The catalyst is effective for electron withdrawing groups on the ring (entries **18d**-**18g** and **18k**, **Table 6**). The catalyst is also effective for electron donating groups on the ring (entries **18b**, **18c** and **18l**, **Table 6**). Both **18c** and **18l** are capable of donating electron density through the ring structure. The steric effects from the proximity of the OMe functional group to the HP reaction centre is therefore the major influence in its reactivity and thus steric hindrance results in a lower yield for the *ortho*-OMe group, **18l**. Halides are also tolerated, with no evidence for dehalogenation. 2- and 4-vinyl pyridine also undergo hydrophosphination, although this is markedly slower that the equivalent styrene, taking 72 h to reach approximately equivalent yields (entries **18m** and **18n**, **Table 6**). This is likely due to coordination of the newly formed P,N ligand to the Fe-centre; these compounds are known to be good ligands.[32] The catalytic system is also active for ^{n}Bu- and Me- acrylate substrates (entries **18o** and **18p**, **Table 6**).

Unsuccessful hydrophosphination reactions are outlined in **Table 7**. After 24 h at room temperature, no products were observed in the case of 4-NH_2 styrene (**18q**, **Table 7**) This is believed to be due to the irreversible coordination of nitrogen to the sterically exposed Fe centre. Alkynes were tested in this system - namely diphenylacetylene and phenylacetylene (entries **18r** and **18s**, **Table 7**), however, even at 80 °C over 24 h, no hydrophosphination product was observed. As discussed previously with alkynes, coordination to the catalytic metal center and deactivation is more likely than with alkenes. α-Methyl styrene was also tested (entry **18t**, **Table 7**), giving a very low yield at rt - which could not be improved with heating or increased reaction time. The reaction is likely to be hindered by the additional steric bulk now present at the reaction centre in comparison to styrene. Equivalently *trans*-β-methyl styrene gave no reaction at rt (entry **18u**, **Table 7**). Nor did *trans*- or *cis*-stilbene give any HP products (entries **18x** and **18w**, **Table 7**). Reactions attempted with 1-hexene and allyl benzene (entries **18y** and **18v**, **Table 7**) gave small quantities of phosphine product at rt over 24 h. These were not improved over longer reaction times and reduced to zero upon increasing the temperature. These alkenes are not as activated as styrenes and hence less susceptible to nucleophilic attack. The straightforward hydrophosphination of styrene was also attempted with different phosphines - Cy_2PH and $CyPH_2$, however, no products were observed either at rt or upon increasing to 60°C in either case. These Cy-based phosphines are less able to stabilise electron density via delocalisation than their phenyl-phosphine counterparts and therefore act as stronger nucleophiles. The result of this is the formation of a stronger bond with the Fe centre which inhibits subsequent attack on the styrene double bond. In support

of a potential mechanism (Chapter 4), products seem to be limited to Michael acceptors.

Table 7. Challenging substrate screening for Fe^{III}_2-μ-oxo(salen)$_2$

Entry	Alkene	Product		Spectroscopic Yield
1	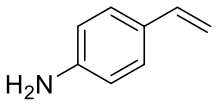	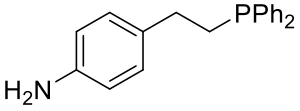	**18q**	*no reaction*
2	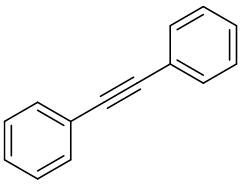	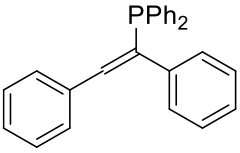	**18r**	*no reaction*
3	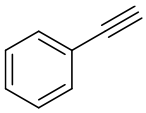	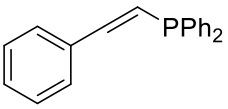	**18s**	*no reaction*
4	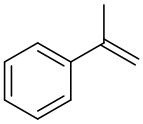	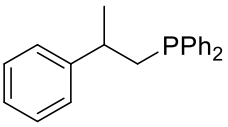	**18t**	trace
5	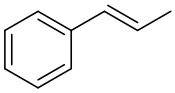	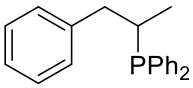	**18u**	*no reaction*
6	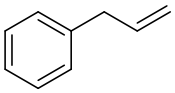	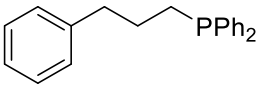	**18v**	trace
7	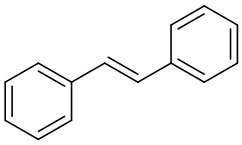	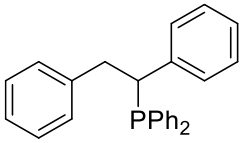	**18w**	*no reaction*

8	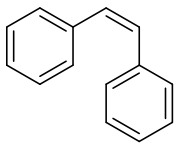	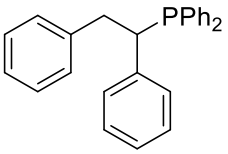	**18x**	*no reaction*
9	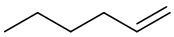	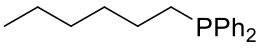	**18y**	trace

Conditions: alkene (1.04 mmol, 1.82 eq), $HPPh_2$ (0.57 mmol, 1 eq), **37** (1.8 mg, 0.5 mol%), MeCN (0.35 mL), using 1,2-DCE as a standard

The turnover frequency for the formation of **18a** over the initial 30 minutes is 80 h^{-1}, slowing to 33 h^{-1} after 3 hours at which point the reaction is 43% complete. It is therefore unnecessary to leave all reactions for the full 24 h reported, unless maximising the yield is of key importance to the experimentalist.

An unusual result was obtained from the reaction with cinnamyl chloride (**Scheme 66**).

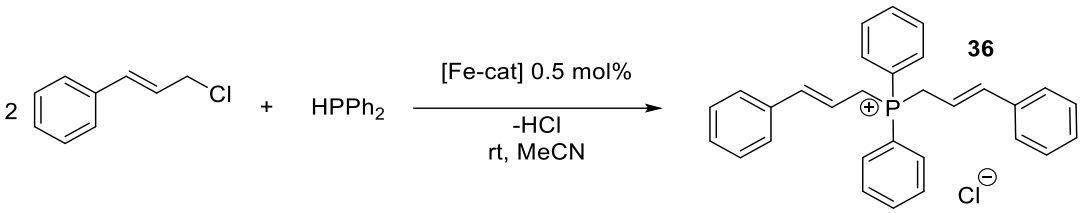

Scheme 66. Reaction of $HPPh_2$ with cinnamyl-Cl

The unusual product formed with cinnamyl chloride, **36** (**Scheme 66**) is likely due to an S_N2 reaction of the phosphine with the styrene.

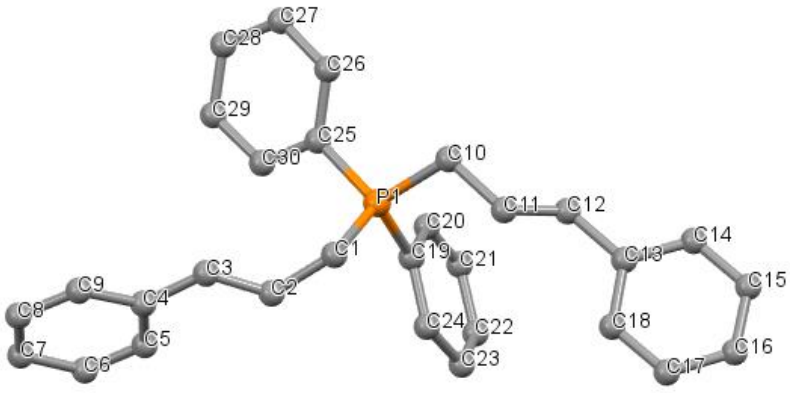

Figure 14. Crystal structure of **36**, Cinnamyl-PPh_2 (counter-ion omitted for clarity)

It was determined to be of value to also test Fe^{II}(salen), **29**, for HP activity. Interestingly, at room temperature, no product was observed for the general HP

reaction. Upon addition of base to the HP reaction with **29**, good yields of HP product were observed (**Table 8**).

Table 8. Hydrophosphination reactions with **29** and base

Entry	Base	Conditions	Spectroscopic Yield **18a**
1	NaO^tBu	2 mol%	20 %
2	NaO^tBu	1 eq	66 %
3	NaO^tBu	1 eq, no catalyst	12 %
4	NaO^tBu	1 eq base, 1 eq cumene	87 %
5	NEt_3	1 eq	6 %
6	-	no catalyst	trace

Conditions: alkene (1.04 mmol, 1.82 eq), $HPPh_2$ (0.57 mmol, 1 eq), **39** (1.8 mg, 1 mol%)), MeCN (0.35 mL), rt, 24 h, using 1,2-DCE as a standard

Upon addition of stoichiometric quantities of diphenylphosphine to **29**, no hydride signal was observed in the ^1H NMR. Which suggests the reaction does not proceed *via* oxidative addition of diphenylphosphine to **29**, with formation of an unstable Fe(IV) complex. These results support the mechanism outlined in **Chapter 4, Section 4.8**, where the formation of an iron-phosphido complex is the initial step in the catalytic cycle. This is supported, in part, by the observations made in **Table 8**, where proton abstraction from $HPPh_2$ is necessary for the HP transformation to take place.

3.3 Hydrophosphination with iron-porphyrin

Further exploration of ligand set was determined to be of value, the preservation of the μ-oxygen moiety was of particular interest for further studies as well as exploration of N-ligands for hydrophosphination. It was determined that the Fe^{III}_2-μ-oxo(porphyrin)$_2$ (**37**, **Figure 15**) embodied these desired features and hence made an ideal candidate for further study.

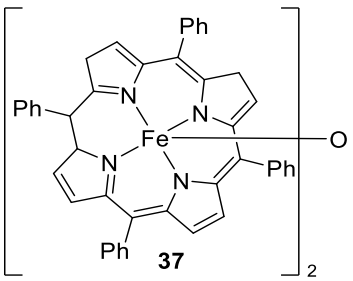

Figure 15. Fe^{III}_2-μ-oxo(porphyrin)$_2$, **37**

Table 9. Solvent screening with *Fe^{III}_2-μ-oxo(porphyrin)$_2$*

Entry	Solvent	Spectroscopic Yield[a], (%)
1	toluene	70
2	dichloromethane	98
3	tetrahydrofuran	88
4	acetonitrile	84
5	pentane	65
6	ethanol	35
7	neat	96

General reaction conditions: styrene (120 mL, 1.04 mmol, 1.82 equiv.), $HPPh_2$ (100 mL, 0.57 mmol), **38b** (0.0029 mmol, 0.5 mol%), 24 h, rt, inert atmosphere.

[a] Yield determined by ^{1}H NMR spectroscopy using 1,2-DCE as a standard.

As no mechanistic studies were planned for this system, it was determined that DCM should be used for further reactivity studies due to the high yield given with styrene (likely due to the solubility of this otherwise low solubility precatalyst).

Once again, variation of functionality on the phenyl ring of styrene resulted in a wide scope of accessible products. The catalyst is effective for electron withdrawing groups on the ring (entries **18c**-**18h**, **Table 10**) as well as for electron donating groups on the ring (entries **18b** and **18c**, **Table 10**).

In the case of **18h**, *ortho*-Me, a reduced yield was seen in comparison to **18b,** *para*-Me, this is attributed primarily to steric effects over electronic effects. Additionally this reduction in yield was seen for entry **18i** versus **18e** – with overall yield being lower in comparison to the catalytic reaction with Fe^{III}_2-μ-oxo(salen)$_2$ (**Table 10** entries **18i** and **18e** respectively) as may be expected when using the bulkier more rigid porphyrin ligand in comparison to the salen ligand.

Halides are well tolerated, with a lower reaction time being noted for para-Cl and pyridyl substrates (**Table 10** entries **18d**, **18l** and **18m** respectively) when using *Fe^{III}_2-μ-oxo(porphyrin)$_2$* versus *Fe^{III}_2-μ-oxo(salen)$_2$*. A lower temperature is required in the case of para-phenyl likely due to the higher solubility of 4-Ph-styrene in DCM versus MeCN.

Table 10. Substrate scope for Fe^{III}_2-μ-oxo(porphyrin)$_2$

Entry	Alkene	Product		Spectroscopic Yield[a] [Yield][b]
1	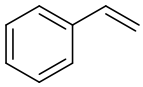	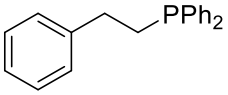	**18a**	96 [73]
2	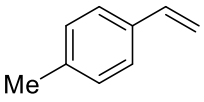	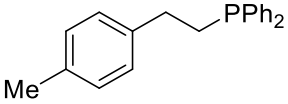	**18b**	[96]
3	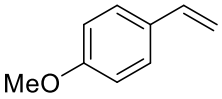	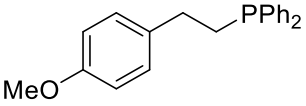	**18c**	75 [71]
4	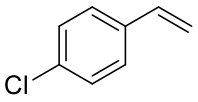	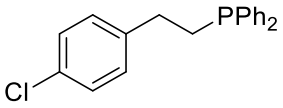	**18d**	83 [72]
5	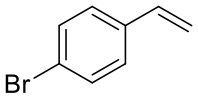	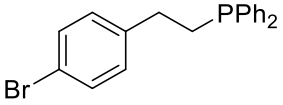	**18e**	85 [67]
6	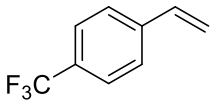	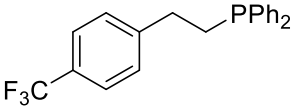	**18h**	[85][a]
7	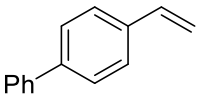	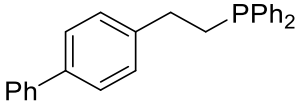	**18i**	75 [35]
8	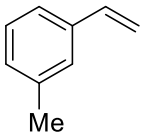	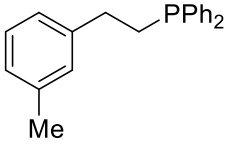	**18j**	[82]

9	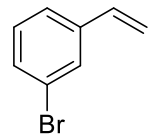	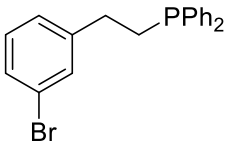	**18k**	96 [62]
10	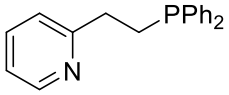	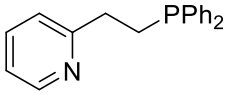	**18l**	79 [71]
11	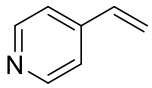	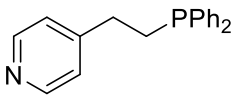	**18m**	75 [72]
12	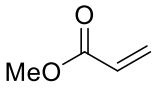	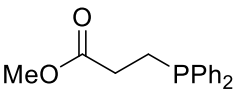	**18n**	79 [71]
13	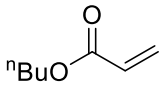	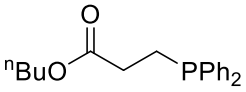	**18o**	99 [74]

General reaction conditions: alkene (1.04 mmol,1.82 equiv), $HPPh_2$ (100 µL, 0.57 mmol), **37** (0.00029 mmol, 0.5 mol%) MeCN (350 µL), 24 h, rt, under argon.

[a] Yield determined using ^1H NMR spectroscopy with 1,2 DCE as a standard.

[b] Isolated yield [%] given in square brackets.

3.4 Hydrophosphination with H_2PPh

In order to explore the limits of this system and the use of primary phosphines in these reactions.

Before this work, the thermal reaction of phenylphosphine with activated alkenes had never been reported. A range of activated substrates were seen to undergo SHP (single hydrophosphination) with minimal conversion to the tertiary phosphine product under these reaction conditions (**Table 11**). Styrenes functionalised in the para-position undergo thermal SHP with only minor amounts of double addition (DHP, where two equivalents of styrene functionalize phenylphosphine furnishing a tertiary phosphine, **Scheme 67**) being observed. EWG and EDG are tolerated, as well as styrenes with a variety of useful functionality. Vinylpyridines undergo hydrophosphination with phenylphosphine, however, this is less selective for the SHP product, with double hydrophosphination taking place readily: 2-vinylpyridine undergoes HP with a 3:2 ratio of SHP:DHP products obtained (**Table 11**, **entry 9**). 4-vinylpyridine gives a poor yield of SHP product, with multiple resonances observed by $^{31}P\{^1H\}$ NMR (**Table 11**, **entry 10**). Acrylates are tolerated under these reaction conditions (entries 11 and 12). Purification of the SHP products, even in the presence of DHP side-products, is straighforward, where the relative volatilities may be

exploited. The reaction mixture is placed under vacuum to remove any unreacted H_2PPh and volatile styrenes, a short path distillation apparatus or cold finger at reduced pressure with gentle heating to 60°C then allows separation of products **38a** to **38l** from any trace DHP product or unreacted, non-volatile, styrenes. Unactivated substrates are unreactive under these conditions; only substrates primed for nucleophilic attack should be used, for example, here use of allylbenzene and 1-hexene resulted in trace amounts of product. Using cyclohexylphosphine in place of phenylphosphine also failed to produce reasonable quantities of product.

Table 11. Substrate scope for Thermal Hydrophosphination with H_2PPh

Entry	Alkene	Product		Spectroscopic Yield[a] [Yield][b]
1	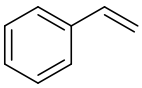	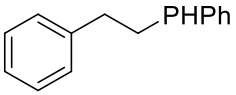	**38a**	61 [53]
2	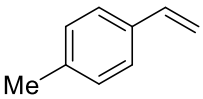	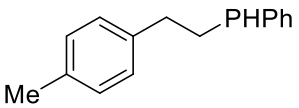	**38b**	44 [40]
3	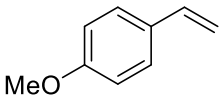	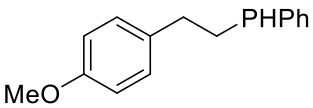	**38c**	82 [70]
4	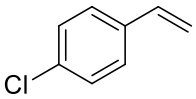	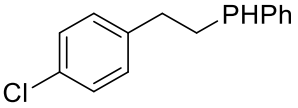	**38d**	76 [66]
5	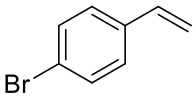	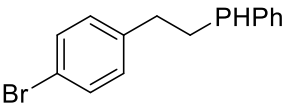	**38e**	93 [78]
6	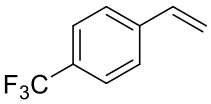	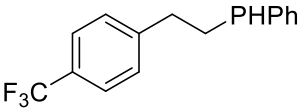	**38f**	60 [55]
7	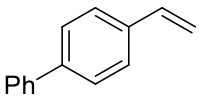	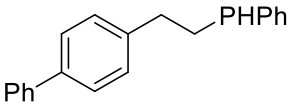	**38g**	79 [76]
8	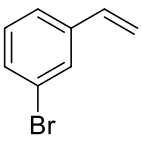	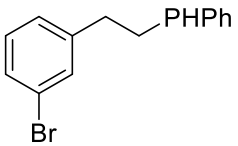	**38h**	76 [61] (34)[c]
9	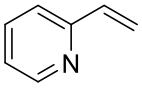	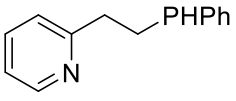	**38i**	60 (40)[c]
10	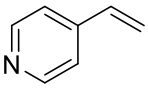	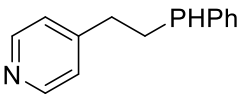	**38j**	35[31]

11	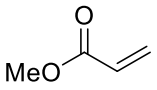	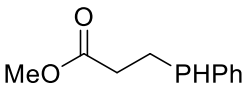	**38k**	81[64]
12	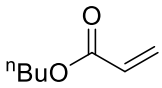	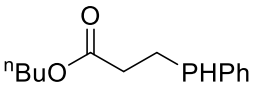	**38l**	74[72]

General reaction conditions: styrene (0.285 mmol, 1equiv.), phenylphosphine (63 mL, 0.57 mmol, 2 equiv.), MeCN (200 mL), 16 h, 80°C, under argon

[a]Yield determined by ^{1}H NMR spectroscopy using THF as a standard.

[b]Isolated yield [%] given in square brackets.

[c]Product of double hydrophosphination observed, spectroscopic yield shown in brackets.

These thermally produced phosphine products, **38a** to **38l,** seemed perfectly setup for introduction into the previously established iron catalysed systems, given their similarity to diphenylphosphine. Indeed, they could undergo iron-catalysed HP in the presence **38b** or **38c**. By alteration of the reaction stoichiometries, the product of double hydrophosphination was observed (**Scheme 34**).

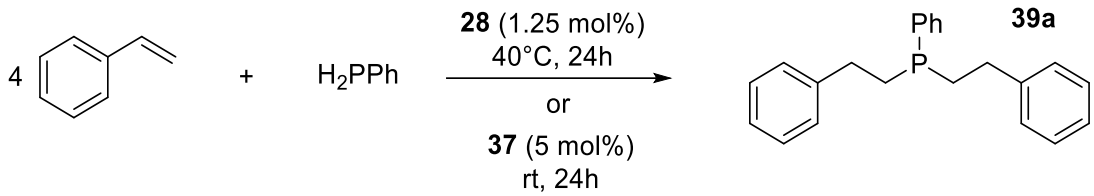

Scheme 67. Iron catalysed reaction of H_2PPh with styrene

This reaction is believed to proceed via thermal SHP and on formation of small amounts of SHP product it is immediately transferred to an iron-catalysed HP cycle where it can undergo DHP, thus helping to drive forward the thermal process. Alternatively, it is possible to undertake thermal SHP at 80°C to afford secondary phosphines, followed by addition of catalyst and further reaction at room temperature to generate products such as **39a**, (**Scheme 67**).Using the one-pot procedure, 1.25 mol% of **37** and heating to 40°C, clean formation of the DHP product was observed, with only small quantities of unreacted SHP product (<15%) and unreacted starting materials. In some Fe-catalysed HP reactions small quantities of side product are observed in the ^{31}P NMR (See **Figure 16** resonance at ~20 ppm, product observed at ~15 ppm and oxidised product also observed at ~30 ppm). These are believed to be products of Michael addition, where styrene starting material undergoes further attack by the HP product.[104]

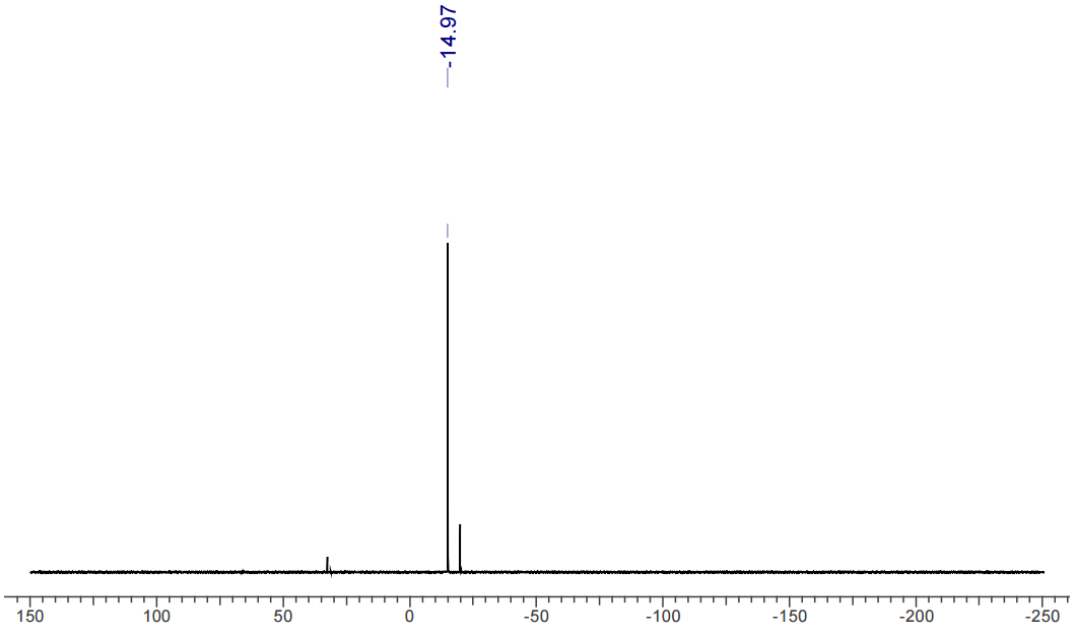

Figure 16. Styrene HP product, product peak labelled

This points towards a potential reaction mechanism which proceeds via a zwitterionic intermediate. The reaction proceeds best neat, with increased concentration likely resulting in more favourable DHP. The catalyst loading was increased in the hope of lowering the reaction temperature; however, the reaction does not proceed cleanly and mixtures of products are seen to form. On the other hand, **28** is an excellent pre-catalyst for DHP at room temperature and, unlike **37**, no side-products were observed at the higher catalyst loading of 5 mol%.

The phosphine products are oils at room temperature, the structure of phosphine **38a** was confirmed by ligation to iron, which is achieved in good yield (65%) by stirring two equivalents of the ligand with $FeCl_2 \cdot THF_{1.5}$ at room temperature in dry THF. Precipitation of the iron complex was observed within minutes and it was isolated by removal of solvent by filtration followed by washing with cold pentane.

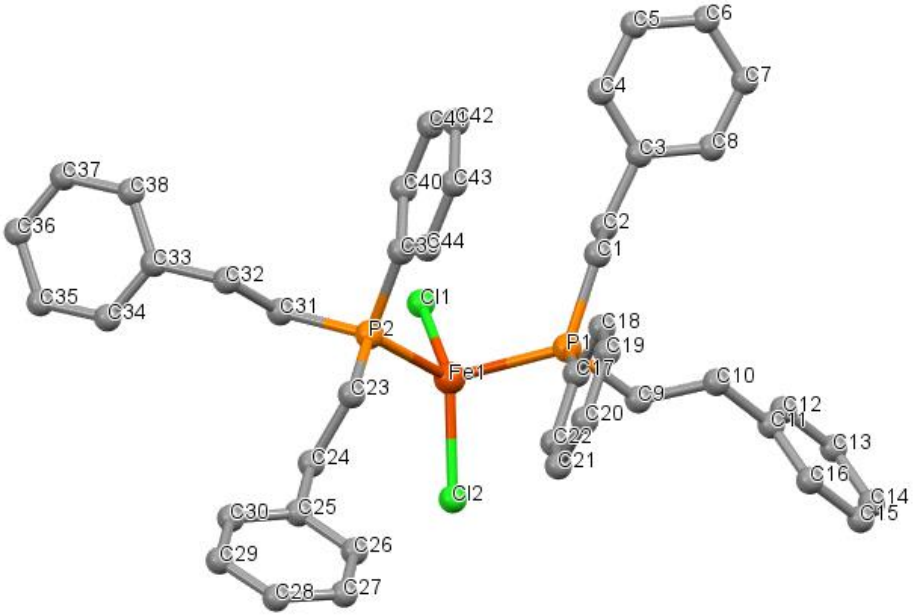

Figure 17. Crystal structure of Fe complex of **39a**

The iron complex (**40**) was obtained as a distorted tetrahedral complex with bond lengths of 2.433(1) and 2.415(1) Å, for Fe-P1 and Fe-P2 respectively and 2.232(1) and 2.238(1) for Fe-Cl1 and Fe-Cl2 respectively.

Table 12. Double hydrophosphination with Fe^{III}_2-μ-oxo(salen)$_2$ **28** and Fe^{III}_2-μ-oxo(porphyrin)$_2$ **37**

Entry	Alkene	Product		Spectroscopic Yield[a] [Yield][b]	
				28	**37**
1	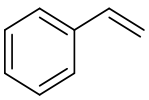	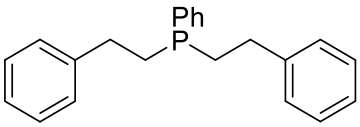	**39a**	66	81[79]
2	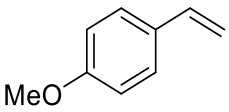	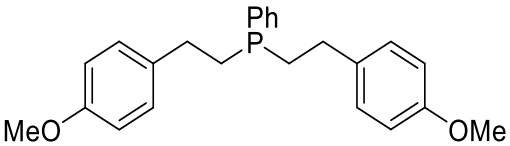	**39b**	30	63[62]
3	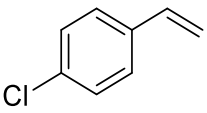	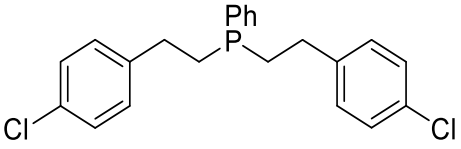	**39c**	78	74[63]
4	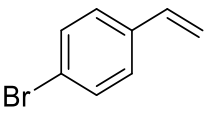	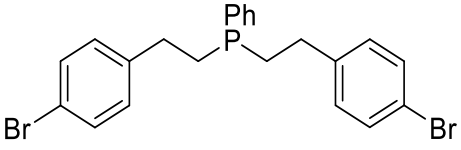	**39d**	60	96 [80]

5		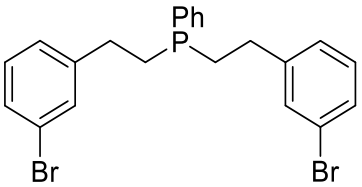	**39e**	58	[82]
6	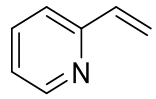	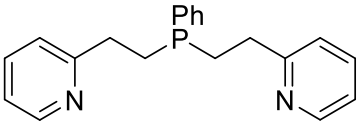	**39f**	36	92 [88]

[a] Conditions: alkene (2.28 mmol, 4 equiv.), H_2PPh (63 µL, 0.57 mmol, 1 equiv.), **28** (1.25 mol%, MeCN (0.35 mL) or **37** (5 mol%), neat, rt – 40 °C, 24 h. 1,2-DCE used as a standard.

[b] Isolated yield given in square brackets.

The potential of this system to access optically active tertiary phosphines seemed promising considering easy access to chiral salen complexes. **38a** could be generated via a thermal reaction, separated and then further reacted under catalytic conditions with an achiral iron precatalyst with a different styrene to produce unsymmetrical phosphine products stereoselectively. These P-chiral phosphines have already found use in asymmetric catalysis applications and as such there is a distinct place for their well-defined synthesis. There are a number of examples of their synthesis in the literature, however, it would be unusual to have an iron catalysed system given literature precedent.[57,76,105–108] Early research form Knowles into asymmetric hydrogenations found use of these stereogenic phosphines.[109]

Jacobsen's ligand, **32**, was once again ligated to iron to yield the desired chiral µ-oxo complex, **34**.

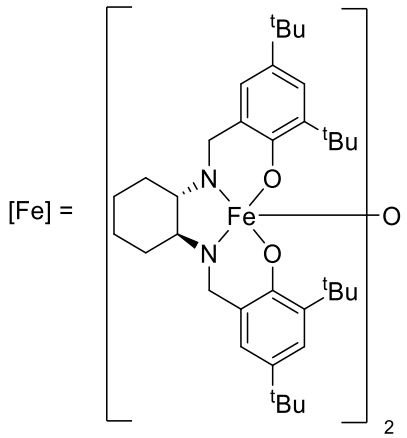

Figure 18. Iron catalyst **34** for unsymmetrical HP

When **38a** was reacted in the presence of two equivalents of 4-chlorostyrene with **34 (**0.5 mol%) at 60°C for 60h, **40** was obtained in 90% yield (**Figure 18**).

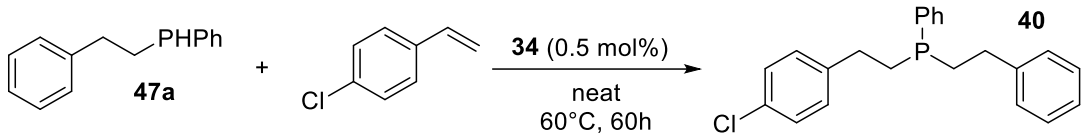

Scheme 68. Iron catalysed unsymmetrical HP

The unsymmetrical phosphine product was formed selectively with only racemic product observed (**Scheme 68**). The isolated and oxidised phosphine product was studied using several tests for chirality. Circular dichroism was used to demonstrate that enantioinduction has not taken place.[110] This could be due to rapid P-inversion at the Fe-centre being more likely at the raised reaction temperature or possibly due to relatively remote stereocentre of the metal complex.[111] Kagan's amide and various lanthanide shift reagents ($Eu(FOD)_3$ and $Eu(hfc)_3$) did not give peak separation for the oxide of **40** by either ^1H or $^{31}P\{^1H\}$ NMR. This is nonetheless a useful method to make unsymmetrically substituted tertiary phosphines.

3.5 Summary

The work contained in this chapter describes the synthesis of an iron catalyst featuring the salen ligand. Under atmospheric conditions, the synthetic procedure yields a bimetallic, oxo-bridged complex (**28**). The presence of the Fe-O-Fe linkage was identified by x-ray crystallography, supported by IR analysis. The same reaction performed under an inert atmosphere yielded the iron(II) salen complex (**29**). The conversion of **28** to **29** is shown to proceed under an atmosphere of air. Several derivatised salen ligands were synthesised and their equivalent Fe-µ-oxo compounds synthesised.

The Fe-µ-oxo compounds were screened for activity towards hydrophosphination of styrene with PPh_2. Since no significant variation in their activity was established, 38 was selected for further study due to ease of synthesis. **28** displayed a wide substrate scope with good functional group tolerance and high yields of phosphine products. Iron(II) salen (**29**) was found to be inactive for hydrophosphination under similar conditions, proceeding only upon addition of a base (NaO^tBu or NEt_3).

Similar studies were conducted with an iron µ-oxo porphyrin complex (**37**). This catalyst gave excellent yields in DCM with a wide substrate scope.

The thermal hydrophosphination of alkenes with a primary phosphine (PH_2Ph) was described. This gave mono addition of the phosphine across the double bond to give terminal phosphino-alkanes.

Double hydrophosphination with 2 equivalents of alkene was shown to proceed with PH_2Ph in the presence of catalytic amounts of **28** or **37**.

An iron-μ-oxo complex of Jacobsen's ligand was synthesised (3X). Catalytic hydrophosphination with 3X gave an asymmetric phosphine, however, no chiral selectivity was observed.

4 Kinetic and Mechanistic Studies of Hydrophosphination with Fe-μ-oxo

4.1 Overview

This chapter describes the kinetic and mechanistic studies of catalytic hydrophosphination with Fe-μ-oxo salen (**28**) with $PHPh_2$

A Hammet study of the catalytic system is conducted to provide insight into the effect of varying substituents (on the phenyl ring of styrene) on relative rates of reaction.

The thermodynamic parameters of the hydrophosphination reaction are determined via Arrhenius and Eyring plots. This study is applied to both the catalysed and uncatalysed hydrophosphination reaction.

Results of these and a number of chemical tests are combined to elucidate a mechanism for the catalytic reaction and a catalytic cycle is proposed.

4.2 Practical considerations for kinetic studies

It was readily apparent in the literature that, although multiple mechanistic pathways for hydrophosphination have been invoked, a comprehensive mechanistic study was yet to be undertaken for an iron catalysed system. It is with this in mind that a thorough kinetic and mechanistic study of the catalytic cycle for hydrophosphination of $HPPh_2$ and styrene with **28** was carried out.

Initial attempts to determine rates proved problematic – within minutes of addition of the final reagent, HP had progressed too far to capture the initial rate of the system. It was therefore necessary to freeze the sample before addition of the styrene via vacuum transfer and defrost the sample immediately prior to loading into the NMR spectrometer.

4.3 Reaction Order

The pre-catalyst, **28**, displays a high level of coordinative saturation which is unlikely to undergo further activation to form an Fe(IV) phosphido complex as the active catalyst. Likewise, reductive disproportionation of **28** from a dimer into two monomers of **29** is unlikely to be the initial step in the catalytic cycle since it was already shown that **29** is not active in catalysis, and only becomes active upon the addition of base. It is therefore useful to determine the order in iron to allow us to generate a speculative catalytic cycle. Reaction monitoring was facilitated by the low loading of **28** used during catalysis. However, it should be noted that increasing the catalyst loading

beyond 1 mol% **28** resulted in poor solubility of the pre-catalyst and a substantial increase in the paramagnetic nature of the NMR spectra, thus the order in iron was determined from the initial rate of reaction at 1.25, 1, 0.5, and 0.25 mol% loadings of **28** (**Figure 19**).

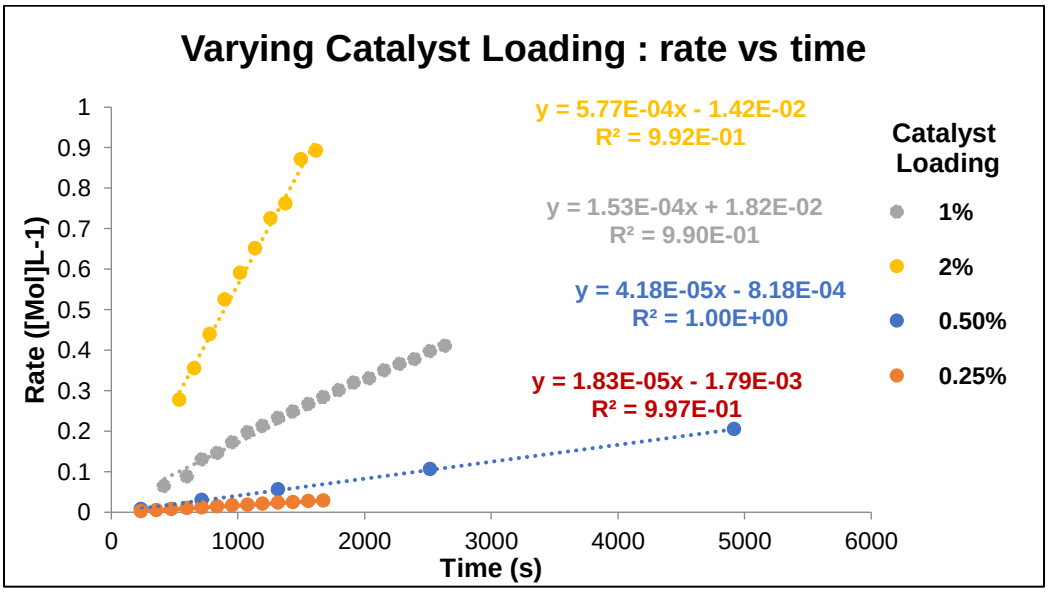

Figure 19. Graph showing initial rate vs time with varying catalyst loading

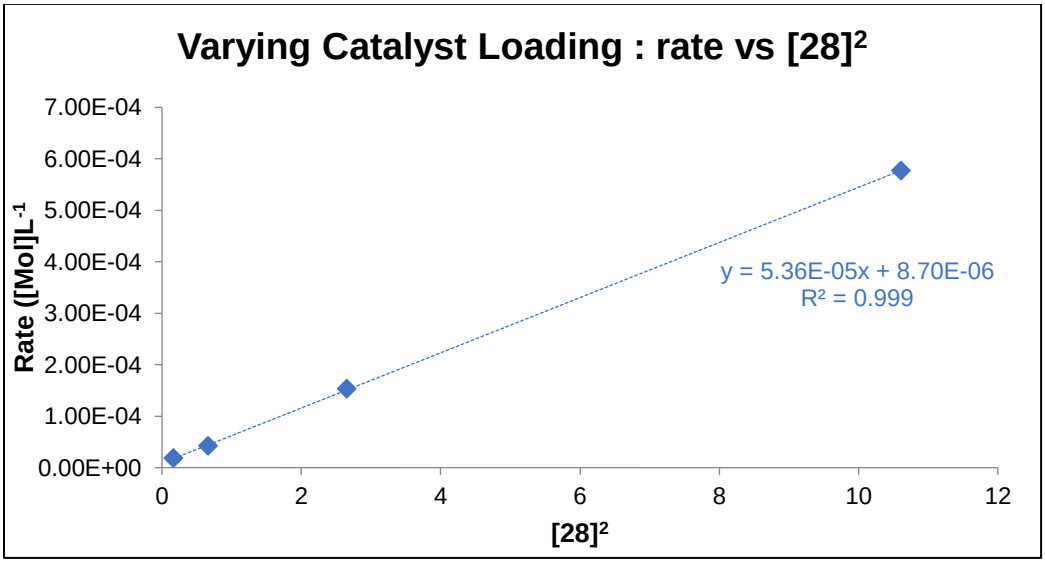

Figure 20. Graph showing initial rate vs [**28**]^2 with varying catalyst loading

Similarly, the reaction order with respect to styrene was determined by plotting the rate of increasing concentrations of styrene.

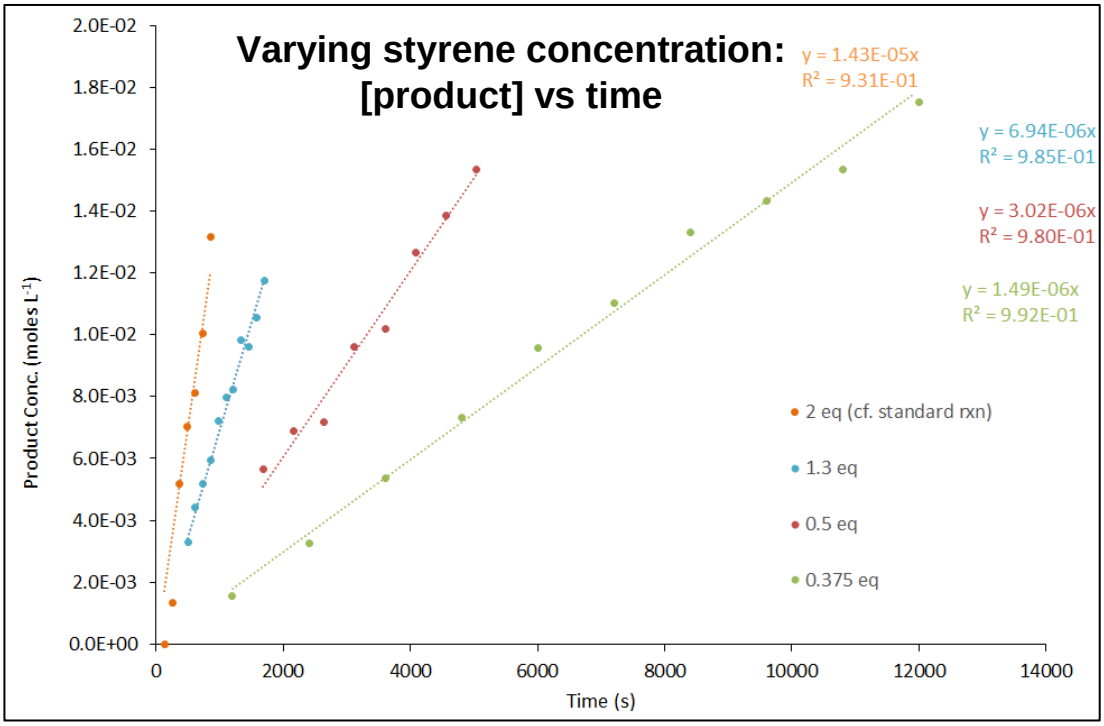

Figure 21. Graph showing increasing concentration of product with time – varying [styrene]

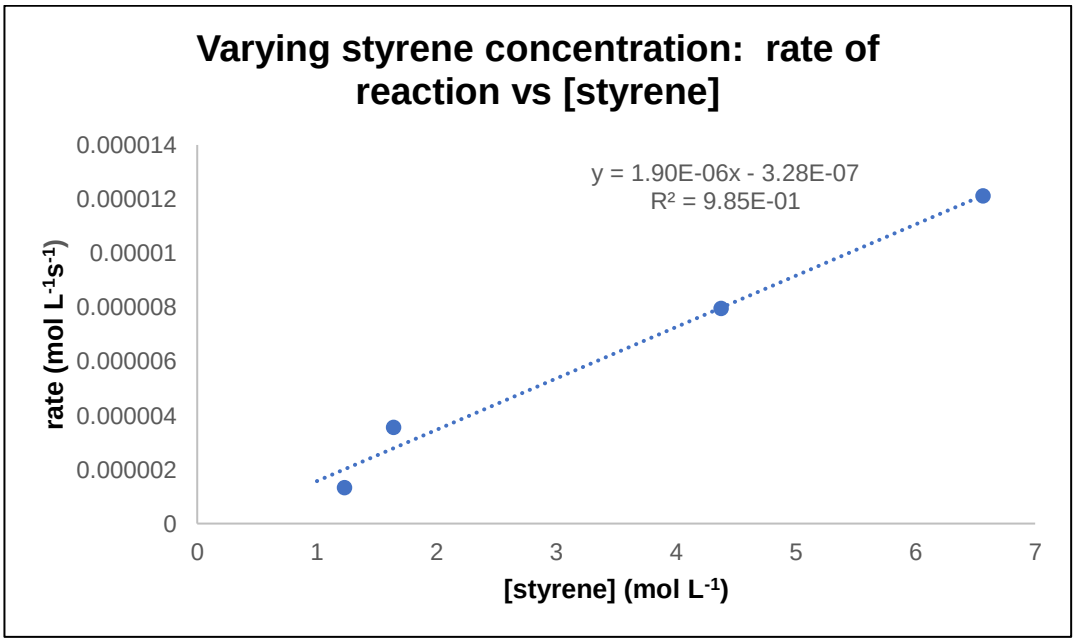

Figure 22. Graph showing initial rate vs [styrene] with varying [styrene]

The rate with respect to $HPPh_2$ was also determined in this manner.

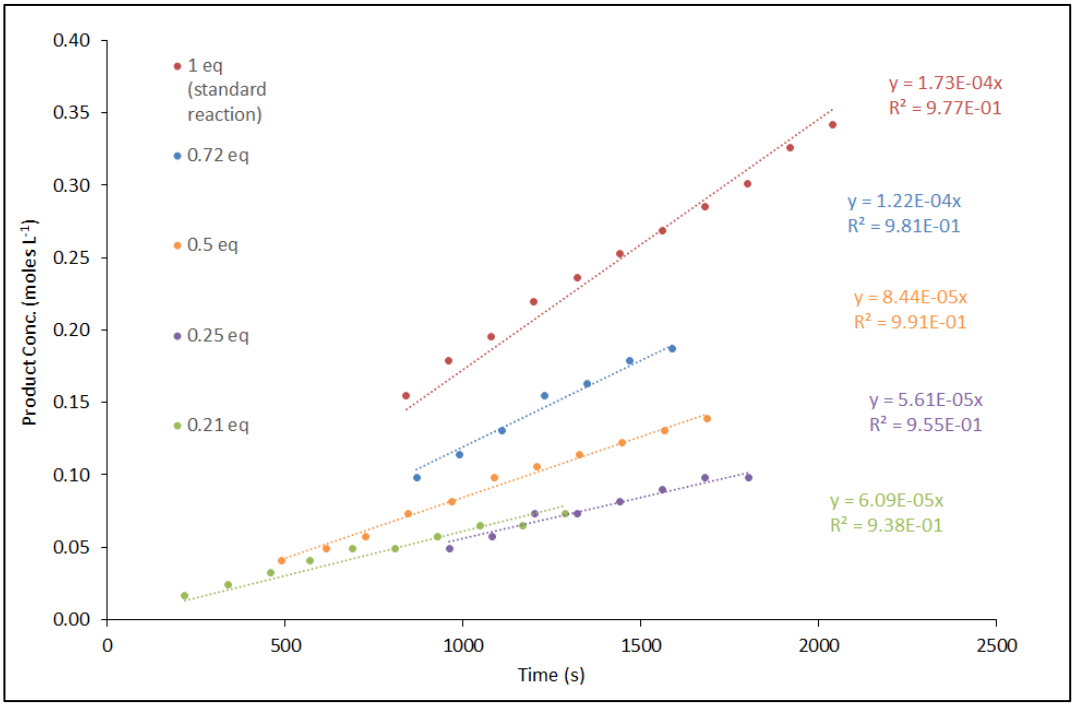

Figure 23. Graph showing initial rate vs [styrene] with varying [$HPPh_2$]

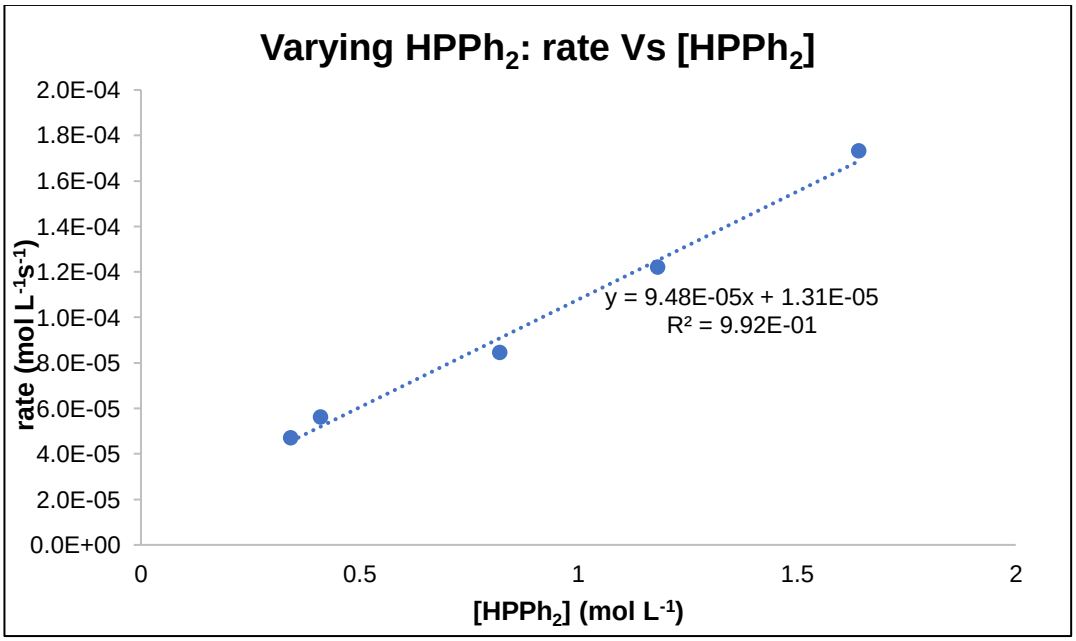

Figure 24. Graph showing increasing concentration of product with time - varying [$HPPh_2$]

The reaction was determined to be 2nd order in catalyst, 1st order in styrene and 1st order in phosphine This allowed for the construction of the rate equation given below;

$$Rate = K[\mathbf{28}]^2[Styrene][HPPh_2]$$

4.4 Hammett Study

It was determined that it would provide great insight to perform a Hammett study on our catalytic system. Varying the R substituent on styrene (**Scheme 69**) and monitoring the resulting rate of reaction enabled us to construct a Hammett plot as follows.

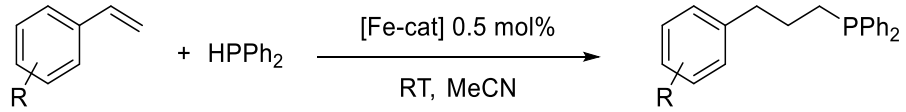

R = 4-MeO, 4-Me, 4-CF_3, 4-Br, 3-Me, 4-CN, 4-H

Scheme 69. General hydrophosphination scheme with R-substituent

In each case the R-substituted styrene was added to the frozen reaction solution already containing the catalyst, solvent and phosphine. The sample was defrosted just before placing in the spectrometer to ensure that the rate of reaction was determined from the initial rate (**Figure 25)**. The earliest data point collected is dependent on the time taken for the instrument to lock and shim. This is particularly seen with electron withdrawing substrates - longer times required to successfully lock and shim potentially suggesting the formation of a high concentration of a transient paramagnetic species in these cases. The gradient of each set of points gives the rate of reaction for various substituted styrenes. As backward extrapolation of these points gives a zero intercept there can be reasonable confidence that these are representative of initial reaction rate.

A Hammett plot (**Figure 26**) may be constructed from these data according to the equation:

$$\sigma\rho = log\frac{X}{H}$$

Where:

σ is the substituent constant for each substituted styrene

ρ is the reaction constant (determined from the gradient of a plot of $log\frac{X}{H}$ vs σ)

X is the rate of reaction for each substituted styrene

and H is the rate of reaction for unsubstituted styrene.

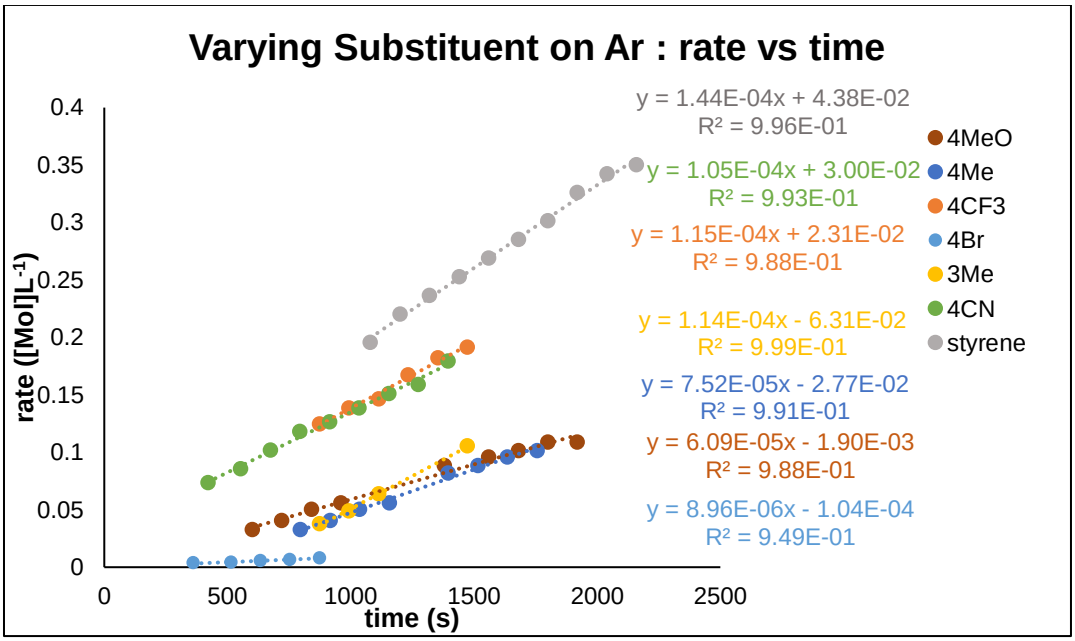

Figure 25. Graph showing the increase in concentration of HP product over time for R-substituted styrenes.

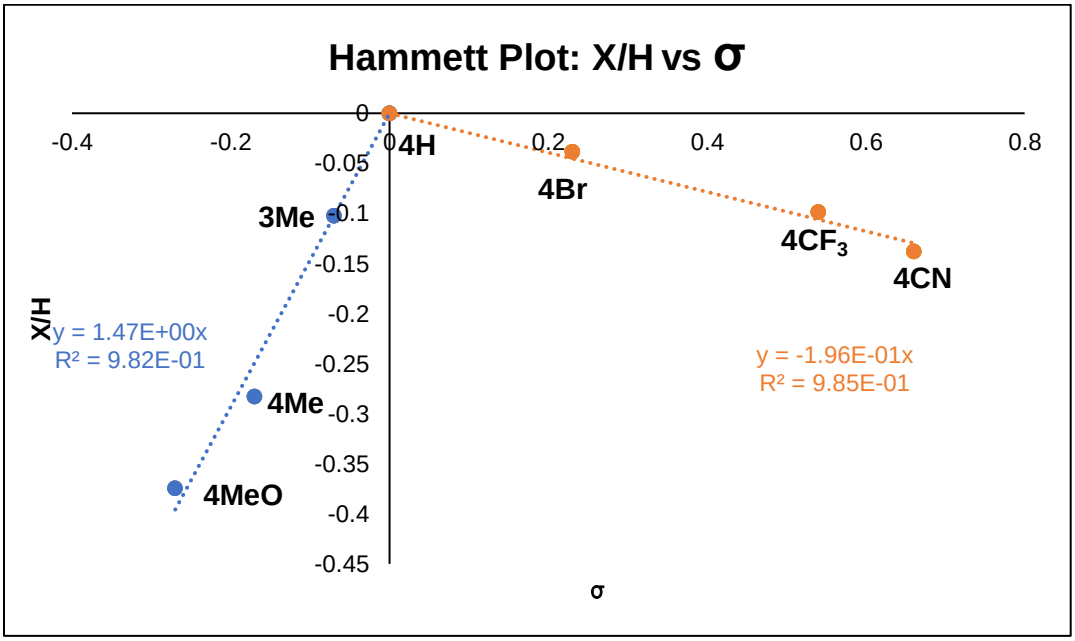

Figure 26. Hammett plot of styrene substituted with EDGs and EWGs

The LHS of the Hammett plot clearly shows that the rate of reaction decreases with increasingly electron donating groups (EDGs). Similarly, the RHS shows a decrease in the rate of reaction with increasingly electron withdrawing groups (EWGs). This point of inflexion at unsubstituted styrene indicates that there is a change in the rate limiting step of the reaction moving from EDGs to EWGs.

Unfortunately, the Hammett plot does not rule out a Michael addition versus a 1,2-insertion mechanism as the observed inflexion could be rationalised for both postulated mechanisms. For example, the LHS of the Hammett plot is indicative of a rate limiting nucleophilic attack of phosphido onto an electron rich styrene if Michael addition were operating. However, it could also indicate a rate limiting step in the 1,2-insertion mechanism, where formation of the metallacyclic transition state is rate limiting for alkenes with EDGs. Moving to increasingly (EWGs) the rate limiting step, irrespective of a Michael addition or 1,2-insertion mechanism, becomes protonolysis - this is a more facile step (from a comparison of gradient) but the transition state is now stabilised by more electron withdrawing groups (EWGs) making protonolysis less favourable.

4.5 Arrhenius and Eyring

Rate measurements for the standard hydrophosphination of styrene with diphenyphosphine at varying temperatures were collected. The activation energy of the reaction was calculated, according to the Arrhenius equation:

$$k = Ae^{-\frac{E_A}{RT}}$$

Which rearranges to give:

$$lnk = -E_A \frac{1}{RT} + lnA$$

Where:

k is the rate constant

A is the pre-exponential factor, unique for each reaction

E_A is the activation energy of the reaction (determined from the gradient of a plot of lnk vs $\frac{1}{T}$)

R is the gas constant

T is the temperature at which the reaction is performed

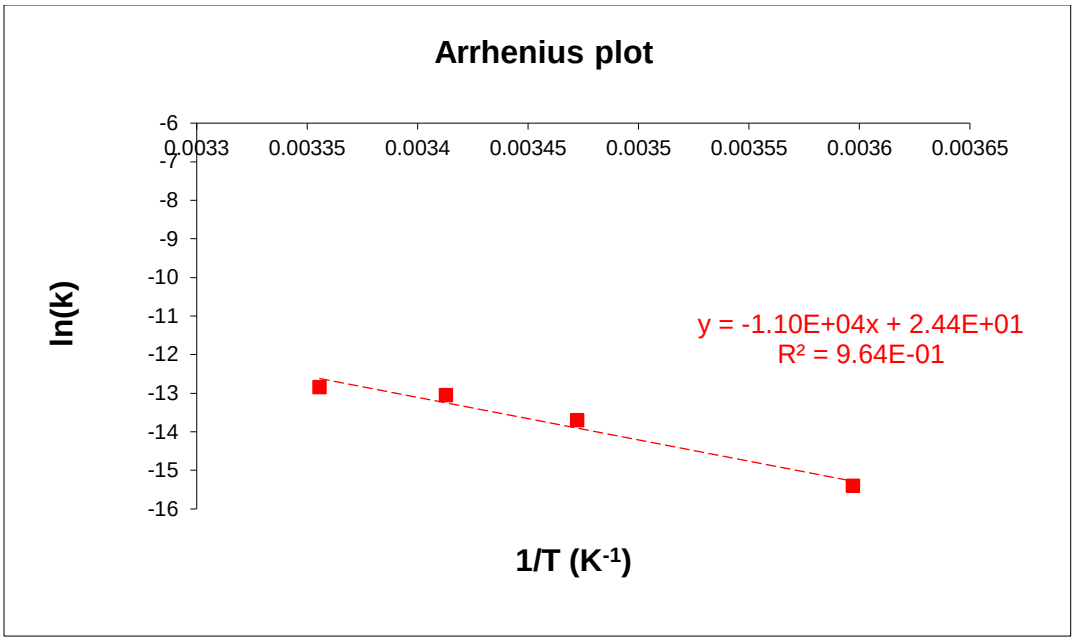

Figure 27. Arrhenius plot for catalysed reaction

The Arrhenius plot for the catalysed reaction yielded a value of E_A= 91.6 kJ mol^{-1}.

Similarly, the Eyring equation was used to obtain the entropy and enthalpy of activation for the reaction.

$$k = \frac{k_B T}{h} e^{-\frac{(\Delta^{\ddagger}H^{\circ} - T\Delta^{\ddagger}S^{\circ})}{RT}}$$

Where:

k_B is Boltzmann's constant

h is Planck's constant

$\Delta^{\ddagger}H^{\circ}$ is the standard enthalpy of activation

$\Delta^{\ddagger}S^{\circ}$ is the standard entropy of activation

Which rearranges to give:

$$ln\frac{k}{T} = -\frac{\Delta^{\ddagger}H^{\circ}}{RT} + \frac{\Delta^{\ddagger}S^{\circ}}{R} + ln\frac{k_B}{h}$$

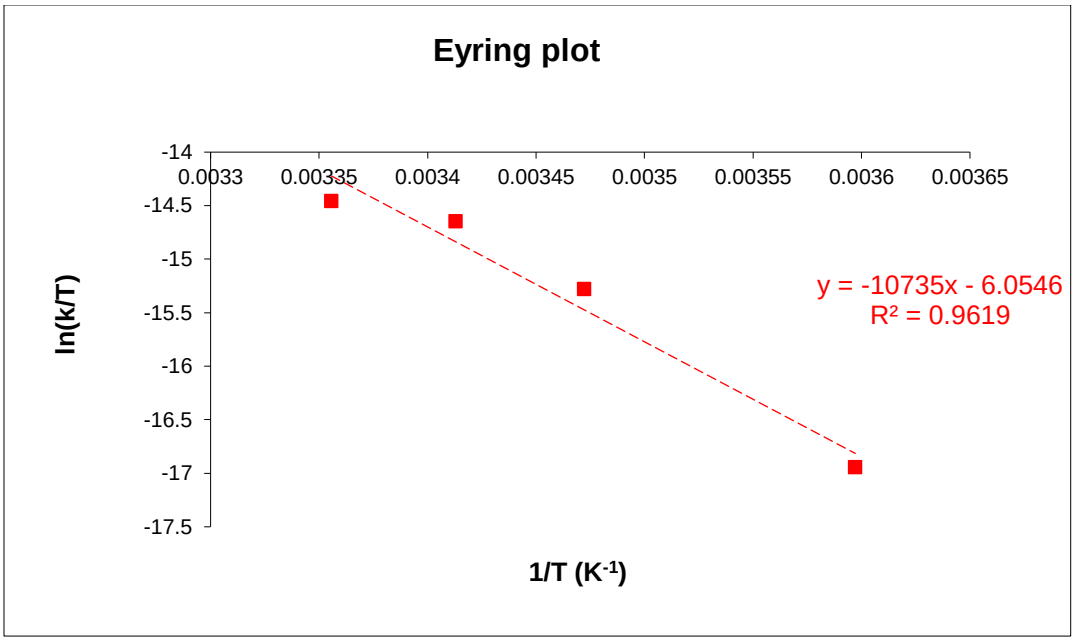

Figure 28. Eyring plot for catalysed reaction

Hence the values for $\Delta^{\ddagger}H^{\circ}$ and $\Delta^{\ddagger}S^{\circ}$ can be calculated from this plot.

$$\text{Gradient} = \frac{\Delta^{\ddagger}H^{\circ}}{R}, \quad \Delta^{\ddagger}H^{\circ} = 89.3 \text{ kJ mol}^{-1}$$

$$\text{y intercept} = \frac{\Delta^{\ddagger}S^{\circ}}{R} + ln\frac{k_B}{h}, \quad \Delta^{\ddagger}S^{\circ} = -247.9 \text{ J mol}^{-1} \text{ K}^{-1}$$

The standard Gibb's free energy change of activation $\Delta^{\ddagger}G^{\circ}$ can then be calculated from the relation:

$$\Delta^{\ddagger}G^{\circ} = \Delta^{\ddagger}H^{\circ} - T\Delta^{\ddagger}S^{\circ}$$

$$\Delta^{\ddagger}G^{\circ} = 163.2 \text{ kJ mol}^{-1}$$

The positive value of $\Delta^{\ddagger}H^{\circ}$ demonstrates that the process required to get to the transition state is endothermic. This is perhaps unsurprising since transition states lie at higher energy than the resting state of their products and reactants.

The negative value of $\Delta^{\ddagger}S^{\circ}$ in the catalysed system demonstrates that the transition state of the rate determining step involves a decrease of entropy. This result suggests that the rate determining step involves an associative process.

The value of $\Delta^{\ddagger}G^{\circ}$ is positive indicating that there is a decrease in free energy during the rate determining step.

A comparative study of the uncatalysed system was also undertaken.

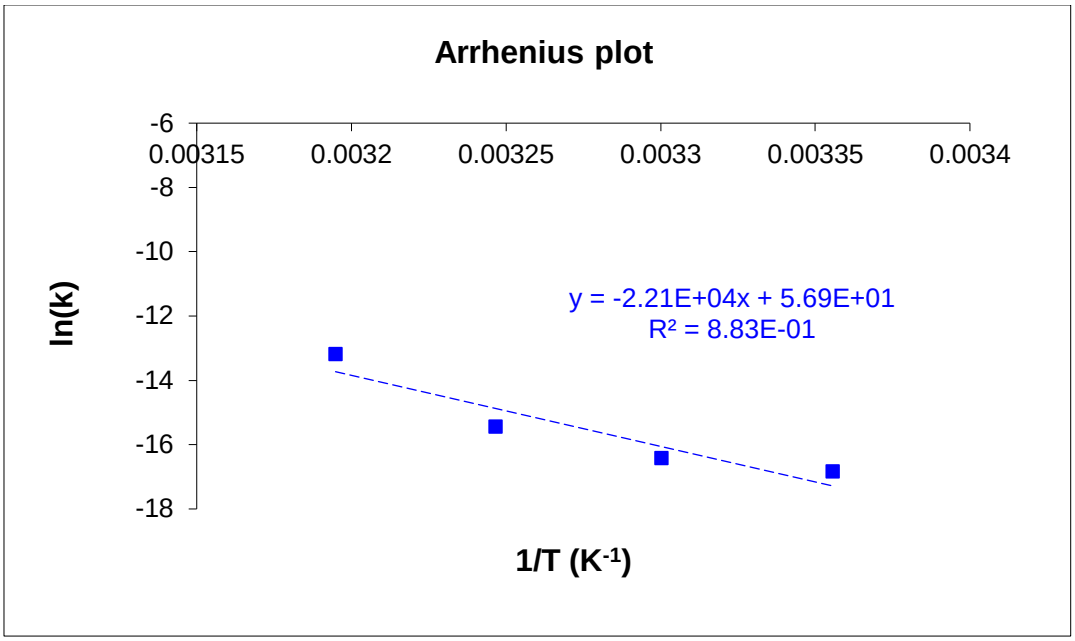

Figure 29. Arrhenius plot for uncatalysed reaction

The Arrhenius plot for the catalysed reaction yielded a value of E_A= 183.7 kJ mol^{-1}.

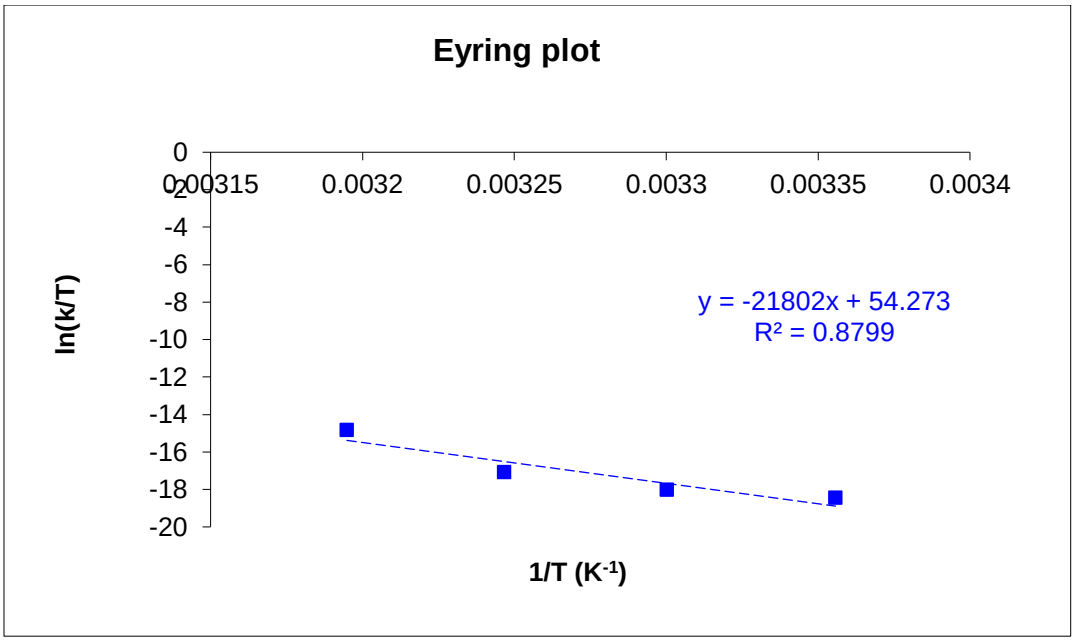

Figure 30. Eyring plot for uncatalysed reaction

Gradient = $\frac{\Delta^{\ddagger}H^{\circ}}{R}$, $\Delta^{\ddagger}H^{\circ} = 181.3\ \text{kJ mol}^{-1}$

y intercept = $\frac{\Delta^{\ddagger}S^{\circ}}{R} + ln\frac{k_B}{h}$, $\Delta^{\ddagger}S^{\circ} = 253.7\ \text{J mol}^{-1}\ \text{K}^{-1}$

$\Delta^{\ddagger}G^{\circ} = 105.7\ \text{kJ mol}^{-1}$

The value of $\Delta^{\ddagger}H^{\circ}$ for the uncatalysed system is greater than that observed for the catalysed system. This signifies that the transition state lies at higher energy in the case of the uncatalysed system, *i.e*. addition of the Fe catalyst lowers the energy of the transition state (**Figure 30**).

The value of $\Delta^{\ddagger}S^{\circ}$ is positive for the uncatalysed system, denoting an increase of entropy during the rate determining step. This often signifies a dissociative mechanism. Clearly, though, the mechanism for hydrophosphination will differ greatly in the absence of a catalyst.

The free energy change $\Delta^{\ddagger}G^{\circ}$ of the uncatalysed system is also positive however the magnitude is less than that of the catalysed system. This signifies that the rate determining step of the uncatalysed system is less endergonic that that of the catalytic system, this is likely due to the significant contribution of the enthalpic term between the two reactions.

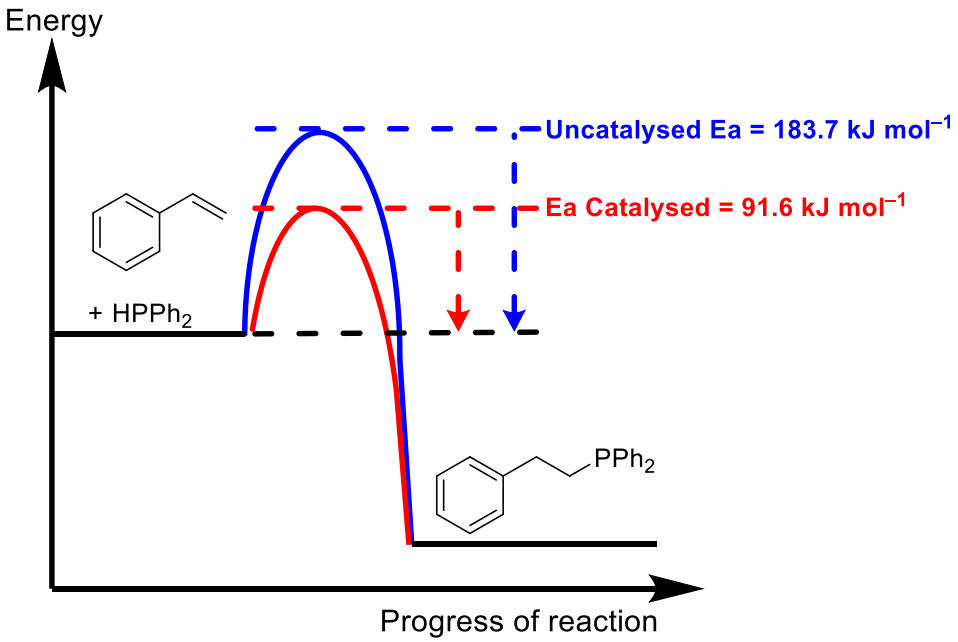

Figure 31. Activation energy difference between catalysed and uncatalysed HP reactions

As can be seen the activation energy of the uncatalysed system (183.7 kJ mol^{-1}) is double that of the catalysed system (91.6 kJ mol^{-1}). Clearly, the barrier to activation has been significantly lowered by addition of the catalyst.

4.6 Reaction Observations

First and foremost, the possibility of a radical catalysed reaction, commonly observed in iron-containing systems, needed to be eliminated. Addition of the radical trapscumene and TEMPO to the standard styrene reaction (**Scheme 70**) resulted in

only a slight reduction in yield of **18a** (**Table 13**) suggesting that this system is not radical mediated.

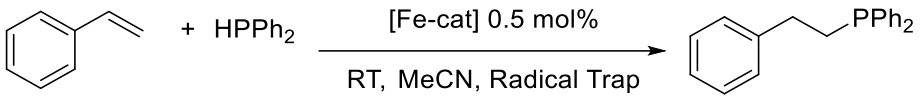

Scheme 70. Radical trapping reactions

Table 13. Radical trap reactions with Fe^{III}_2-μ-oxo(salen)$_2$

Entry	Radical Trap	Conditions	Spectroscopic Yield **18a**
1	Cumene	3 mol%	94 %
2	Cumene	1 eq	89 %
3	TEMPO	3 mol%	87 %
4	TEMPO	1 eq	31 %[a]

Conditions: alkene (1.04 mmol, 1.82 eq), HPPh2 (0.57 mmol, 1 eq), 31a (1.8 mg, 0.5 mol%, MeCN (0.35 mL), rt, 24 h. 1,2-DCE used as a standard. [a] reaction carried out in darkness. It is likely that the quantity of TEMPO impeded the reaction in this case.

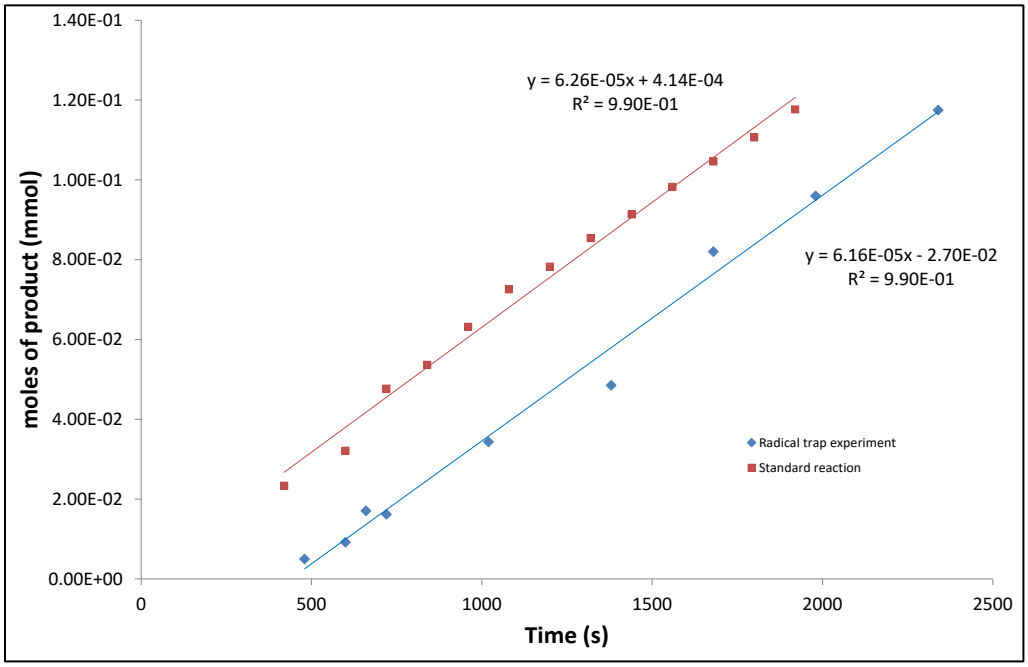

Figure 32. Reaction rates with and without a radical trap

A ^{31}P NMR spectrum of the crude reaction solution for the hydrophosphination of styrene shows only a broadening of the resonance corresponding to $HPPh_2$ with no change in chemical shift. This could be indicative of a weak coordination of the phosphine to the iron centre as described by Corma and co-workers who report that for $FeCl_3(PPh_3)_2$ only the free phosphine is recorded by ^{31}P NMR. They found that

solid state NMR, however, gave the expected down-field shift in NMR signal. In fact they go on to say that this may indicate the low affinity of Fe(III) for phosphines in solution makes them ideal candidates for catalytic transformations using phosphine reactants such as hydrophosphination.[112]

Looking for evidence which could rule out one of the postulated mechanisms of HP, mass spectrometry was used to analyse the crude reaction mixtures. Whilst they do not provide definitive proof of the Michael addition pathway, evidence for a Michael addition HP pathway would be provided by observation of telomerisation products in the mass spectrometry analysis of the crude reaction mixtures (**Scheme 70**). Indeed, the unsubstituted styrene, which should only be moderately prone to telomerisation shows that dimers are formed in the crude reaction mixture of **18a** (**Figure 33**). This effect is also observed in the crude reaction mixture of **18g** (**Figure 34**). It is possible that these products are formed by the initial dimerisation of styrene, followed by reaction with phosphine, so although it does not rule out a 1,2-insertion process, it hints that Michael addition may be operating.

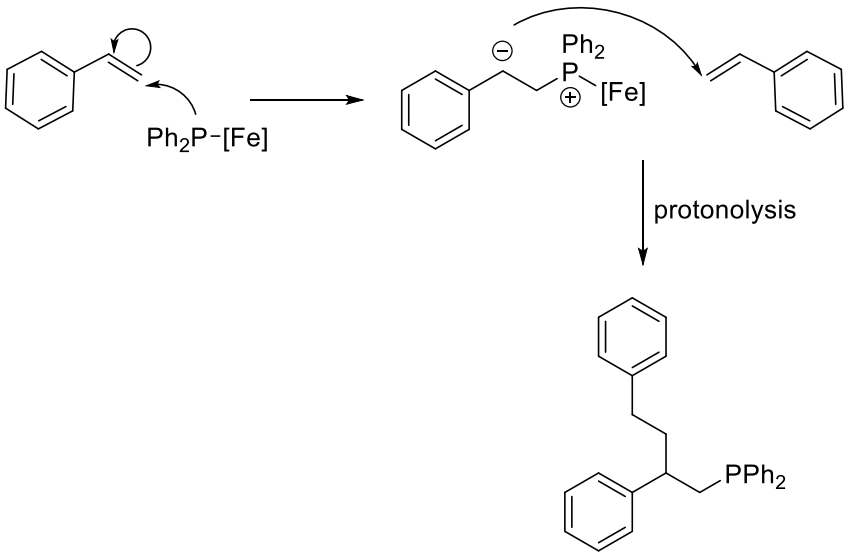

Scheme 71. Potential telomerisation pathway

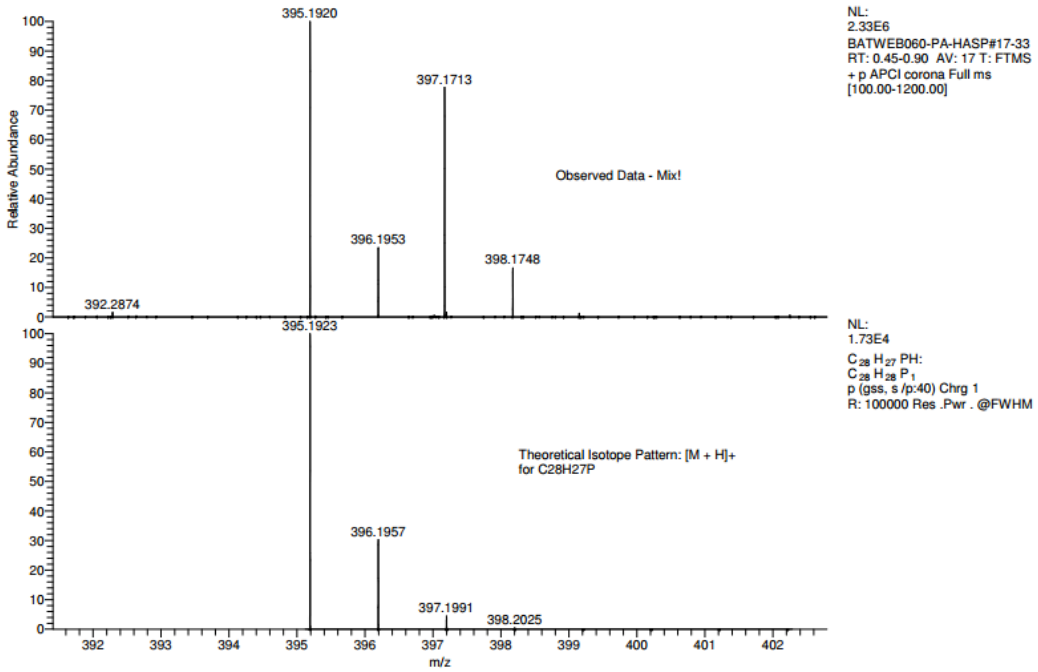

Figure 33. Mass spectrometry analysis of crude reaction mixture of **18a** showing telomerisation product.

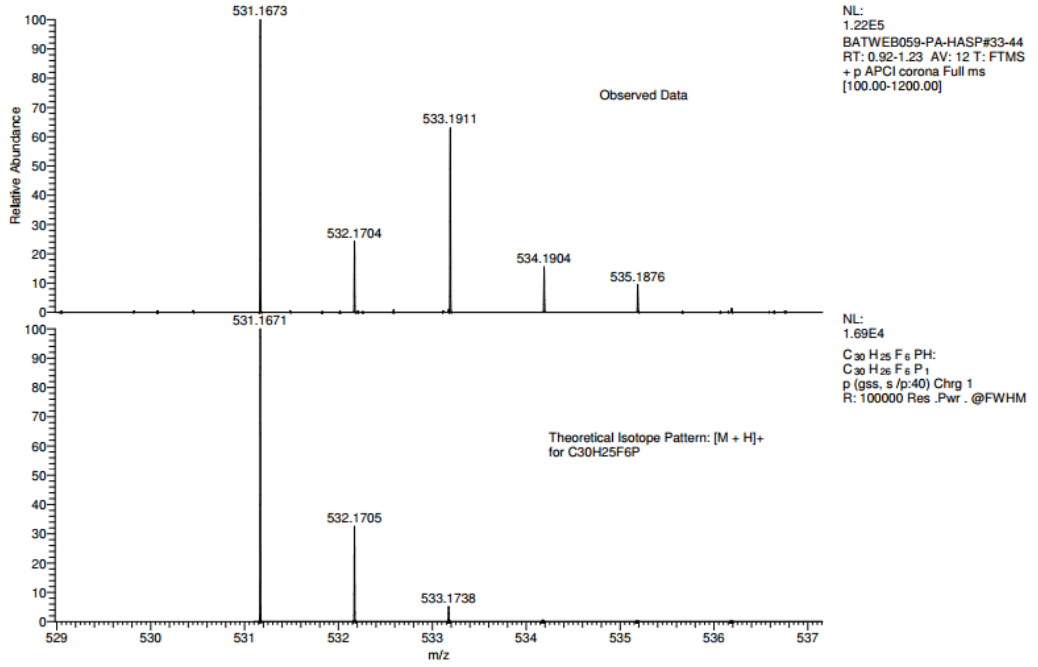

Figure 34. Mass spec analysis of crude reaction mixture of **18g** showing telomerisation product.

Addition of benzaldehyde to the reaction solution, in an attempt to trap the zwitterionic species according to an adapted Morits-Baylis-Hillman reaction (as in the work of Glueck, **Chapter 1, Section 1.8**), was unfortunately unsuccessful. Although it is not clear why these products were not observed, it is potentially due to the extremely high rate of the catalytic transformation, in direct competition with the reaction of

benzaldehyde with the zwitterionic species. Where the zwitterion is short-lived, the reaction with benzaldehyde is disfavoured.

4.7 Labelling studies

To characterise the reaction pathway more thoroughly deuterium labelling studies were carried out. The kinetic isotope effect can then be used to give an indication of how directly D-labelled atoms are involved in the overall chemical transformation. In this catalytic system, it is a ratio of the rate of HP for the protonated styrene over the rate for the deuterated styrene. The value may be used to make assertions on the nature of the primary reaction site.

For βD-styrene the kinetic isotope effect, the ratio of the rate of hydrophosphination of the protonated styrene to the deuterated styrene, was calculated as 1.3 ± 0.2; this value is consistent with a secondary kinetic isotope effect. This indicates, as expected, that the D-labelled atoms are adjacent to the reaction site and are not involved directly in the reaction.

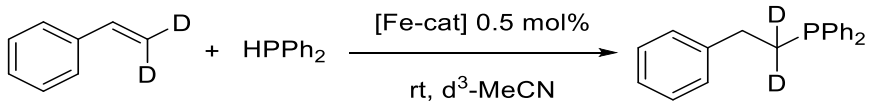

Scheme 72. D-labelling reaction: βD-styrene

Unexpectedly, upon addition of D-labelled phosphine to the standard reaction set up, the reaction did not proceed. On further attempts – using freshly prepared $DPPh_2$ – this negative result was found repeatedly. This would seem to imply an infinite kinetic isotope effect. Upon addition of base, the reaction proceeded as in **Scheme 72**.

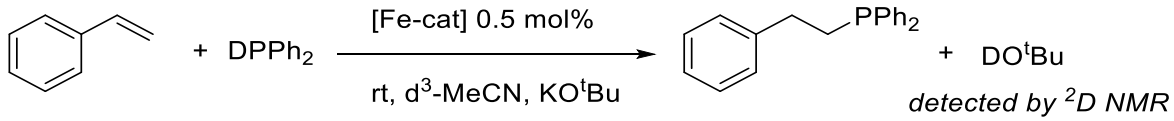

Scheme 73. D-labelling reaction: $DPPh_2$

It is therefore unclear whether the initial activation of the catalyst is inhibited (**Scheme 75**, **Section 4.9**), or if the change from $HPPh_2$ to $DPPh_2$ indeed results in a much larger kinetic barrier. This would further imply that the rate determining step for the reaction is the breaking of the P-H bond, or protonolysis. Given these considerations and the apparent break from consistency with the Hammett studies conducted in **Section 4.3**, an additional kinetic study was performed with $DPPh_2$, wherein the reaction solution is left for several days to give additional time to react. Indeed, this reaction proceeded to ~60% conversion to the deuterated product, suggesting that the initial activation step may be more complex than initially anticipated.

Based on these results, further clarification was sought. Due to lack of availability of αD-styrene, it was not possible to study the effect on KIE of the complementary deuteration on the substrate to that of $DPPh_2$ as seen in **Scheme 74**. However, the literature revealed a method of examining the α-position on the styrene substrate via ^{13}C NMR.

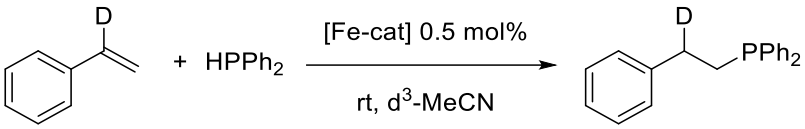

Scheme 74. D-labelling reaction: αD-styrene

As mentioned previously, in support of this, it was found that **29** alone was not active for the catalysis of hydrophosphination at room temperature. Addition of $HPPh_2$ to **29** revealed no resonance by ^1H NMR corresponding to the formation of a metal hydride species effectively ruling this out as a product of the disproportionation of **28**.

Scheme 75. Potential D-labelled phosphine

Another interesting observation that was made was that small quantities of H_2O were also perceived to build up at the beginning of reaction monitoring (**Figure 35**). It was questioned whether this was an important process in the catalytic cycle and whether it was related to the activation of **28**. This is discussed further in **Section 4.9**.

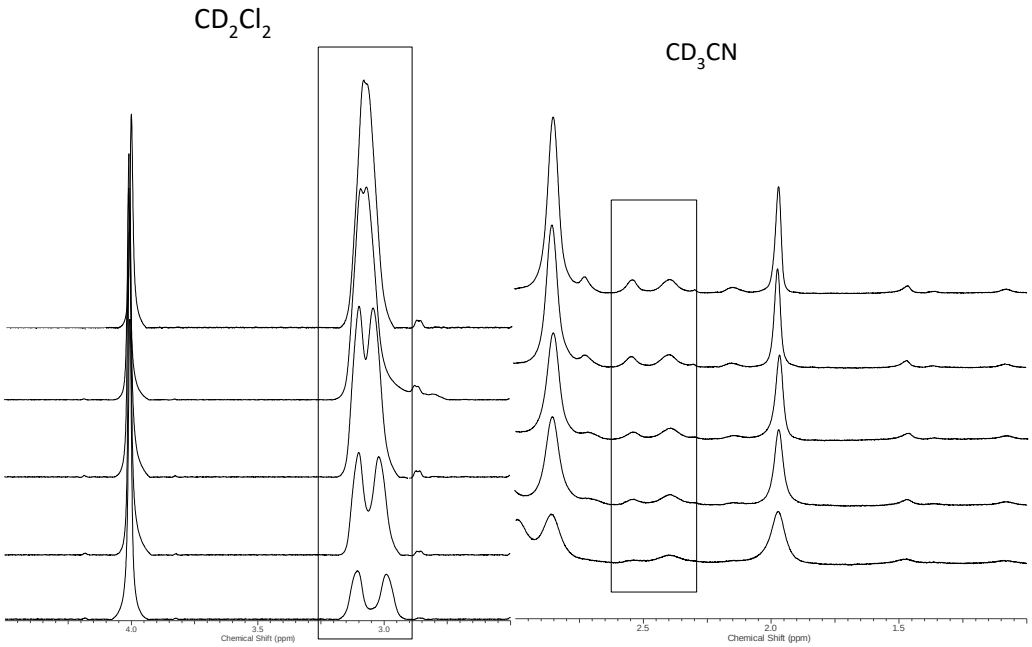

Figure 35. Coalescing resonances in CD_2Cl_2 NMR versus MeCN (boxed regions show -CH_2CH_2- phosphine product). The time scale over which these reactions are monitored are not equivalent

Table 14. Hydrophosphination reactions with **29** and base

Entry	Base	Conditions	Spectroscopic Yield **18a**
1	NaO^tBu	2 mol%	20 %
2	NaO^tBu	1 eq	66 %
3	NaO^tBu	1 eq, no catalyst	12 %
4	NaO^tBu	1 eq base, 1 eq cumene	87 %
5	NEt_3	1 eq	6 %
6	-	no catalyst	trace

Conditions: alkene (1.04 mmol, 1.82 eq), $HPPh_2$ (0.57 mmol, 1 eq), **39** (1.8 mg, 1 mol%)), MeCN (0.35 mL), rt, 24 h, using 1,2-DCE as a standard

This difference in theoretical and observed percentages allows a comparison of complete incorporation of deuterium versus actual deuterium incorporation.

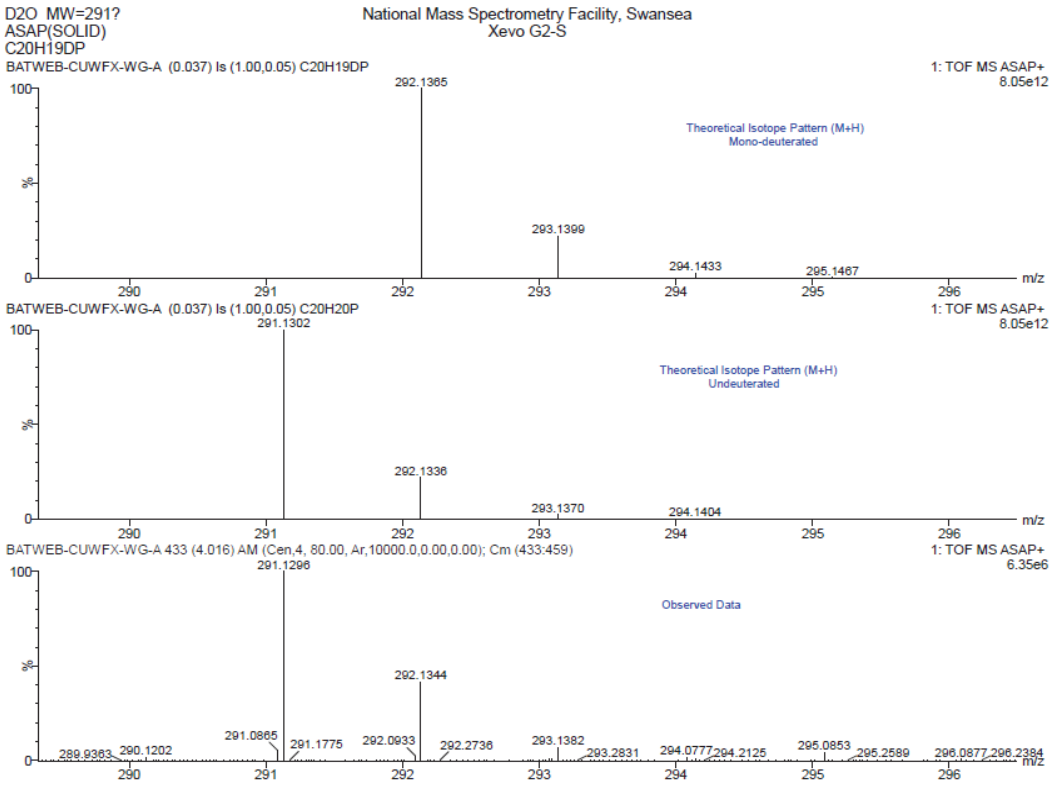

Figure 36. Theoretical isotope patterns for deutero and non-deutero products versus observed data

Use of a 50/50 mix of $HPPh_2$ and $DPPh_2$ resulted in incorporation of deuterium in the final products also. It was determined that formation of primarily the proteo HP product occurred – this product was previously identified via MS as [M+H] = 291.13 (as opposed to the possible deutero product [M_D+H] = 292.14). However, the ratio of the observed peak at 292.13 to that of the theoretical pattern for [M+H] of the undeuterated product suggests some deuterium incorporation (approximately 20% higher than for the theoretical pattern). As one component of the mix of phosphines used was 86% deuterated $DPPh_2$ this means that the true ratio was closer to 57%/43% $HPPh_2$/$DPPh_2$

To determine the outcome of this experiment accurately, analysis was performed by multinuclear NMR as well as Mass Spectrometry

A reaction with pure $DPPh_2$ allowed to react for ~96 h resulted in the formation of deutero product, suggesting that the induction time required for this reaction was higher due not to the KIE, but suggests a series of complex reactions as a precursor to formation of the catalytically active species. This is indicative of the formation of a multi-metallic complex. Mass spec analysis of this sample determined that the deutero product was the primary product present. Using 86% $DPPh_2$ a ratio of 14:86

% intensity of final products, the actual ratio is closer to 40:100. This indicates that the non-deutero reaction is favoured (turnover approximately x3 greater) which corresponds with the much longer induction time of catalysis for $DPPh_2$ than for $HPPh_2$.

4.8 Cyclic voltammetry

Cyclic voltammetry (CV) measurements were performed to probe the electrochemical properties of the various stages of the reaction. A simple experiment was constructed where sequential addition of reactants to the catalytic species were probed *via* CV measurements. The CV of the pre-catalytic species was examined, then a quantity of styrene was added, and the CV of the mixture was examined to check for any changes in the CV profile. A quantity of phosphine was then added to complete the conditions for the catalytic reaction and the CV of this mixture was examined again. In this way several hypothetical stages of the catalytic cycle can be explored. Initially the scan rate was varied to establish the consistent position of the cathodic and anodic peak potentials. The CV profile reveals a reversible one-electron reduction for the Fe^{III}_2-μ-oxo(salen)$_2$ (peak current proportional to square root of scan rate for diffusion limited processes).

Scans were taken following successive additions of increasing quantities of styrene. A clear shift in peak position is seen from following the reaction with styrene (**Appendix**, **Figure 37**). Scans were then taken following successive additions of increasing quantities of diphenylphosphine. A clear shift in peak position is seen following the reaction with $HPPh_2$ this is seen to shift back towards the position of the pure catalyst (**Appendix**, **Figure 38**).

A cyclic voltammetry study was also conducted for the Fe^{III}_2-μ-oxo(porphyrin)$_2$ system (and its reactants) in the same fashion as for the salen system.

Addition of styrene to the Fe^{III}_2-μ-oxo(porphyrin)$_2$ solution results in an irreversible CV trace. This is likely the result of a reversible electrochemical reduction which affects an irreversible chemical change in the system. Addition of increasing quantities of styrene appears to partially restore the reversibility of this process. Nevertheless, this is in direct contrast to the salen-containing system, which exhibited only a reversible electrochemical reduction under similar conditions.

Scans were then taken following successive additions of increasing quantities of diphenylphosphine.

4.9 Proposed Catalytic Cycle

All of the observations described so far support the catalytic cycle proposed (Scheme 76). Knowing that **29** requires addition of base to become catalytically active, it is clear that the catalytic cycle must involve the deprotonation of phosphine by the metal complex **28**. Heteroleptic cleavage of **28** into Fe(salen) (**29**) and Fe–PPh_2 (**41**) could be envisaged to be the first step in the process with further activation of the Fe(salen)OH taking place in-keeping with the order in Fe and the observation of increasing quantities of H_2O in the crude reaction mixture as shown previously (**Figure 12**).

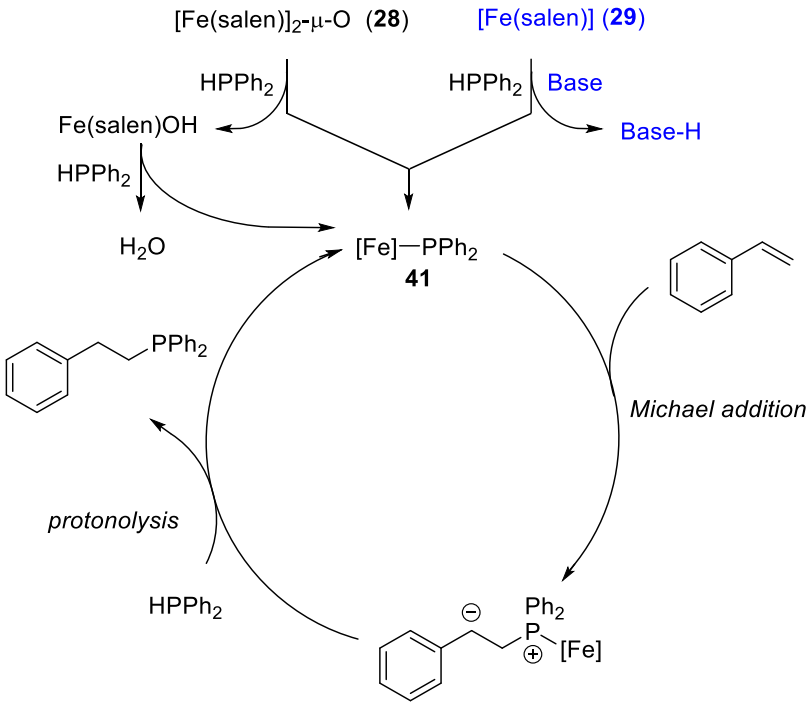

Scheme 76. Proposed catalytic cycle

Therefore, based on our observations to date, a speculative catalytic cycle could be proposed which starts with the heteroleptic cleavage of **28** into iron-phosphido intermediate **41** and Fe(salen)OH complex. Based on the order in Fe, the hydroxide complex is not a final, inactive resting state and could become re-activated and be reincorporated into the catalytic cycle. This is supported by the small quantities of water that are observed to form by ^{1}H NMR, where activation of the iron hydroxide in the presence of another equivalent of diphenylphosphine liberates H_2O and another equivalent of **41**. **41** undertakes Michael addition of styrene to form a highly reactive zwitterion. The zwitterion can then undertake two processes 1) further attack of styrene to form the dimer observed by mass spectrometry or 2) the rapid protonolysis event needed to release product. Since the Hammett data shows less of a rate-

limiting effect for electron poor substrates, it could be envisaged that protonolysis is sufficiently rapid to prevent protracted telomerisation events taking place.

4.10 Summary

The work detailed in this chapter describes the kinetic and mechanistic studies of Fe-μ-oxo salen (**28**) for the catalytic hydrophosphination of styrene with $PHPh_2$.

Initial kinetic studies revealed the reaction to be 2nd order in catalyst (**28**), 1st order in styrene and 1st order in phosphine.

A Hammett study of the catalytic system revealed that the unsubstituted styrene gave the highest rate of reaction with substitution of electron withdrawing or electron donating groups on the phenyl ring reducing the rate of reaction. A change in the rate determining step is also observed for the moving from electron withdrawing to electron donating substituents.

The thermodynamic parameters of the catalysed and uncatalyzed hydrophosphination reactions were determined via Arrhenius and Eyring plots. The activation energy of the uncatalysed system was calculated to be 183.7 kJ mol^{-1}, while the activation energy of the catalysed system was calculated to be 91.6 kJ mol^{-1}, clearly showing that, as expected, addition of the catalyst lowered the barrier to activation. Values of $\Delta^{\ddagger}H^{\circ}$, $\Delta^{\ddagger}S^{\circ}$ and $\Delta^{\ddagger}G^{\circ}$ were calculated for the catalysed and uncatalyzed reactions compared.

Addition of radical traps cumene or TEMPO showed no effect on the reaction yield or rate, ruling out a radical-based mechanism.

Studies of the reaction solution through mass spectrometry revealed telomerisation products suggesting the presence of a zwitterionic species as part of the reaction mechanism. Addition of benzaldehyde was unsuccessful in trapping this species, however, this is likely due to its high rate or conversion to the phosphine product.

Deuterium labelling studies yielded a kinetic isotope effect of 1.3(2) for β-deuterated styrene, consistent with a secondary kinetic isotope effect. $PDPh_2$ was unreactive in the catalytic reaction, giving an infinite kinetic isotope effect – this signifies that cleavage of the P-D bond did not occur over the observation period.

Based on these experimental and spectroscopic observations a catalytic cycle was proposed to take place via a Michael addition mechanism. The catalytic mechanism proposed is consistent with all experimental observations

5 Conclusions and Future Work

A range of reactions were developed to produce a variety of unique 1,1-diphos compounds through hydrophosphination. This motif is only visited upon in the literature in the case of a palladium templated reaction and is otherwise inaccessible via current methods.

Further, A mild synthesis of a variety of activated phosphines has been developed utilising a low-cost iron catalyst which is un-paralleled in its ability to catalyse hydrophosphination, in terms of catalyst loading and room temperature reactivity. The Fe^{III}_2-μ-oxo(salen)$_2$ pre-catalyst remains at the forefront of hydrophosphination catalysts, in terms of expense, activity and its wide substrate scope. The astoundingly low catalyst loading required for this system is paralleled only by the Fe^{III}_2-μ-oxo(porphyrin)$_2$ system discussed herein and a select few others. Both electron withdrawing and electron donating groups are well tolerated by these iron-μ-oxo systems. The phosphine products were isolated and have been further found use in the literature as ligands in catalysis themselves. Initial investigations in to hydrophosphination focused on the use of diphenylphosphine in these hydrophosphination reactions, however, these systems were also found to be active with a phenylphosphine source. This led to the development of products with two substitutions onto the phosphorus moiety.

A thorough kinetic and mechanistic study was carried out for hydrophosphination with Fe^{III}_2-μ-oxo(salen)$_2$.

Development of a catalytic system able to impart chirality to phosphines would provide an ideal extension to this study.

The high activity of the catalysts is suspected to be imparted by the μ-oxo bridge. A series of catalysts utilising this motif would be of great interest. Indeed, there is clear potential in these systems for small molecule activation purposes.

6 Experimental

6.1 General considerations

Reagents were purchased from Sigma Aldrich or prepared as stated. CH_3CN was dried over CaH_2 (reflux), distilled and then degassed using three freeze-pump-thaw cycles. NMR data was collected at 300, 400 or 500 MHz on Bruker instruments in $CDCl_3$ or CD_3CN at 293 K and referenced to residual protic solvent. Elemental analyses were carried out by Dr S. Boyer at London Metropolitan University. Mass Spectrometry data was collected by the EPSRC NMSF at the University of Swansea.

4-Methoxystyrene, 4-chlorostyrene, 3-methylstyrene and 4-trifluoromethylstyrene were purchased and purified by trap-to-trap distillation then degassed using three freeze-pump-thaw cycles before transferring to the glove box.

6.2 Synthesis of Styrene Derivatives

A benzaldehyde derivative (5 mmol) was added to potassium carbonate (1.1 g, 8 mmol) and methyltriphenylphosphonium bromide (2.1 g, 6 mmol) in anhydrous 1,4-dioxane (5 mL) and heated at reflux for 16 h. The reaction mixture was then cooled, filtered and washed with pentane and then concentrated *in vacuo.*

Two methods of isolation can be used:

[a] The residue was dissolved in hot pentane, cooled to 0 °C, filtered (to remove triphenylphosphine oxide: sparingly soluble in cold pentane) and washed with cold pentane. The filtrate was dried ($MgSO_4$) and concentrated *in vacuo* to give the styrene derivative.

[b] Isolate *via* silica gel column chromatography in 40% EtOAc/pentane (ensuring dioxane is removed prior to isolation).

All styrene derivatives were then vacuum distilled (may require gentle heating) and degassed before transferring to the glove box.

6.3 Synthesis of 30, representative of 32 and 33

A mixture of salicylaldehyde (2.49 g, 18.3 mmol, 3.5 eq) and ethylenediamine (0.31 g, 5.2 mmol, 1 eq) in dry EtOH (40 mL) was heated at reflux for 2 h. The solution was cooled to 0 °C and filtered, and the resultant yellow solid was washed with cold EtOH. The product was then dried *in vacuo* (**30**, 1.07g, 77%)(**32**, 0.414g, 78%). **30** comparable to the commercially available compound (CAS: 94-93-9). **32** and **33** prepared as in literature and require further characterisation.[75]

6.4 Synthesis of 34

A mixture of 1,2 diaminocyclohexane·tartrate (0.34 g, 1.3 mmol, 1 eq) and K_2CO_3 (0.35 g, 1.5 mmol, 2 eq) in distilled water (1.8 mL) was stirred until dissolution. EtOH was added and the mixture was heated to reflux. A solution of 3,5-ditertbuyl-2-hydroxybenzaldehyde (0.6 g, 2.6 mmol, 2 eq) in EtOH (3 mL) was added in a steady stream over 5 mins which formed a yellow slurry. The mixture was heated to reflux with vigorous stirring over for 2 h. Distilled water (1.8 mL) was added to the mixture which was then cooled in an ice bath. The product was collected via vacuum filtration and washed with cold EtOH (1.2 mL). The crude solid was redisolved in CH_2Cl_2 (2.5 mL) and washed with distilled water (3.5 mL x 2) and brine (1.2 mL). The solvent was dried over Na_2SO_4 before it was removed *in vacuo*. A yellow powder was isolated in good yield (0.52g, 76%). Comparable to the commercially available compound (CAS: 135616-40-9).

6.5 Synthesis of 31a, 35 and 36

$Fe(OAc)_2$ (109 mg, 0.6 mmol, 1 eq) was weighed into a flask and dissolved in ethanol (5 mL) leaving a brown solution. To this, a solution of N,N′-Bis(salicylidene)ethylenediamine (200 mg, 0.7 mmol, 1.2 eq) in ethanol (10 mL) was added forming a red solution. The mixture was then stirred at 80 °C for 2 h. The flask was allowed to cool to rt before filtering off the solid and washing it with ethanol. The dark red solid was dried under vacuum.

6.6 Synthesis of 37

Manipulations carried out under an inert atmosphere (Ar) with rigorous air sensitive handling. $FeCl_2$ (142 mg, 1.12 mmol, 1 eq., 99.9% purity) and *N*,*N*′-Bis(salicylidene)ethylenediamine (300 mg, 1.12 mmol, 1 eq, dried under vacuum) were combined in an ampule. Freshly dried THF (15 mL) was cannulated onto the mixture which was then stirred at 80 °C for 2 h before cooling to rt. Using a metal cannula with a glass paper frit, the reaction solution was filtered away from the precipitate leaving a straw yellow solid which was then washed with THF (2 x 5 mL). The solid was then dried under vacuum before storing in a glovebox freezer (-30 °C).

6.7 Method of synthesis of styrenes

A benzaldehyde derivative (5 mmol) was added to potassium carbonate (1.1g, 8 mmol) and methyltriposphonium bromide (2.1g, 6 mmol) in anhydrous 1,4-dioxane (5mL) and heated at reflux for 16h. The reaction mixture was cooled, filtered and washed with pentane and then concentrated *in vacuo.*

I. The residue was dissolved in hot pentane, cooled to 0°C, filtered (to remove triphenylphosphine oxide: sparingly soluble in cold pentane) and washed with cold pentane. The filtrate was dried ($MgSO_4$) and concentrated in vacuo to give the styrene derivative.

II. Isolation via silica gel column chromatography (ensuring dioxane removed prior to isolation).

All styrene derivatives were then vacuum distilled (may require gentle heating) and degassed before transferring to the glove box.

6.8 Hydrophosphination with 28

The procedure was carried out under an inert argon atmosphere in an M-Braun glove box. Compound **28** (1.8 mg, 1 mol% Fe-centre) was weighed out into a Schlenk tube. CH_3CN (350 µL)[a] was added to this (forming a deep red solution) followed by styrene (1.04 mmol, 1.86 eq) and finally diphenylphosphine (100 µL, 0.57 mmol, 1 eq).[b] After stirring at room temperature for 24 h, the Schlenk tube was placed under vacuum and the excess starting styrene and solvent removed leaving an orange/red oil.[c]

For spectroscopic yields reaction solutions were exposed to air and filtered through a silica gel plug using CH_2Cl_2. This removed the iron residue leaving a colourless oil.[d] Solvent was removed by blowing nitrogen over the oil before addition of 45 µL 1,2-dichloroethane as an integration standard. $CDCl_3$ was used as the NMR solvent.[e] Products were then isolated by column chromatography 1 - 5% EtOAc/pentane. The products oxidised slowly over time (this can be observed in some $^{31}P\{^1H\}$ spectra as a peak at ~20 ppm).

[a] In the case of 4-phenyl-styrene, 750 µL CH_3CN were used to wash the insoluble styrene into an ampule which was then heated at 60 °C for 24 h.

[b] Upon addition of diphenylphosphine to 2-vinylpyridine reaction, solution turned aubergine purple.
In the case of 2-vinylstyrene a lavender-coloured oil remained

[c] 4-vinylstyrene and 2-vinylstyrene reacted for 72 h; 4-chlorostyrene reacted for 114 h.

[d] In the case of 4-vinylstyrene a yellow oil remained.

[e] In the case of 3-methylstyrene, 4-vinylstyrene and 2-vinylstyrene no additional purification was necessary.

[f] Non deutero THF (4.1 mg) was used for an integration standard in the case of 4-MeO-, 4-Me- and 3-methylstyrene.

6.9 Hydrophosphination with radical trap

Carried out using the general method for hydrophosphination (**7.1.7**). The appropriate quantity of Cumene or TEMPO added to the Schlenk tube after loading the pre-catalyst and CH_3CN.

6.10 Hydrophosphination with 38

Carried out using the general method for hydrophosphination (**7.1.7**). The appropriate quantity of base added to the Schlenk after loading the pre-catalyst and CH_3CN. Colour change – yellow to colourless upon addition of NEt_3. Upon addition of diphenylphosphine to NaO^tBu and an orange solution formed which gradually returned to colourless after 30 mins.

6.11 Method for hydrophosphination without catalyst.

Carried out using the general method for hydrophosphination (**7.1.7**, without catalyst). Addition of diphenylphosphine to NaO^tBu solution an orange solution formed which did not go back to colourless until the solution was opened to air.

6.12 General method for kinetic studies of hydrophosphination

31a (1.8 mg, 0.01 eq) was weighed out into a vial. CD_3CN (350 µL) was added to this (forming a deep red solution) followed by diphenylphosphine (100 µL, 0.056 mmol). This solution was syringed into a vial containing an integration standard - 1,3,5-trimethoxybenzene (3.4 mg). This solution was then syringed into a J-Young NMR tube and sealed. Styrene derivative was syringed into a separate J-Young NMR tube and sealed. The two J-Young NMR tubes were then attached to a Schlenk line through vacuum transfer apparatus. The samples were degassed using three freeze-pump-thaw cycles. With the CD_3CN containing tube kept frozen, the styrene was allowed to warm to rt and transferred on top of the CD_3CN solution. Once all the styrene was transferred, the sample was removed from liquid N_2 and placed in acetone/solid CO_2 the NMR tube was then refilled with argon and kept frozen. When ready to collect kinetic data the sample was allowed to defrost – the sample was inverted to speed up this process. Once all solid had melted the outside of the tube was wiped down to remove condensation/ice forming on the outside and placed in the spectrometer.

6.13 General Method for Catalytic Double Hydrophosphination

Carried out under an inert argon atmosphere in an M-Braun glove box.

2a (4.7 mg, 1.25 mol%) was weighed out into a Schlenk tube. Styrene (2.28mmol, 4 eq) was added to this (forming a deep red solution) followed by and phenylphosphine (62 mg, 0.57 mmol, 1 eq).[a] After stirring at 40°C for 24 h, the Schlenk tube was placed under vacuum and the excess starting styrene removed leaving an orange/red oil.

For spectroscopic yields reaction solutions were filtered through a silica gel plug using CH_2Cl_2. This removed the iron residue leaving a colourless oil. Solvent was removed under vacuum before addition of 40 µL THF as an integration standard. C_6D_6 was used as the NMR solvent.

4MeO-styrene DHP and styrene DHP were isolated by column chromatography 5% EtOAc/pentane. 2-vinylpyridine, 4-vinylpyridine and 4Cl-Styrene DHP were all isolated by sublimation of SHP away from the desired product.
The products oxidised slowly over time (this can be observed in some $^{31}P\{^1H\}$ spectra as a peak around 20 ppm).

6.14 Hydrophosphination with $Fe(HMDS)_2THF$

$Fe(HMDS)_2THF$ (16 mg, 10 mol %) was weighed into a vial before transferring to a schlenck. MeCN (200 µL) was added to this using a mirco-pipettor. The alkyne (0.5 mmol) was added to this solution followed by $HPPh_2$ (174 µL,1 mmol). The reaction was stirred over night for 18 h before evacuating. A DCE standard was added and an NMR sample was taken in CDCl3 to indicate spectroscopic yield. The sample was evacuated and filtered through a cotton wool plug with EtOAc. A small volume of water was added to this, followed by 2-3 drops of hydrogen peroxide, to yield the oxidised phosphine product. A separation was performed with EtOAc and water and the oxidised phosphine (present in the EtOAc fraction) dried with $MgSO_4$ before separating from side products via a narrow silica-gel column with Et_2O eluent.

6.15 Hydrophosphination with KHMDS

The substrate (0.5 mmol) was added to a schlenck, followed by MeCN (100 µL) was added to this using a mirco-pipettor and $HPPh_2$ (174 µL, 1 mmol). KHMDS (20 mg, 20 mol %) was weighed into a vial before transferring to the schlenk. The reaction was stirred for 16 h before evacuating to remove solvent. The sample was and filtered through an alumina plug with a 3:1 Pentane:CH_2Cl_2 mix, affording the desired product as a white solid.

6.16 Cyclic voltammetry measurements

Cyclic voltammetry measurements were taken on an Ivium CompactStat at an applied potential range of ±4V, 0.01mV res. (20bit)/±10V, 0.02mV res. A Standard Calomel reference electrode and platinum counter electrode were used for all measurements.

A 0.1M buffer solution of $Bu_4N^+PF^-_6$ was made up with acetonitrile. 25 ml of this buffer solution was used to dissolve the of iron compound. An appropriate sweep width and was selected to observe fully the reversible peaks for the iron compound. 4 scans were collected at $50mVs^{-1}$ before adding 5 µL of styrene. 10 µL of styrene was then added before increasing addition by increments of 5 µL up to 35 µL taking 4 scans for each. Successive increments of 10 µL of $HPPh_2$ were then added taking 4 scans between them up to 50 µL.

6.17 General Method for Catalytic Unsymmetrical Double Hydrophosphination

The reaction mixture was prepared under an argon atmosphere in an M-Braun glove box; 6 (0.5 mol%) was weighed out into a Schlenk tube.CH3CN (200 mL) was added to this followed by 4a (0.5 mmol, 1equiv.) and a substituted styrene (1 mmol, 2equiv.) was added. After stirring at 60°C for 60 h, the Schlenk tube was placed under vacuum and the excess starting styrene and solvent removed. A spectroscopic yield was obtained prior to purification by column chromatography(1%EtOAc/petroleum ether).

6.18 General Method for Thermal Single Hydrophosphination

Carried out under an inert argon atmosphere in an M-Braun glove box.
Styrene (0.285 mmol, 1 eq) was placed in a Schlenk tube, acetonitrile (200µL) and phenylphosphine (62 mg, 0.57 mmol, 2 eq) were added. After stirring at 80°C for 16 h, the Schlenk tube was placed under vacuum and the excess starting styrene and solvent removed leaving a colourless oil. THF (40 µL) was added as an integration standard. C_6D_6 was used as the NMR solvent.

The clean product was thus obtained via short-path distillation under reduced pressure(2×10^{-2} mbar, 60°C).

7 Product Characterisation

36a (Table 3, Entry 1)

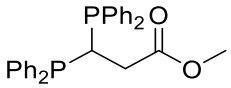

Off-white powder (86%). ^{1}H NMR (500 MHz, 298 K, C_6D_6) δ 7.75-7.72 (m, 4H), 7.59-7.56 (m, 4H), 7.05 (app. T, *J* = 7.2 Hz, 4H), 7.02-6.95(m, 8H), 4.27 (t,$^{3}J_H$ = 5.9 Hz, 1H), 2.90 (s, 3H); ^{13}C{^{1}H} NMR (126 MHz, 298 K, C_6D_6) δ 172.8 (t, J_p = 3.3 Hz), 137.0 (app. t, *J* = 4.2 Hz), 136.6 (app. t, *J* = 5.4 Hz), 135.2 (app. t, *J* = 11.2 Hz), 133.9 (app. t, *J* = 10.9 Hz), 129.2, 128.9, 128.7 (app. t, *J* = 3.5 Hz), 128.4 (app. t, *J* = 3.8 Hz) 51.2, 34.7 (t, J_P = 9.4 Hz), 28.3 (t, J_P = 25.5 Hz); ^{31}P{^{1}H} NMR (202 MHz, 298 K, C_6D_6) δ -6.6; IR (solid) ν 1726 cm^{-1}; HRMS (EI) 457.1486 (calcd.), 457.1487 (obs.).

36b (Table 3, Entry 2)

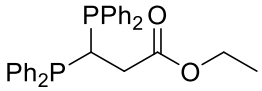

Off-white solid (79%). ^{1}H NMR (500 MHz, 298 K, C_6D_6) δ 7.77 - 7.74 (m, 4H), 7.60 - 7.57 (m, 4H), 7.05 (app. t, J_H = 7.2 Hz, 4H), 7.02 - 6.98 (m, 8H), 4.31 (t, $^{3}J_H$ = 5.8 Hz, 1H), 3.47 (q, $^{3}J_H$ = 7.2 Hz, 2H)), 2.65 (td, ^{3}J$_P$ = 9.0 Hz, ^{3}J$_H$ = 5.9 Hz, 2H), 0.69 (t, $^{3}J_H$ = 7.2 Hz, 3H); ^{13}C{^{1}H} NMR (126 MHz, 298 K, C_6D_6) δ 172.4 (m), 137.1 (app. t, *J* = 4.2 Hz), 136.7 (app. dd, *J* = 5.8 Hz, 5.1 Hz), 135.2 (app. t, *J* = 3.8 Hz) 133.9 (app. t, *J* = 10.5 Hz) 129.2, 128.9, 128.7 (app. t, *J* = 3.4 Hz) 128.4 (app. t, *J* = 3.8 Hz), 60.4, 34.9 (t, J_P = 9.3 Hz), 28.2 (t, J_P = 25.3 Hz) 13.9; ^{31}P{^{1}H} NMR (202 MHz, 298 K, C_6D_6) δ -6.3; IR (solid) ν 1722 cm^{-1}; HRMS (EI) 471.1643 (calcd.), 471.1647 (obs.).

Table 15. Crystal data and structure refinement for **36b**

Identification code	s16rlw5
Empirical formula	C29 H28 O2 P2
Formula weight	470.45
Temperature/K	150.00(10)
Crystal system	triclinic
Space group	P-1
a/Å	6.2505(2)
b/Å	22.1889(9)
c/Å	18.8017(6)
α/°	90
β/°	93.871(3)

γ/°	90
Volume/Å^3	1222.00(11)
Z	2
ρ_{calc}mg/mm^3	1.279
m/mm^{-1}	1.799
F(000)	496.0
Radiation	CuKα (λ = 1.54184)
2Θ range for data collection	4.209 to 73.343°
Index ranges	-12 ≤ h ≤ 10, -14 ≤ k ≤ 14, -15 ≤ l ≤ 15
Reflections collected	10428
Independent reflections	6225
Data/restraints/parameters	6225/0/280
Goodness-of-fit on F^2	1.042
Final R indexes [I>=2σ (I)]	R_1 = 0.0360, wR_2 = 0.0965
Final R indexes [all data]	R_1 = 0.0390, wR_2 = 0.0989
Largest diff. peak/hole / e Å^{-3}	0.53/-0.33

36c (Table 3, Entry 3)

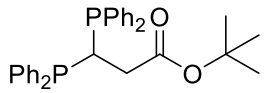

Off-white solid (75%). ^{1}H NMR (500 MHz, 298 K, C_6D_6) δ 7.77 - 7.74 (m, 4H), 7.06 (t, J_H = 7.2 Hz, 4H) 7.03 - 6.99 (m, 8H), 4.31 (t, ^3J_H = 5.5 Hz, 1H), 2.72 (td, ^3J_P = 9.3 Hz, ^3J_H = 5.4 Hz, 2H), 1.12 (s, 7H), 1.04 (s, 2H); ^{13}C{^{1}H} NMR (126 MHz, 298 K, C_6D_6) δ 171.6 (t, *J* = 2.9 Hz), 137.4 (app. t, *J* = 4.5 Hz), 136.9 (app. t, *J* = 5.7 Hz), 135.1 (app. t, *J* = 11.2 Hz), 134.0 (app. t, *J* = 10.5 Hz), 129.1, 128.9, 128.7(app. t, *J* = 3.5 Hz), 128.5(app. t, *J* = 4.1 Hz), 80.2, 35.9, 27.9, 27.8, 27.6 (t, J_P = 25.6 Hz); ^{31}P{^{1}H} NMR (202 MHz, 298 K, C_6D_6) δ -5.0; IR (solid) ν 1722 cm^{-1}; HRMS (EI) 499.1956 (calcd.), 499.1954 (obs.).

18a (Table 6, Entry 1)

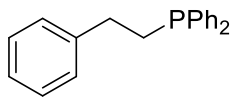

Colourless oil, 147 mg (88%). ^{1}H NMR (300 MHz, 298 K, $CDCl_3$) δ 7.47 – 7.15 (m, 14H), 2.73 - 2.67 (m, 2H), 2.39 - 2.33 (m, 2H); ^{13}C{^{1}H} NMR (75 MHz, 298 K, $CDCl_3$) δ 142.7 (d, *J* = 12.7 Hz), 138.6 (d, *J* = 19.2 Hz), 132.8 (d, *J* = 13.2 Hz), 128.9, 128.6 (d, *J* = 6.2 Hz), 128.2, 128.0, 126.1, 32.3 (d, *J* = 3.3 Hz), 30.2 (d, *J* = 7.7 Hz); ^{31}P{^{1}H}

NMR (121.5 MHz, 298 K, $CDCl_3$) δ -15.0; IR (solid) v 3055, 2936, 1603, 1585, 1481 cm^{-1}; HRMS (EI) 291.1303 (calcd.), 291.1297 (obs.). Small amounts of oxidised product observed by NMR.

18b (Table 6, Entry 2)

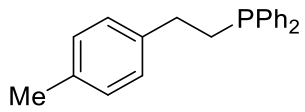

Colourless oil, 136 mg (79%). ^1H NMR (300 MHz, 298 K, $CDCl_3$) δ 7.58 - 7.55 (m, 4H), 7.43 - 7.41 (m, 6H), 7.17 (s, 4H), 2.83 - 2.75 (m, 2H), 2.48 - 2.40 (m, 2H), 2.40 (s, 3H); $^{13}C\{^1H\}$ NMR (75 MHz, 298 K, $CDCl_3$) δ 139.6 (d, *J* = 13.4 Hz), 138.5 (d, *J* = 12.7 Hz), 135.6, 132.8 (d, *J* = 18.3 Hz), 129.2, 128.7, 128.6 (d, *J* = 6.5 Hz), 128.1, 31.8 (d, *J* = 17.6 Hz), 30.4 (d, *J* = 12.5 Hz), 21.13; $^{31}P\{^1H\}$ NMR (121.5 MHz, 298 K, $CDCl_3$) δ -15.1; IR (solid) v 3052, 2915, 1590, 1516, 1482, 1437, 801, 862, 738, 693 cm^{-1}; HRMS (EI) $[M + H]^+$ 305.1454 (calcd.), 305.1452 (obs.)

18c (Table 6, Entry 3)

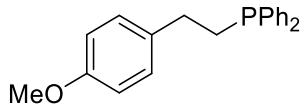

Colourless oil, 163 mg (89%). ^1H NMR (300 MHz, 298 K, $CDCl_3$) δ 7.63 - 7.60 (m, 4H), 7.46 - 7.43 (m, 6H), 7.23 (d, 2H, *J* = 8.7, 2.1 Hz), 6.99 - 6.92 (dd, 2H, *J* = 8.6, 2.3 Hz), 3.90 (s, 3H), 2.84 - 2.81 (m, 2H), 2.52 - 2.46 (m, 2H); $^{13}C\{^1H\}$ NMR (75 MHz, 298 K, $CDCl_3$) δ 158.0, 138.7 (d, *J* = 13.0 Hz), 134.6 (d, *J* = 13.3 Hz), 132.8 (d, *J* = 18.3 Hz), 129.1, 128.6, 128.5 (d, *J* = 6.5 Hz), 113.9, 55.3, 31.2 (d, *J* = 17.7 Hz), 30.4 (d, *J* =12.7 Hz); $^{31}P\{^1H\}$ NMR (121.5 MHz, 298 K, $CDCl_3$) δ -15.3; IR (solid) v 3053, 2934, 2904, 2833, 1610, 1584, 1510, 1464, 818, 734, 695, 717 cm^{-1}; HRMS (EI) $[M + H]^+$ 321.1403 (calcd.), 321.1403 (obs.)

18d (Table 6, Entry 4)

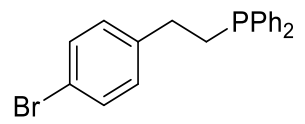

Colourless oil, 136 mg (65%). ^1H NMR (300 MHz, 298 K, $CDCl_3$) δ 7.54 - 7.33 (m, 12H), 7.09 (d, 2H, *J* = 8.3 Hz), 2.78 - 2.70 (m, 2H), 2.43 - 2.37 (m, 2H); $^{13}C\{^1H\}$ NMR (75 MHz, 298 K, $CDCl_3$) δ 141.5 (d, *J* = 12.7 Hz), 138.3 (d, *J* = 13.0 Hz), 132.8 (d, *J* = 18.3 Hz), 131.5, 130.1, 128.8, 128.6 (d, *J* = 6.5 Hz), 119.9, 31.7 (d, *J* = 18.0 Hz), 30.1 (d, *J* = 13Hz); $^{31}P\{^1H\}$ NMR (121.5 MHz, 298 K, $CDCl_3$) δ -15.4; IR (solid) v 3052,

2933, 1487, 1433, 842, 799, 736, 693 cm^{-1}; HRMS (EI) $[M + H]^+$ 369.0402 (calcd.), 369.0397 (obs.)

18e (Table 6, Entry 5)

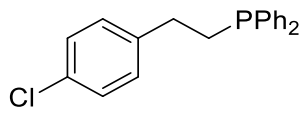

Colourless oil, 136 mg (74%, 114 h). ^{1}H NMR (300 MHz, 298 K, $CDCl_3$) δ 7.50 - 7.47 (m, 4H), 7.38 - 7.31 (m, 6H), 7.25 (dd, 2H, *J* = 8.6, 2.1 Hz), 7.10 (dd, 2H, *J* = 8.6, 2.1 Hz), 2.76 -2.68 (m, 2H), 2.39 - 2.34 (m, 2H); $^{13}C\{^1H\}$ NMR (75 MHz, 298 K, $CDCl_3$) δ 141.1 (d, *J* 13.0 Hz), 138.4 (d, *J* = 13.0 Hz), 132.9 (d, *J* = 18.6 Hz), 130.9 (d, *J* = 9.3 Hz), 129.7, 128.8, 128.7, 128.6 (d, *J* = 2.8 Hz), 31.7 (d, *J* = 18.0 Hz), 30.3 (d, *J* = 13.3 Hz); $^{31}P\{^1H\}$ NMR (121.5 MHz, 298 K, $CDCl_3$) δ -15.2; IR (solid) v 3064, 2898, 1591, 1492, 1435, 843, 801, 736, 720, 693 cm^{-1}; HRMS (EI) $[M + H]^+$ 325.0907 (calcd.), 325.0903 (obs.)

18f (Table 6, Entry 6)

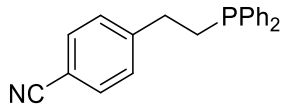

Colourless oil, 77 mg (43%). ^{1}H NMR (300 MHz, 298 K, $CDCl_3$) δ 7.56 (d, 2H, *J* = 8.4 Hz), 7.49 - 7.43 (m, 4H), 7.38 - 7.35 (m, 6H), 7.28 (d, 2H, *J* = 8.4 Hz), 2.92 - 2.67 (m, 2H), 2.47 - 2.31 (m, 2H); $^{13}C\{^1H\}$ NMR (75 MHz, 298 K, $CDCl_3$) δ 148.1 (d, *J* = 12.7 Hz), 137.9 (d, *J* = 12.2 Hz), 132.8 (d, *J* = 18.6 Hz), 132.4, 130.8 (d, *J* = 9.3Hz), 129.1 (d, *J* = 12.1 Hz), 128.7 (d, *J* = 6.8 Hz) 119.1, 110.0, 32.5 (d, *J* = 17.3 Hz), 29.7 (d, *J* = 13.4 Hz); $^{31}P\{^1H\}$ NMR (121.5 MHz, 298 K, $CDCl_3$) δ -15.4; IR (solid) v 3060, 2943, 2905, 2227, 1605, 1506, 1480, 1435, 822, 741, 695 cm^{-1}; HRMS (EI) $[M + H]^+$ 316.1250 (calcd.), 316.1245 (obs.)

18g (Table 6, Entry 7)

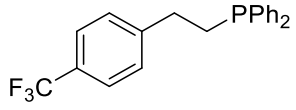

Colourless oil, 170 mg (83%). ^{1}H NMR (300 MHz, 298 K, $CDCl_3$) δ 7. 51 - 7.41 (m, 6H), 7.37 - 7.30 (m, 6H), 7.24 (d, 2H, *J* = 8.1 Hz), 2.80 - 2.72 (m, 2H), 2.38 - 2.33 (m, 2H); $^{13}C\{^1H\}$ NMR (75 MHz, 298 K, $CDCl_3$) δ 146.7 (d, *J* = 12.7 Hz), 138.3 (d, *J* = 12.7 Hz), 132.8 (d, *J* = 18.6 Hz), 128.7, 128.53. 128.45, 128.0 (d, *J* = 10.5 Hz), 126.1, 125.3 (q, *J* = 3.7 Hz), 32.2 (d, *J* = 18.3 Hz), 30.0 (d, *J* = 13.4 Hz); $^{31}P\{^1H\}$ NMR (121.5

MHz, 298 K, $CDCl_3$) δ -15.3; IR (solid) v 3049, 2922, 1590, 1567, 1480, 1434, 1323, 844, 820, 748, 735, 695 cm^{-1}; HRMS (EI) $[M + H]^+$ 359.1171 (calcd.), 359.1166 (obs.)

18h (Table 6, Entry 8)

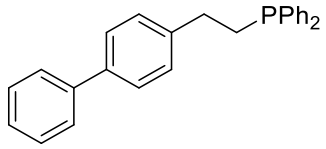

Colourless oil, 122 mg (58% at 60°C). ^1H NMR (300 MHz, 298 K, $CDCl_3$) δ 7.70 - 7.33 (m, 19H), 2.90 - 2.85 (m, 2H), 2.55 - 2.50 (m, 2H); $^{13}C\{^1H\}$ NMR (75 MHz, 298 K, $CDCl_3$) δ 141.7 (d, *J* = 13.0 Hz), 141.1, 139.0, 138.5 (d, *J* = 12.4 Hz), 132.7 (d, *J* = 18.6 Hz), 128.7, 128.62, 128.56, 128.50 (d, *J* = 6.5 Hz), 127.2, 127.03, 126.98, 31.9 (d, *J* =17.7 Hz), 30.2 (d, *J* = 12.4 Hz); $^{31}P\{^1H\}$ NMR (121.5 MHz, 298 K, $CDCl_3$) δ -14.9; IR (solid) v 3050, 2944, 2903, 1586, 1481, 1433, 821, 744, 693 cm^{-1}; HRMS (EI) $[M + H]^+$ 367.1610 (calcd.), 367.1606 (obs.)

18i (Table 6, Entry 9)

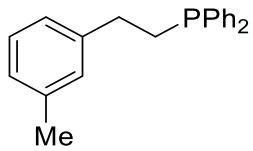

Colourless oil, 164 mg (95%). ^1H NMR (300 MHz, 298 K, $CDCl_3$) δ 7.63 - 7.60 (m, 4H), 7.46 - 7.42 (m, 6H), 7.29 (dd, 1H, *J* = 8.1, 7.2 Hz), 7.13 - 7.09 (m, 3H), 2.88 - 2.80 (m, 2H), 2.53 - 2.42 (m, 2H), 2.44 (s, 3H); $^{13}C\{^1H\}$ NMR (75 MHz, 298 K, $CDCl_3$) δ 142.6 (d, *J* = 13.4 Hz), 138.6 (d, *J* =13.0 Hz), 138.0, 134.0 (d, *J* = 16.8 Hz), 132.8 (d, *J* = 18.6 Hz), 129.0, 128.6 (*J* = 8.1 Hz), 128.4 (d, *J* = 5.3 Hz), 126.8, 125.2, 32.2, 30.3, 21.5; $^{31}P\{^1H\}$ NMR (121.5 MHz , 298 K, $CDCl_3$) δ -14.8; IR (solid) v 3052, 2917, 2856, 1608, 1586, 1480, 1433, 1377, 735, 695 cm^{-1}; HRMS (EI) $[M + H]^+$ 305.1454 (calcd.), 305.1454 (obs.)

18j (Table 6, Entry 10)

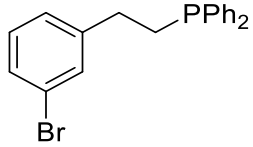

Colourless oil, 202 mg (96%). ^1H NMR (300 MHz, 298 K, $CDCl_3$) δ 7.55 - 7.52 (m, 4H), 7.42 - 7.36 (m, 8H), 7.18 - 7.15 (m, 2H), 2.80 - 2.72 (m, 2H), 2.44 - 2.39 (m, 2H); $^{13}C\{^1H\}$ NMR (75 MHz, 298 K, $CDCl_3$) δ 144.9 (d, *J* = 13.4 Hz), 138.1 (d, *J* = 12.4 Hz),

132.8 (d, *J* =18.6 Hz), 131.2, 130.0, 129.2, 128.8, 128.6 (d, *J* = 6.9 Hz), 126.9, 122.5, 31.9 (d, *J* = 18.3 Hz), 30.0 (d, *J* = 12.8 Hz); $^{31}P\{^{1}H\}$ NMR (121.5 MHz, 298 K, $CDCl_3$) δ -15.2; IR (solid) v 3057, 2943, 2923, 2830, 1583, 1567, 1491, 1475, 1464, 1431, 885, 796, 775, 739, 695 cm^{-1}; HRMS (EI) 369.0402 (calcd.), 369.0406 (obs.)

18k (Table 6, Entry 11)

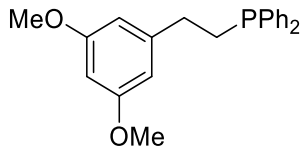

Colourless oil, 178 mg (89%). ^{1}H NMR (300 MHz, 298 K, $CDCl_3$) δ 7.54 - 7.42 (m, 4H), 7.41 - 7.39 (m, 6H), 6.41 (d, 2H, *J* = 2.3 Hz), 6.37 (t, 1H, *J* = 2.3 Hz), 3.81 (s, 6H) 2.78 - 2.70 (m, 2H) 2.47 - 2.41 (m, 2H); $^{13}C\{^{1}H\}$ NMR (75 MHz, 298 K, $CDCl_3$) δ 160.9, 145.1 (d, *J* = 13.4 Hz), 138.5, 133.0 (d, *J* = 18.6 Hz), 128.8, 128.6 (d, *J* = 6.5 Hz), 106.3, 98.0, 55.3, 32.6 (d, *J* = 18.0 Hz), 30.0 (d, *J* =12.4 Hz); $^{31}P\{^{1}H\}$ NMR (121.5 MHz, 298 K, $CDCl_3$) δ -14.9; IR (solid) v 3048, 2920, 2849, 1591, 1567, 1470, 1433, 843, 782 cm^{-1}; HRMS (EI) 351.1508 (calcd.), 351.1505 (obs.)

18l (Table 6, Entry 12)

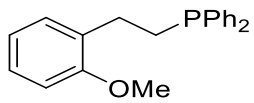

Colourless oil, 113 mg (62%). ^{1}H NMR (300 MHz, 298 K, $CDCl_3$) δ 7.64 - 7.59 (m, 2H), 7.47 - 7.42 (m, 6H), 7.32 - 7.23 (m, 2H), 7.01 (app. td, 1H, *J* = 7.4, 1.0 Hz), 6.93 (d, 1H, *J* = 8.1 Hz) 3.88 (s, 3H), 2.94 - 2.86 (m, 2H), 2.52 - 2.47 (m, 2H); $^{13}C\{^{1}H\}$ NMR (75 MHz, 298 K, $CDCl_3$) δ 157.3, 138.7 (d, *J* = 12.7 Hz), 132.8 (d, *J* = 18.3 Hz), 131.0 (d, *J* = 13.6 Hz), 129.6, 128.4 (d, *J* = 6.5 Hz), 127.4, 120.4, 110.2, 55.1, 28.4 (d, *J* = 12.1 Hz), 27.2 (d, *J* = 18.3 Hz); $^{31}P\{^{1}H\}$ NMR (121.5 MHz, 298 K, $CDCl_3$) δ -14.5; IR (solid) v 3059, 2948, 2922, 2902, 2830, 1600, 1583, 1490, 1464, 1432, 852, 742, 696 cm^{-1}; HRMS (EI) $[M + H]^+$ 321.1403 (calcd.), 321.1404 (obs.)

18m (Table 6, Entry 13)

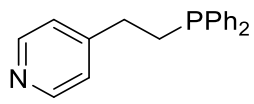

Colourless oil, 125 mg (75%, after 72 h). ^{1}H NMR (300 MHz, 298 K, $CDCl_3$) δ 8.46 (dd, 2H, *J* = 4.3, 1.7 Hz), 7.47 - 7.42 (m, 4H), 7.36 - 7.31 (m, 6H), 7.07 (dd, 2H, *J* = 4.3, 1.7 Hz), 2.76 -2.58 (m, 2H), 2.44 - 2.25 (m, 2H); $^{13}C\{^{1}H\}$ NMR (75 MHz, 298 K,

$CDCl_3$) δ 151.4 (d, *J* = 13.0 Hz), 149.9, 138.1 (d, *J* = 12.7 Hz), 132.8 (d, *J* = 18.6 Hz), 129.0, 128.7 (d, *J* = 6.8 Hz), 123.7, 31.6 (d, *J* = 18.7 Hz), 29.1 (d, *J* = 13.3 Hz); $^{31}P\{^1H\}$ NMR (121.5 MHz, 298 K, $CDCl_3$) δ -15.2; IR (solid) v 3051, 2928, 1599, 1559, 1480, 1433, 850, 801, 737, 694 cm^{-1}; HRMS (EI) $[M + H]^+$ 292.1250 (calcd.), 292.1246 (obs.)

18n (Table 6, Entry 14)

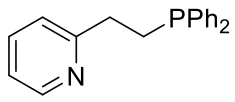

Colourless oil, 143 mg (86%, after 72 h). ^1H NMR (300 MHz, 298 K, $CDCl_3$) δ 8.56 (d, 1H, *J* = 4.1 Hz), 7.62 - 7.43 (m, 5H), 7.43 - 7.29 (m, 6H), 7.20 - 7.03 (m, 2H), 3.05-2.82 (m, 2H), 2.64 - 2.48 (m, 2H); $^{13}C\{^1H\}$ NMR (75 MHz, 298 K, $CDCl_3$) δ 161.9 (d, *J* = 13.3 Hz), 149.5, 138.5 (d, *J* = 13.0 Hz), 136.4, 132.9 (d, *J* = 18.6 Hz), 128.7, 128.6 (d, *J* = 6.8 Hz), 122.8, 121.3, 34.7 (d, *J* = 17.7 Hz), 28.1 (d, *J* = 12.4 Hz); $^{31}P\{^1H\}$ NMR (121.5 MHz, 298 K, $CDCl_3$) δ -14.6; IR (solid) v 3046, 2920, 2949, 1590, 1567, 1470, 1479, 1433, 843, 781, 749, 735, 723, 697, cm^{-1}; HRMS (EI) $[M + H]^+$ 292.1250 (calcd.), 292.1249 (obs.)

18o (Table 6, Entry 15)

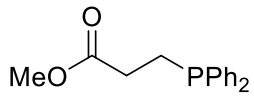

Colourless oil, 120 mg (69%). ^1H NMR (300 MHz, 298 K, $CDCl_3$) δ 7.50 - 7.47 (m, 4H), 7.37 - 7.35 (m, 6H), 3.66 (s, 3H), 2.45 - 2.42 (m, 4H); $^{13}C\{^1H\}$ NMR (75 MHz, 298 K, $CDCl_3$) δ 173.5 (d, *J* = 14.9 Hz), 137.7 (d, *J* =12.1 Hz), 132.7 (d, *J* = 18.3 Hz), 128.8, 128.5 (d, *J* = 6.5 Hz), 51.7, 30.5 (d, *J* = 19.3 Hz), 22.9 (d, *J* = 11.5 Hz); $^{31}P\{^1H\}$ NMR (121.5 MHz, 298 K, $CDCl_3$) δ -14.9; IR (solid) v 3054, 2950, 1735, 1585, 1481, 1433, 1354, 848, 736, 694 cm^{-1}; HRMS (EI) $[M + H]^+$ 273.1039 (calcd.), 273.1040 (obs.)

18p (Table 6, Entry 16)

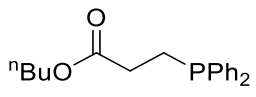

Colourless oil, 142 mg (76%). ^1H NMR (300 MHz, 298 K, $CDCl_3$) δ 7.49 - 7.46 (m, 4H), 7.37 - 7.35 (m, 6H), 4.08 (t, 2H, *J* = 6.7 Hz), 2.44 - 2.39 (m, 4H), 1.61 (m, 2H), 1.37 (m, 2H), 0.95 (t, 3H, *J* = 7.4 Hz); $^{13}C\{^1H\}$ NMR (75 MHz, 298 K, $CDCl_3$) δ 173.3 (d, *J* = 15.2 Hz), 137.8 (d, *J* = 18.6 Hz), 132.8 (d, *J* = 18.6 Hz), 128.9, 128.6 (d, *J* = 6.8 Hz), 64.6, 30.9, 30.7, 23.0 (d, *J* = 11.5 Hz), 19.2, 13.8; $^{31}P\{^1H\}$ NMR (121.5 MHz,

298 K, $CDCl_3$) δ -14.9; IR (solid) v 3054, 2958, 2872, 1731, 1586, 1481, 1465, 1433, 1348, 737, 696 cm^{-1}; HRMS (EI) 315.1508 (calcd.), 315.1509 (obs.)

38a (Table 11, Entry 1)

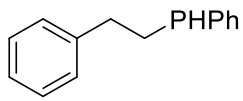

Colourless oil (61% SHP). ^1H NMR (500 MHz, 298 K, C_6D_6) δ 7.34 (s, 2H), 7.13 - 7.07 (m, 6H), 6.94 - 6.93 (m, 2H), 4.09 (dm, 1H, *J* = 210 Hz), 2.61 - 2.56 (m, 2H), 1.93 - 1.84 (m, 2H); $^{13}C\{^1H\}$ NMR (125 MHz, 298 K, $CDCl_3$) δ 142.1, 139.7, 135.7 (d, *J* = 4.8 Hz), 133.6 (d, *J* = 1.9 Hz), 128.3 (d, *J* = 4.8 Hz), 128.1, 127.9, 125.9, 34.5 (d, *J* = 2.9 Hz), 25.2 (d, *J* = 3.8 Hz); $^{31}P\{^1H\}$ NMR (202 MHz, 298 K, $CDCl_3$) δ -52.3; IR (solid) v 2912.37, 2283.31, 1602.82, 1495.35, 1434.47, 740.47, 720.58, 692.95 cm^{-1}; HRMS (EI) 213.0828 (calcd.), 213.0834 (obs.).

38b (Table 11, Entry 2)

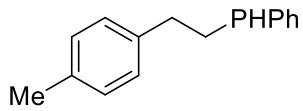

Colourless oil (18% SHP). ^1H NMR (500 MHz, 298 K, C_6D_6) δ 7.36 - 7.33 (m, 2H), 7.07 - 7.04 (m, 3H), 6.95 (d, 2H, *J* = 7.9 Hz), 6.88 (d, 2H, *J* = 7.9 Hz), 4.10 (dm, 1H, *J* = 206.3 Hz), 2.67 - 2.53 (m, 2H), 2.12 (s, 3H), 1.90 - 1.80 (m, 2H); $^{13}C\{^1H\}$ NMR (125 MHz, 298 K, $CDCl_3$) δ 139.1 (d, *J* = 7.3 Hz), 135.8 (d, *J* = 12.3 Hz), 133.5 (d, *J* = 15.5 Hz), 129.1, 129.0, 128.3 (d, *J* = 5.6 Hz), 128.1, 128.0, 34.0 (d, *J* = 8.1 Hz), 25.3 (d, *J* = 13.5 Hz), 20.7; $^{31}P\{^1H\}$ NMR (202 MHz, 298 K, $CDCl_3$) δ -53.01; IR (solid) v 2920, 2283, 1591, 1515, 1436, 807, 740 cm^{-1}; HRMS (EI) 227.0984 (calcd.), 227.0987 (obs.). (Oxidised product present)

38c (Table 11, Entry 3)

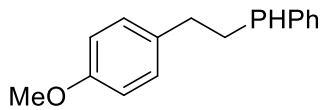

Colourless oil (4.9 SHP : 1 DHP IG^{31}P)(82% SHP/ 17% DHP based on THF). ^1H NMR (500 MHz, 298 K, C_6D_6) δ 7.40 - 7.32 (m, 2H), 7.09 - 7.00 (m, 3H), 6.88 (d, 2H, *J* = 10 Hz), 6.76 (d, 2H, *J* = 10 Hz), 4.12 (dm, 1 H, *J* = 206.3 Hz), 3.33 (s, 3H), 2.65 - 2.56 (m, 2H), 1.98 - 1.86 (m, 2H); $^{31}P\{^1H\}$ NMR (202 MHz, 298 K, $CDCl_3$) δ -52.8; IR (solid) v cm^{-1} 2930.06, 2283.25, 1610.63, 1511.18, 1434.35, 820.19, 741.99, 695.98; HRMS (EI) 243.0933 (calcd.), 243.0936 (obs.).

38d (Table 11, Entry 4)

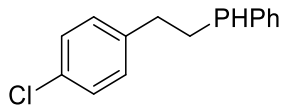

Colourless oil (76% SHP). ^{1}H NMR (500 MHz, 298 K, C_6D_6) δ 7.34 - 7.32 (m, 2H), 7.10 - 7.08 (m, 3H), 7.06 (d, 2H, *J* = 8.3 Hz), 6.58 (d, 2H, *J* = 8.3 Hz), 4.05 (ddd, 1 H, *J* = 206.4, 7.8, 5.9 Hz), 2.46 - 2.35 (m, 2H), 1.80 - 1.66 (m, 2H); ^{13}C{^{1}H} NMR (125 MHz, 298 K, C_6D_6) δ 139.8 (d, *J* = 7.6 Hz), 134.7 (d, *J* = 12.4 Hz), 132.9 (d, *J* = 16.2 Hz) 131.1, 128.9, 127.7, 127.5, 127.3, 33.0 (d, *J* = 8.6 Hz), 24.2 (d, *J* = 14.3 Hz); ^{31}P{^{1}H} NMR (202 MHz, 298 K, $CDCl_3$) δ -53.0; IR (solid) v 2923, 2285, 1490, 1434, 734, 695 cm^{-1}; HRMS (EI) 265.0544 (calcd.), 265.0548 (obs.).

38e (Table 11, Entry 5)

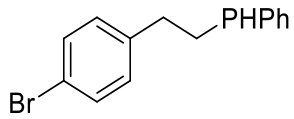

Colourless oil (80% SHP/14% DHP based on IG^{31}P)(93% SHP/3% DHP based on THF). ^{1}H NMR (500 MHz, 298 K, C_6D_6) δ 7.34 - 7.30 (m, 2H), 7.20 (d, 2H, *J* = 8.3 Hz), 7.08 - 7.07 (m, 3H), 6.51 (d, 2H, *J* = 8.3 Hz), 4.03 (ddd, 1H, *J* = 206.4, 7.3, 5.9 Hz), 2.41 - 2.32 (m, 2H), 1.81 - 1.64 (m, 2H); ^{13}C{^{1}H} NMR (125 MHz, 298 K, C_6D_6) δ 133.5 (d, *J* = 15.6 Hz), 131.3, 129.8, 128.3 (d, *J* = 5.7 Hz), 128.2, 128.1, 128.0, 127.9, 33.6 (d, *J* = 8.3 Hz) 24.8 (d, *J* = 13.7 Hz); ^{31}P{^{1}H} NMR (202 MHz, 298 K, $CDCl_3$) δ -52.73; IR (solid) v 2924, 2283, 1586, 1487, 1434, 801, 741, 695 cm^{-1}; HRMS (EI) 291.1297 (calcd.), 291.1304 (obs.).

38f (Table 11, Entry 6)

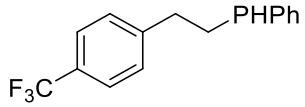

Colourless oil (60% SHP). ^{1}H NMR (400 MHz, 298 K, C_6D_6) δ 7.43 - 7.39 (m, 1H), 7.31 - 7.25 (m, 4H), 7.08 - 7.05 (m, 2H), 6.74 - 6.72 (m, 1H), 6.65 - 6.63 (m, 1H), 4.00 (d, 1H, *J* = 205.8 Hz), 2.43 - 2.37 (m, 2H), 1.74 - 1.62 (m, 2H);); ^{13}C{^{1}H} NMR (100 MHz, 298 K, C_6D_6) δ 135.8, 134.3 (d, *J* = 15.6 Hz), 133.3 (d, *J* = 19.5 Hz), 130.0, 129.2, 129.1, 128.9, 125.9, 34.8 (d, *J* = 8.1 Hz), 25.3 (d, *J* = 14.5 Hz); ^{31}P{^{1}H} NMR (162 MHz, 298 K, C_6D_6) δ -52.6; IR (solid) v 3073, 2310, 1550, 1479, 1366, 759, 655 cm^{-1}.

38g (Table 11, Entry 7)

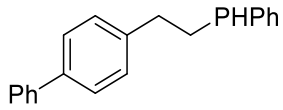

Colourless oil (79% SHP). ^{1}H NMR (400 MHz, 298 K, C_6D_6) δ 7.55 - 7.51 (m, 1H), 7.50 - 7.47 (m, 2H), 7.43 - 7.34 (m, 4H), 7.23 - 7.19 (m, 2H), 7.09 - 7.03 (m, 3H), 6.97 - 6.95 (m, 2H), 4.11 (ddd, 1H, *J* = 207.4, 7.6, 6.4 Hz), 2.72 - 2.57 (m, 2H), 1.97 - 1.85 (m, 2H); ^{13}C{^{1}H} NMR (100 MHz, 298 K, C_6D_6) δ 141.8 (d, *J* = 11.3 Hz), 141.2, 139.1 (d, *J* = 2.2 Hz), 133.6 (d, *J* = 15.5 Hz), 128.7, 128.6, 127.2, 127.1, 127.0, 127.0, 126.9, 34.1 (d, *J* = 8.2 Hz), 25.1 (d, *J* = 13.7 Hz); ^{1}P{^{1}H} NMR (162 MHz, 298 K, C_6D_6) δ -52.7; IR (solid) ν 3065, 2284, 1602, 1432, 820, 747, 695 cm^{-1}; HRMS (EI) 291.1304 (calcd.), 291.1297 (obs.).

38h (Table 11, Entry 8)

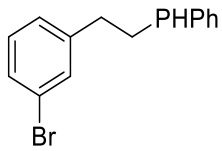

Colourless oil (76% SHP). ^{1}H NMR (400 MHz, 298 K, C_6D_6) δ 7.28 - 7.26 (m, 2H), 7.15 (m, 2H, partially obscured by solvent), 7.08 - 7.04 (m, 3H), 6.69 - 6.65 (m, 1H), 6.60 - 6.59 (m, 1H), 3.98 (dm, 1H, *J* = 206.5 Hz), 2.38 - 2.29 (m, 2H), 1.74 - 1.57 (m, 2H); ^{13}C{^{1}H} NMR (101 MHz, 298 K, C_6D_6, C-P not observed) δ 133.5 (d, *J* = 15.3 Hz), 131.2, 129.8, 129.7, 129.0, 128.4 (d, *J* = 5.6 Hz), 128.0, 126.6, 122.5, 33.9 (d, *J* = 8.6 Hz), 24.6 (d, *J* = 14.0 Hz); ^{31}P{^{1}H} NMR (162 MHz, 298 K, $CDCl_3$) δ -52.6; IR (solid) ν 2923, 2283, 1593, 1567, 1475, 1434, 882, 781, 741, 694 cm^{-1}; HRMS (EI) 293.0089 (calcd.), 293.0095 (obs.).

38i (Table 11, Entry 9)

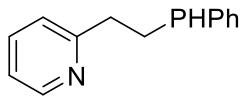

Colourless oil (60% SHP). ^{1}H NMR (500 MHz, 298 K, C_6D_6) δ 8.54 - 8.53 (m, 1H), 7.59 - 7.57 (m, 1H), 7.54 - 7.51 (m, 2H), 7.34 - 7.32 (m, 3H), 7.12 - 7.10 (m, 2H), 4.18 (ddd, 1H, *J* = 211.0, 7.9, 6.3 Hz), 2.98 - 2.91 (m, 2H), 2.31 - 2.22 (m, 2H); ^{13}C{^{1}H} NMR (125 MHz, 298 K, $CDCl_3$) δ 161.4 (d, *J* = 7.8 Hz), 149.3, 136.3, 133.6 (d, *J* = 15.4 Hz), 128.5, 128.4, 128.2, 122.7. 121.2, 36.8 (d, *J* = 7.5 Hz), 23.2 (d, *J* = 12.5 Hz); ^{31}P{^{1}H} NMR (202 MHz, 298 K, $CDCl_3$) δ -51.71; IR (solid) ν 2913.84, 2279.32,

1590.97, 1474.00, 1433.93, 811.73, 741.52 cm^{-1}; HRMS (EI) 216.0937 (calcd.), 216.0939 (obs.).

38j (Table 11, Entry 10)

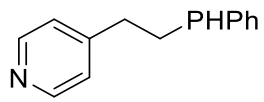

Colourless oil (75% SHP). ^{1}H NMR (500 MHz, 298 K, C_6D_6) δ 8.51 - 8.50 (m, 2H), 7.32 - 7.29 (m, 2H), 7.09 - 7.07 (m, 3H), 6.51 - 6.50 (m, 2H), 4.00 (ddd, 1H, *J* = 206.9, 7.8, 5.9 Hz), 2.36 - 2.25 (m, 2H), 1.73 - 1.62 (m, 2H); $^{13}C\{^{1}H\}$ NMR (125 MHz, 298 K, $CDCl_3$) δ 150.0, 133.5 (d, *J* = 15.6 Hz), 128.4 (d, *J* = 5.7 Hz), 128.2, 128.1 (d, *J* = 8.6 Hz), 127.9,123.2, 33.4(d, *J* = 7.6 Hz), 23.7 (d, *J* = 14.3 Hz); $^{31}P\{^{1}H\}$ NMR (202 MHz, 298 K, $CDCl_3$) δ -52.47; HRMS (EI) 232.0886 (calcd.), 232.0889 (obs.).

38k (Table 11, Entry 11)

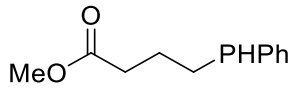

Colourless oil (81% SHP). ^{1}H NMR (500 MHz, 298 K, C_6D_6) δ 7.34 - 7.29 (m, 2H), 7.03 (m, 3H), 4.02 (d, 1H, *J* = 207.4 Hz), 3.28 (s, 3H), 2.18 - 2.17 (m, 2H), 1.88 - 1.86 (m, 2H); $^{31}P\{^{1}H\}$ NMR (202 MHz, 298 K, $CDCl_3$) δ -51.2; IR (solid) ν 2923, 2280, 1593, 1568, 1475, 1434 cm^{-1}; HRMS (EI) 181.0413 (calcd.), 181.0414 (obs.).

38l (Table 11, Entry 12)

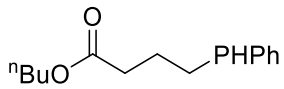

Colourless oil (74 % SHP). ^{1}H NMR (500 MHz, 298 K, C_6D_6) δ 7.32 - 7.29 (m, 2H), 7.03 - 7.02 (m, 3H), 4.06 (ddd, 1H, *J* = 207.9, 8.3, 5.9 Hz), 3.95 - 3.92 (m, 2H), 2.28 - 2.19 (m, 2H), 2.00 - 1.89 (m, 2H), 1.38 - 1.32 (m, 2H), 1.18 - 1.12 (m, 2H), 0.76 - 0.73 (m, 3H); $^{13}C\{^{1}H\}$ NMR (125 MHz, 298 K, $CDCl_3$, Carbonyl Carbon not observed) δ 134.4, 129.1 (d, *J* = 5.7 Hz), 128.8 (d, *J* = 18.1 Hz), 128.7, 64.6, 33.5 (d, *J* = 8.6), 31.3, 19.7, 19.3, 19.2, 14.1; $^{31}P\{^{1}H\}$ NMR (202 MHz, 298 K, $CDCl_3$) δ -51.19; IR (solid) ν 2958.59, 2873.06, 2285.06, 1730.36, 1600.85, 1464.89, 1435.01, 1388.81, 803.34, 737.19 cm^{-1}; HRMS (EI) 291.1303 (calcd.), 291.1297 (obs.).

7.1 Double Hydrophosphination Products

39a (Table 12, Entry 1)

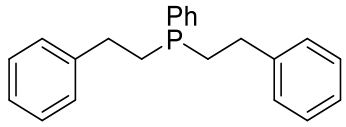

Colourless oil (81% DHP). ^{1}H NMR (500 MHz, 298 K, C_6D_6) δ 7.50 - 7.48 (m, 2H), 7.20 - 7.18 (m, 6H), 7.14 - 7.04 (m, 3H), 7.00 - 6.99 (m, 4H), 2.67 - 2.54 (m, 4H), 1.93 - 1.81 (m, 4H); ^{13}C{^{1}H} NMR (125 MHz, 298 K, $CDCl_3$) δ 142.8 (d, *J* = 11.6 Hz), 138.0 (d, *J* = 14.9 Hz), 132.6 (d, *J* = 18.9 Hz), 129.1, 128.6, 128.5, 128.2, 126.0, 32.3 (d, *J* = 15.3 Hz), 30.3 (d, *J* = 12.9 Hz); ^{31}P{^{1}H} NMR (121.5 MHz, 298 K, $CDCl_3$) δ -23.40; HRMS (EI) 319.1610 (calcd.), 319.1614 (obs.).

39b (Table 12, Entry 2)

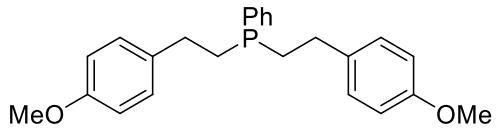

Colourless oil (64% DHP). ^{1}H NMR (500 MHz, 298 K, C_6D_6) δ 7.66 - 7.63 (m, 2H), 7.47 - 7.42 (m, 3H), 7.13 (d, 4H, *J* = 8.6 Hz), 6.88 (d, 4H, *J* = 8.6 Hz), 3.82 (s, 6H), 2.75 - 2.64 (m, 4H), 2.13 - 2.01 (m, 4H); ^{13}C{^{1}H} NMR (125 MHz, 298 K, $CDCl_3$) δ 157.9, 134.9 (d, *J* = 11.7 Hz), 132.6 (d, *J* = 18.8 Hz), 129.3 (d, *J* = 6.3 Hz), 129.1, 129.0, 128.5 (d, *J* = 7.0), 113.9, 55.3, 31.4 (d, *J* = 15.3 Hz), 30.6 (d, *J* = 12.9 Hz); ^{31}P{^{1}H} NMR (202 MHz, 298 K, $CDCl_3$) δ -24.44; IR (solid) ν 2931.59, 1610.38, 1583.41, 1509.68, 1463.68, 1434.16, 817.61, 742.98, 696.58 cm^{-1}; HRMS (EI) 379.1821 (calcd.), 379.1826(obs.).

39c (Table 12, Entry 3)

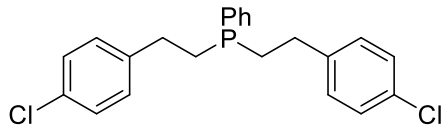

Colourless oil (74% DHP). ^{1}H NMR (300 MHz, 298 K, C_6D_6) δ 7.53 - 7.52 (m, 2H), 7.27 - 7.25 (m, 3H), 7.17 (d, 4H, *J* = 8.3 Hz), 6.74 (d, 4H, *J* = 8.3 Hz), 2.54 - 2.46 (m, 4H), 1.84 - 1.74 (m, 4H); ^{13}C{^{1}H} NMR (125 MHz, 298 K, $CDCl_3$) δ 142.8 (d, *J* = 11.6 Hz), 132.5 (d, *J* = 18.9 Hz), 129.0, 128.6, 128.5, 128.4, 128.1, 126.0, 32.2 (d, *J* = 15.3 Hz), 30.3 (d, *J* = 12.9 Hz); ^{31}P{^{1}H} NMR (202 MHz, 298 K, $CDCl_3$) δ -24.6

39d (Table 12, Entry 4)

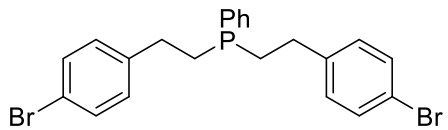

Colourless oil (96% DHP). ^{1}H NMR (500 MHz, 298 K, C_6D_6) δ 7.49 - 7.47 (m, 2H), 7.34 - 7.30 (m, 7H), 6.95 - 6.93 (m, 4H), 2.60 - 2.48 (m, 4H), 1.99 - 1.86 (m, 4H); ^{13}C{^{1}H} NMR (125 MHz, 298 K, $CDCl_3$) δ 141.4 (d, *J* = 11.3 Hz), 137.3 (d, *J* = 14.5 Hz), 132.5 (d, *J* = 19.2 Hz), 131.4, 129.8, 129.2, 128.5 (d, *J* = 7.2 Hz), 119.7, 31.6 (d, *J* = 15.7 Hz) 30.2 (d, *J* = 13.2 Hz); ^{31}P{^{1}H} NMR (202 MHz, 298 K, C_6D_6) δ -24.2.

39e (Table 12, Entry 5)

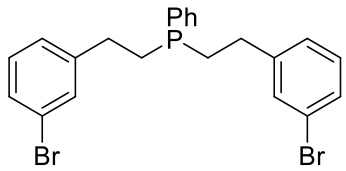

Colourless oil (64% DHP). ^{1}H NMR (400 MHz, 298 K, C_6D_6) δ 7.36 (m_{br}, 2H), 7.16 - 7.15 (m, 3H, partially obscured by solvent), 7.13 - 7.12 (m, 4H, partially obscured by solvent), 6.73 - 6.64 (m, 4H), 2.39 - 2.32 (m, 4H), 1.67 - 1.55 (m, 4H); ^{13}C{^{1}H} NMR (101 MHz, 298 K, $CDCl_3$) δ 144.9 (d, *J* = 11.5 Hz), 132.7, 132.5, 131.2, 130.0, 129.3, 129.2, 128.7 (d, *J* = 7.3 Hz), 126.9, 122.5, 32.0 (d, *J* = 16.0 Hz), 30.1 (d, *J* = 13.3 Hz); ^{31}P{^{1}H} NMR (162 MHz, 298 K, $CDCl_3$) δ -23.5.

39f (Table 1, Entry 6)

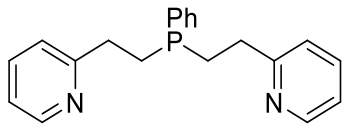

Colourless oil (92% DHP). ^{1}H NMR (400 MHz, 298 K, $CDCl_3$) δ 8.56 - 8.55 (m, 2H), 7.66 - 7.58 (m, 4H), 7.42 - 7.40 (m, 3H), 7.15 - 7.12 (m, 4H), 2.96 - 2.89 (m, 4H), 2.27 - 2.23 (m, 4H); ^{13}C{^{1}H} NMR (125 MHz, 298 K, $CDCl_3$) δ 161.9, 149.2, 136.5, 132.6 (d, *J* = 19.1 Hz), 129.0, 128.5, 128.4, 122.6, 121.1, 34.5 (d, *J* = 16.2 Hz), 28.0 (d, *J* =12.4 Hz); ^{31}P{^{1}H} NMR (162 MHz, 298 K, $CDCl_3$) δ -22.9; HRMS (EI) 336.1392 (calcd.), 336.1395 (obs.).

40

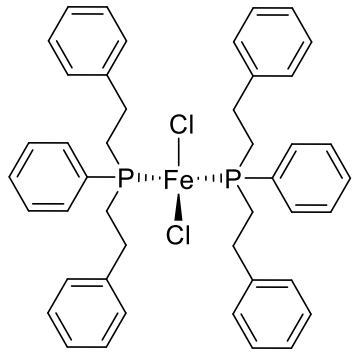

Table 7: Crystal data and structure refinement for **40**.

Identification code	e15rlw5
Empirical formula	$C_{44}H_{46}Cl_2FeP_2$
Formula weight	763.54
Temperature/K	150(2)
Crystal system	monoclinic
Space group	P 21/c
a/Å	19.8018(7)
b/Å	10.4550(4)
c/Å	19.1365(7)
α/°	90
β/°	90.463(3)
γ/°	90
Volume/Å^3	3961.7(3)
Z	4
ρ_{calc}mg/mm^3	1.280
m/mm^{-1}	0.626
F(000)	1600
Radiation	MoKα (λ = 0.71073)
2Θ range for data collection	3.7170 to 28.1710°
Index ranges	-20 ≤ h ≤ 20, -13 ≤ k ≤ 13, -24 ≤ l ≤ 24
Reflections collected	21880
Independent reflections	12709
Data/restraints/parameters	12709/0/443
Goodness-of-fit on F^2	0.938
Final R indexes [I>=2σ (I)]	R_1 = 0.0600, wR_2 = 0.1445
Final R indexes [all data]	R_1 = 0.1036, wR_2 = 0.1550
Largest diff. peak/hole / e Å^{-3}	0.93/-0.55

36

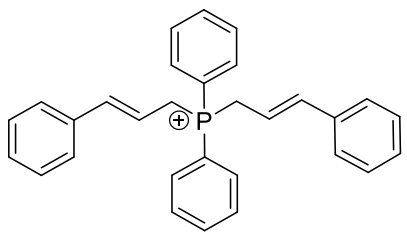

Table 16. Crystal data and structure refinement for **36**.

Identification code	k14rlw2
Empirical formula	$C_{30}H_{28}P$
Formula weight	419.49
Temperature/K	293(2)
Crystal system	triclinic
Space group	P-1
a/Å	9.2360(2)
b/Å	13.0810(3)
c/Å	13.8270(3)
α/°	114.9100(10)
β/°	97.3700(10)
γ/°	109.0750(10)
Volume/Å^3	1361.27(5)
Z	2
ρ_{calc}mg/mm^3	1.023
m/mm^{-1}	0.113
F(000)	446.0
Radiation	MoKα (λ = 0.71073)
2Θ range for data collection	5.956 to 55.058°
Index ranges	-12 ≤ h ≤ 11, -16 ≤ k ≤ 16, -17 ≤ l ≤ 17
Reflections collected	30283
Independent reflections	6225
Data/restraints/parameters	6225/0/280
Goodness-of-fit on F^2	1.062
Final R indexes [I>=2σ (I)]	R_1 = 0.0560, wR_2 = 0.1490
Final R indexes [all data]	R_1 = 0.0828, wR_2 = 0.1585
Largest diff. peak/hole / e Å^{-3}	0.27/-0.35

28

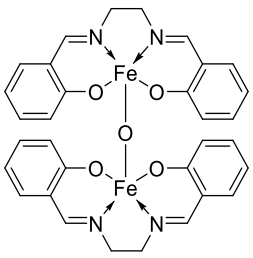

Dark red solid (143 mg, 72%). IR (solid) v 3049, 1610, 1597, 851 cm^{-1}; m.p. (decomp.) 296 °C.

Crystal structure obtained, with compound data being comparable to other published methods.[113-82]

Table 17. Crystal data and structure refinement for **28**.

Identification code	k14rlw1
Empirical formula	C_{32} H_{28} Fe_2 N_4 O_5
Formula weight	660.28
Temperature	150(2) K
Wavelength	0.71073 Å
Crystal system	Triclinic
Space group	P-1
Unit cell dimensions	a = 10.7340(3)Å alpha = 67.142 (1)°
	b = 10.8150(2)Å beta = 85.858 (1)°
	c = 13.7380(4)Å gamma = 73.156 (2)°
Volume	1405.06 (6) $Å^3$
Z	2
Density (calculated)	1.561 Mg/m^3
Absorption coefficient	1.083 mm^{-1}
F(000)	680
Crystal size	0.15 x 0.1 x 0.07 mm
Theta range for data collection	3.71 to 24.99 °.
Index ranges	-12<=h<=12; -12<=k<=12; -16<=l<=16
Reflections collected	20793
Independent reflections	4911 [R(int) = 0.0669]
Reflections observed (>2sigma)	3673
Data Completeness	0.992
Absorption correction	Semi-empirical from equivalents
Max. and min. transmission	0.989 and 0.899
Refinement method	Full-matrix least-squares on F^2
Data / restraints / parameters	4911 / 0 / 388
Goodness-of-fit on F^2	1.035
Final R indices [I>2sigma(I)]	R1 = 0.0404 *wR*2 = 0.0837
R indices (all data)	R1 = 0.0672 *wR2* = 0.0933
Largest diff. peak and hole	0.319 and -0.365 $eÅ^{-3}$

Table 18. elemental analysis for **28**.

Element	Expected (%)	Found (1)	Found (2)
Carbon	59.66	59.47	59.45
Hydrogen	4.38	4.30	4.26
Nitrogen	8.70	8.61	8.55

29

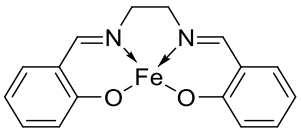

Yellow solid (276 mg, 77%). IR (solid) v 2966, 1638, 1606 cm^{-1}; m.p. (decomp.) 174 °C. Compound data is comparable to other published data.[83,84]

Table 19. elemental analysis for **29**

Element	Expected (%)	Found (1)	Found (2)
Carbon	58.21	58.29	58.22
Hydrogen	4.27	4.12	4.16
Nitrogen	8.49	8.11	8.17

8 Appendix

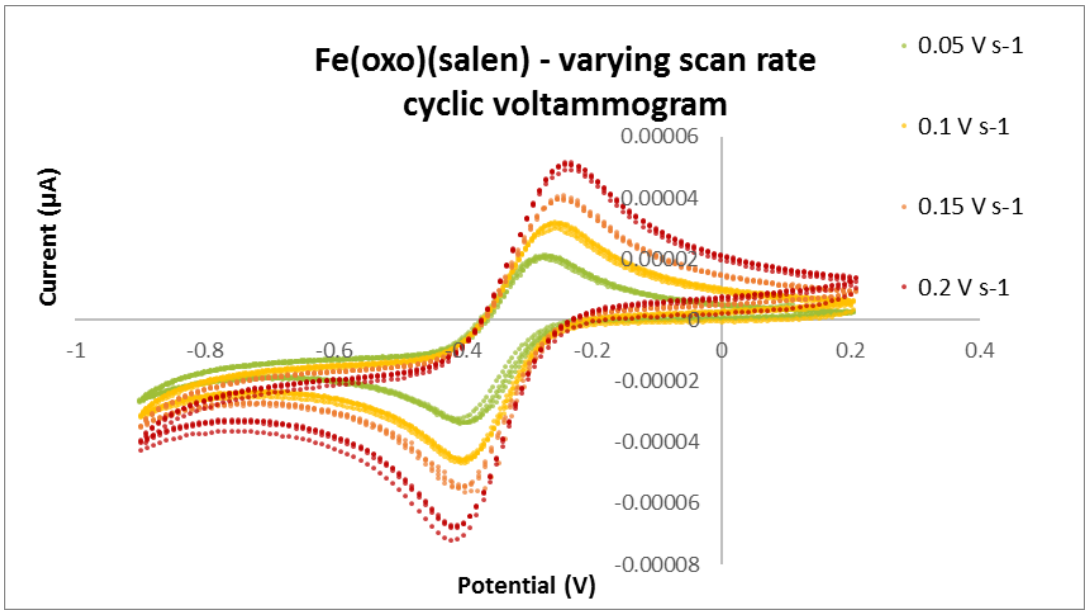

Figure 37. Fe^{III}_2-μ-oxo(salen)$_2$ voltammogram with varying scan rates (mV s^{-1})

Scans were taken following successive additions of increasing quantities of styrene. A clear shift in peak position is seen from following the reaction with styrene (**Figure 36**).

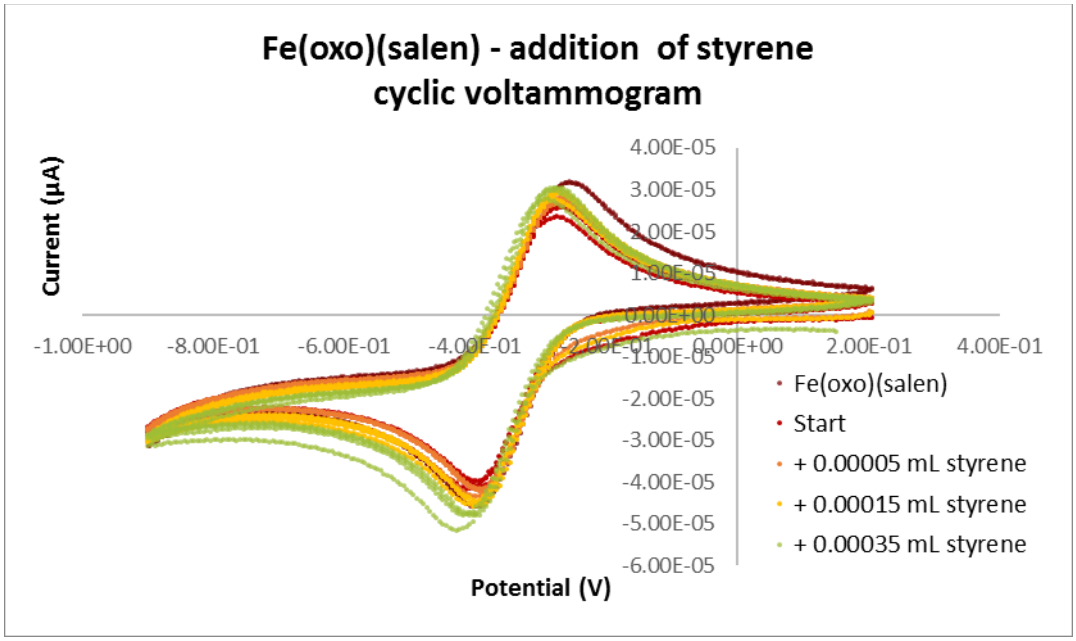

Figure 38. Fe^{III}_2-μ-oxo(salen)$_2$ –styrene addition - scan rate 50 mVs^{-1}

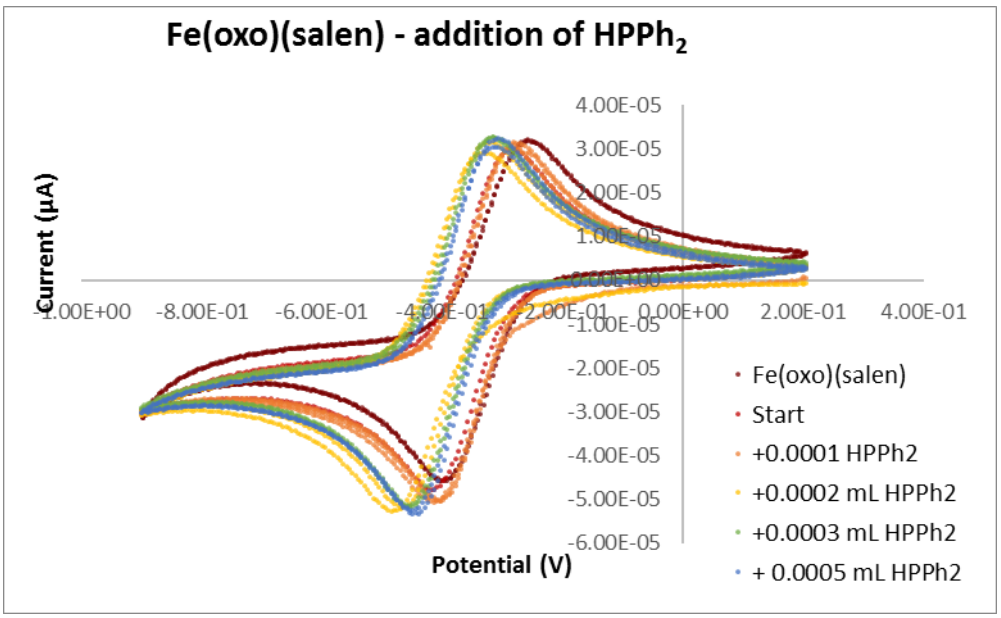

Figure 39. Fe^{III}_2-μ-oxo(salen)$_2$ – $HPPh_2$ addition - scan rate 50 mVs^{-1}

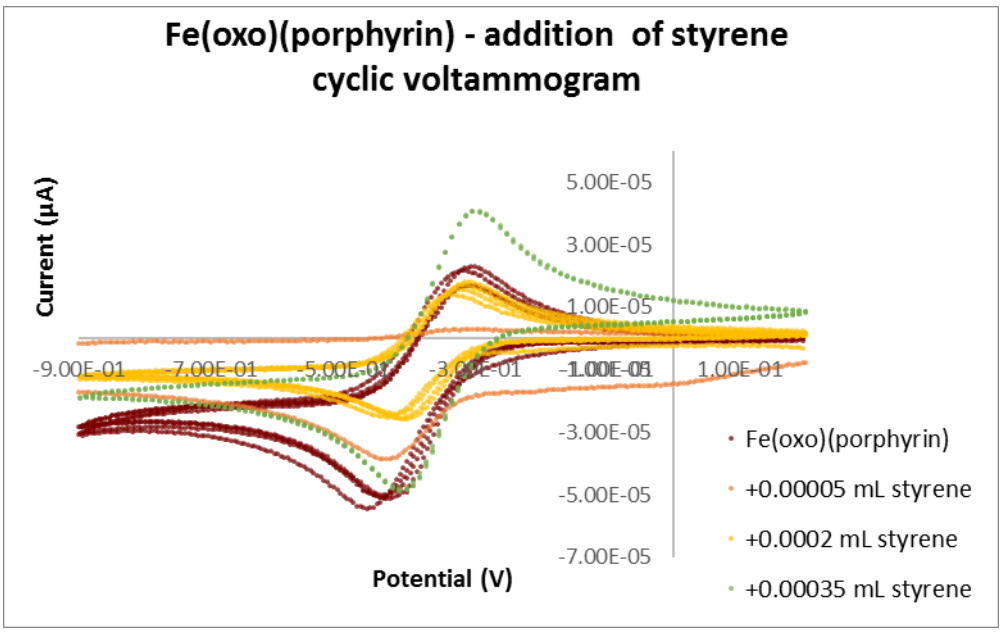

Figure 40. Fe^{III}_2-μ-oxo(porphyrin)$_2$ – $HPPh_2$ addition - scan rate 50 mVs^{-}

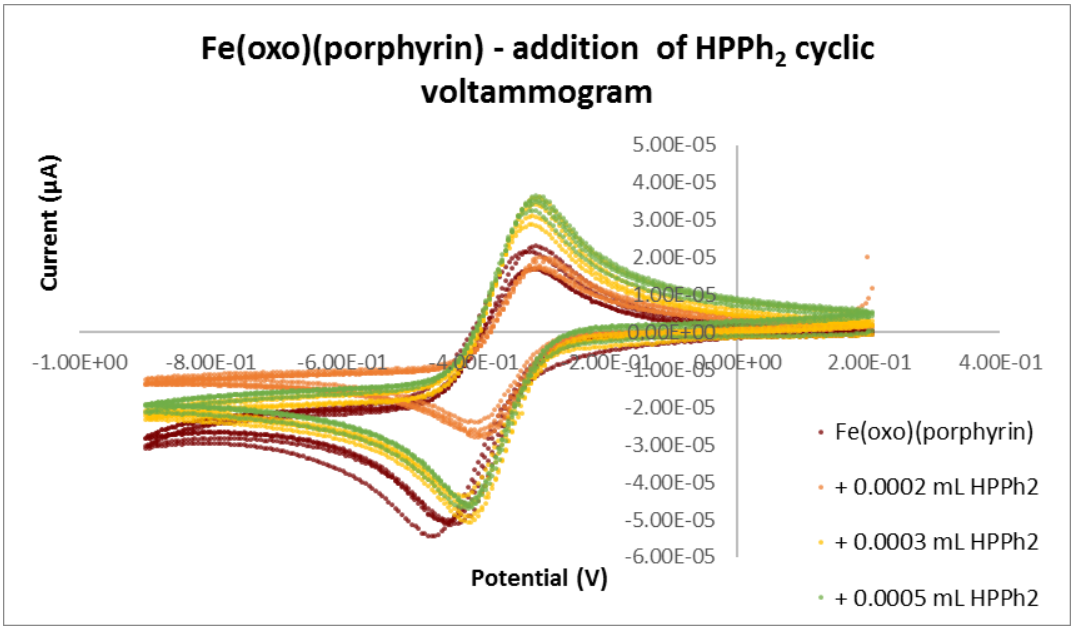

Figure 41. Fe^{III}_2-μ-oxo(porphyrin)$_2$ – $HPPh_2$ addition - scan rate 50 mVs^{-1}

References

1 K. J. Gallagher and R. L. Webster, *Chem. Commun.* , 2014, **50**, 12109–11.

2 K. J. Gallagher, M. Espinal-Viguri, M. F. Mahon and R. L. Webster, *Adv. Synth. Catal.*, 2016, **358**, 2460–2468.

3 W. Reppe and H. Vetter, *Justus Liebigs Ann. Chem.*, 1953, **582**, 133–161.

4 C.-L. Sun, B.-J. Li and Z.-J. Shi, *Chem. Rev.*, 2011, **111**, 1293–1314.

5 K. Junge, K. Schröder and M. Beller, *Chem. Commun.*, 2011, **47**, 4849.

6 R. H. Morris, *Chem. Soc. Rev.*, 2009, **38**, 2282.

7 C. Bolm, J. Legros, J. Le Paih and L. Zani, *Chem. Rev.*, 2004, **104**, 6217–6254.

8 B. E. Plietker, *Topics in Organometallic Chemistry, Iron Catalysis: Fundamentals and Applications*, 2011.

9 B. E. Plietker, *Iron Catalysis in Organic Chemistry: Reactions and Applications*, 2008.

10 K. Gopalaiah, *Chem. Rev.*, 2013, **113**, 3248–96.

11 M. T. Reetz, *Organocatalysis*, Springer-Verlag, Berlin, 2008.

12 A. Behr and P. Neubert, *Applied Homogeneous Catalysis.*, WILEY-VCH Weinheim, Weinheim, 2012, vol. 52.

13 J. Clayden, N. Greeves, S. Warren and P. Wothers, *Organic Chemistry*, 2001.

14 S. J. Berners-Price, R. K. Johnson, C. K. Mirabelli, L. F. Faucette, F. L. McCabe and P. J. Sadler, *Inorg. Chem.*, 1987, **26**, 3383–3387.

15 Y. Huang, S. a Pullarkat, Y. Li and P.-H. Leung, *Chem. Commun.* , 2010, **46**, 6950–6952.

16 A. Börner, .

17 I. Wauters, W. Debrouwer and C. V Stevens, *Beilstein J. Org. Chem.*, 2014, **10**, 1064–1096.

18 M. Espinal-Viguri, M. F. Mahon, S. N. G. Tyler and R. L. Webster, *Tetrahedron*, 2017, **73**, 64–69.

19 C. A. Brown, T. A. Nile, M. F. Mahon and R. L. Webster, *Dalton Trans.*, 2015, **44**, 12189–12195.

20 M. Espinal-Viguri, A. K. King, J. P. Lowe, M. F. Mahon and R. L. Webster, *ACS Catal.*, 2016, **6**, 7892–7897.

21 M. D. Greenhalgh and S. P. Thomas, *J. Am. Chem. Soc.*, 2012, **134**, 11900–11903.

22 H. R. Sharpe, A. M. Geer, W. Lewis, A. J. Blake and D. L. Kays, *Angew. Chemie*, 2017, **129**, 4923–4926.

23 C. A. Tolman, *Chem. Rev.*, 1977, **77**, 313–348.

24 A. G. Orpen and N. G. Connelly, *Organometallics*, 1990, **9**, 1206–1210.

25 G. Besenyei, L. Párkányi, E. Gács-Baitz and B. R. James, *Inorg. Chim. Acta*, 2002, **327**, 179–187.

26 T. Murahashi and H. Kurosawa, *Coord. Chem. Rev.*, 2002, **231**, 207–228.

27 C. P. Kubiak and R. Eisenberg, *J. Am. Chem. Soc.*, 1977, **99**, 6129–6131.

28 M. C. J. M. Van Hooijdonk, G. Gerritsen and L. Brandsma, *Phosphorus. Sulfur. Silicon Relat. Elem.*, 2000, **162**, 39–49.

29 W. Voskuil and J. F. Arens, *Recl. des Trav. Chim. des Pays-Bas*, 2010, **82**, 302–304.

30 E. H.-H. Katarzyna Blazewska, Jozef Drabowicz, Jean-Claude Fiaud, Dietrich Gudat, *Science of Synthesis: Houben-Weyl Methods of Molecular Transformations Vol. 42*, Georg Thieme Verlag, 2014.

31 L. Rosenberg, *ACS Catal.*, 2013, **3**, 2845–2855.

32 P. A. Aguirre, C. A. Lagos, S. A. Moya, C. Zúñiga, C. Vera-Oyarce, E. Sola, G. Peris and J. C. Bayón, *Dalton Trans.*, 2007, 5419.

33 H.-H. Chou and R. T. Raines, *J. Am. Chem. Soc.*, 2013, **135**, 14936–14939.

34 L. Routaboul, F. Toulgoat, J. Gatignol, J.-F. Lohier, B. Norah, O. Delacroix, C. Alayrac, M. Taillefer and A.-C. Gaumont, *Chem. Eur. J.*, 2013, **19**, 8760–8764.

35 Y. Song, J. J. Vittal, N. Srinivasan, S.-H. Chan and P.-H. Leung, *Tetrahedron: Asymmetry*, 1999, **10**, 1433–1436.

36 Y. Huang, S. A. Pullarkat, Y. Li and P.-H. Leung, *Inorg. Chem.*, 2012, **51**, 2533–2540.

37 F. Alonso, Y. Moglie, G. Radivoy and M. Yus, *Green Chem.*, 2012, **14**, 2699.

38 Y. Moglie, M. J. González-Soria, I. Martín-García, G. Radivoy and F. Alonso, *Green Chem.*, 2016, **18**, 4896–4907.

39 D. Semenzin, G. Etemad-Moghadam, D. Albouy, O. Diallo and M. Koenig, *J. Org. Chem.*, 1997, **62**, 2414–2422.

40 F. F. P. Rust, A. R. Stiles, F. F. P. Rust and W. E. Vaughan, *J. Am. Chem. Soc.*, 1952, **74**, 3282–3284.

41 T. N. Mitchell and K. Heesche, *J. Organomet. Chem.*, 1991, **409**, 163–170.

42 T. Bunlaksananusorn, P. Knochel and L. M. Universita, *Tet. Lett.*, 2002, **43**, 5817–5819.

43 A. Perrier, V. Comte, C. Moïse, P. Richard and P. Le Gendre, *Eur. J. Org. Chem.*, 2010, **2010**, 1562–1568.

44 C. Scriban, D. S. Glueck, L. N. Zakharov, W. S. Kassel, A. G. DiPasquale, J. A. Golen and A. L. Rheingold, *Organometallics*, 2006, **25**, 5757–5767.

45 I. V Basalov, S. C. Roşca, D. M. Lyubov, A. N. Selikhov, G. K. Fukin, Y. Sarazin, J.-F. Carpentier and A. a Trifonov, *Inorg. Chem.*, 2014, **53**, 1654–1661.

46 A. M. Kawaoka, M. R. Douglass and T. J. Marks, *Organometallics*, 2003, **22**, 4630–4632.

47 M. R. Crimmin, A. G. M. Barrett, M. S. Hill, P. B. Hitchcock and P. A. Procopiou, *Organometallics*, 2007, **26**, 2953–2956.

48 M. R. Crimmin, A. G. M. Barrett, M. S. Hill, P. B. Hitchcock and P. A. Procopiou, *Organometallics*, 2008, **27**, 497–499.

49 A. D. Sadow and A. Togni, *J. Am. Chem. Soc.*, 2005, **127**, 17012–17024.

50 F. Jérôme, F. Monnier, H. Lawicka, S. Dérien and P. H. Dixneuf, *Chem. Commun.*, 2003, 696–697.

51 P. G. Pringle and M. B. Smith, *J. Chem. Soc., Chem. Commun.*, 1990, 1701.

52 D. K. Wicht, I. V. Kourkine, B. M. Lew, J. M. Nthenge and D. S. Glueck, *J. Am. Chem. Soc.*, 1997, **119**, 5039–5040.

53 W. Han and A. R. Ofial, *Chem. Commun.*, 2009, 6023.

54 W. Han, P. Mayer and A. R. Ofial, *Adv. Synth. Catal.*, 2010, **352**, 1667–1676.

55 S. Murata, M. Miura and M. Nomura, *J. Chem. Soc., Chem. Commun.*, 1989, 116.

56 Z. Li, D. S. Bohle and C.-J. Li, *Proc. Natl. Acad. Sci.*, 2006, **103**, 8928–8933.

57 P. Muthupandi and G. Sekar, *Org. Biomol. Chem.*, 2012, **10**, 5347.

58 T. Yokomatsu, T. Yamagishi and S. Shibuya, *J. Chem. Soc. Perkin Trans. 1*, 1997, 1527–1534.

59 A. J. Wooten, P. J. Carroll and P. J. Walsh, *J. Am. Chem. Soc.*, 2008, **130**, 7407–7419.

60 W. Chen, Y. Hui, X. Zhou, J. Jiang, Y. Cai, X. Liu, L. Lin and X. Feng, *Tet. Lett.*, 2010, **51**, 4175–4178.

61 F. Yang, D. Zhao, J. Lan, P. Xi, L. Yang, S. Xiang and J. You, *Angew. Chem. Int. Ed.*, 2008, **47**, 5646–5649.

62 R. Boobalan and C. Chen, *Adv. Synth. Catal.*, 2013, **355**, 3443–3450.

63 J. Sugiura, T. Kakizawa, H. Hashimoto, H. Tobita and H. Ogino, *Organometallics*, 2005, **24**, 1099–1104.

64 M. Kamitani, M. Itazaki, C. Tamiya and H. Nakazawa, *J. Am. Chem. Soc.*, 2012, **134**, 11932–11935.

65 G. Zhao, F. Basuli, U. J. Kilgore, H. Fan, H. Aneetha, J. C. Huffman, G. Wu and D. J. Mindiola, *J. Am. Chem. Soc.*, 2006, **128**, 13575–13585.

66 H. Ohmiya, H. Yorimitsu and K. Oshima, *Angew. Chem. Int. Ed. Engl.*, 2005, **44**, 2368–2370.

67 M. A. Kazankova, I. V Efimova, A. N. Kochetkov, V. Afanas, I. P. Beletskaya and P. H. Dixneuf, *Syn. Lett.*, 2001, 497–500.

68 M. A. Kazankova, I. V Efimova, A. N. Kochetkov, V. V Afanas and I. P. Beletskaya, *Russ. J. Org. Chem.*, 2002, **38**, 1465–1474.

69 M. Liu, C. Sun, F. Hang, N. Sun and D. Chen, *Dalton Trans.*, 2014, **43**, 4813.

70 M. Itazaki, S. Katsube, M. Kamitani and H. Nakazawa, *Chem. Commun.*, 2016, **52**, 3163–3166.

71 P. M. Murray, J. F. Bower, D. K. Cox, E. K. Galbraith, J. S. Parker and J. B. Sweeney, *Org. Process Res. Dev.*, 2013, **17**, 397–405.

72 A. Suzuki, *J. Organomet. Chem.*, 1999, **576**, 147–168.

73 B. H. Yang and S. L. Buchwald, *J. Organomet. Chem.*, 1999, **576**, 125–146.

74 R. J. Chew, K. Sepp, B.-B. Li, Y. Li, P.-C. Zhu, N. S. Tan and P.-H. Leung, *Adv. Synth. Catal.*, 2015, **357**, 3297–3302.

75 K. Gan, A. Sadeer, C. Xu, Y. Li and S. A. Pullarkat, *Organometallics*, 2014, **33**, 5074–5076.

76 R. J. Chew and P.-H. Leung, *Chem. Rec.*, 2016, **16**, 141–158.

77 Y.-X. Jia, R. Jonathan Chew, B.-B. Li, P. Zhu, Y. Li, S. A. Pullarkat, N. Soon Tan and P.-H. Leung, *Dalton Trans.*, 2015, **44**, 17557–17564.

78 B.-B. Li, Y.-X. Jia, P.-C. Zhu, R. J. Chew, Y. Li, N. S. Tan and P.-H. Leung, *Eur. J. Med. Chem.*, 2015, **98**, 250–255.

79 X.-Y. Yang, J. H. Gan, Y. Li, S. A. Pullarkat and P.-H. Leung, *Dalton Trans.*, 2015, **44**, 1258–1263.

80 X.-Y. Yang, W. S. Tay, Y. Li, S. A. Pullarkat and P.-H. Leung, *Organometallics*, 2015, **34**, 1582–1588.

81 X.-Y. Yang, W. S. Tay, Y. Li, S. A. Pullarkat and P.-H. Leung, *Chem. Commun.*, 2016, **52**, 4211–4214.

82 J. Yang and T. D. Tilley, *Angew. Chem. Int. Ed.*, 2010, **49**, 10186–8.

83 M. Lappert, A. Protchenko, P. Power and A. Seeber, *Metal Amide Chemistry*, John Wiley & Sons, Ltd, Chichester, UK, 2008.

84 R. A. Andersen, K. Faegri, J. C. Green, A. Haaland, M. F. Lappert, W. P. Leung and K. Rypdal, *Inorg. Chem.*, 1988, **27**, 1782–1786.

85 A. Jacobi von Wangelin, D. Brenna, M. Villa, T. N. Gieshoff, M. Hapke and F. Fischer, *Angew. Chemie*, 2017, 8451–8454.

86 Y. Zhang, L. Tang, Y. Ding, J.-H. Chua, Y. Li, M. Yuan and P.-H. Leung, *Tet. Lett.*, 2008, **49**, 1762–1767.

87 P. Hofmann, C. Meier, W. Hiller, M. Heckel, J. Riede and M. U. Schmidt, *J. Organomet. Chem.*, 1995, **490**, 51–70.

88 M. M. P. Grutters, J. I. Van Der Vlugt, Y. Pei, A. M. Mills, M. Lutz, A. L. Spek, C. Müller, C. Moberg and D. Vogt, *Adv. Synth. Catal.*, 2009, **351**, 2199–2208.

89 G. M. Lee, C. M. Vogels, A. Decken and S. A. Westcott, *Eur. J. Inorg. Chem.*, 2011, 2433–2438.

90 A. B. Chaplin, J. F. Hooper, A. S. Weller and M. C. Willis, *J. Am. Chem. Soc.*, 2012, **134**, 4885–4897.

91 A. Zanardo, R. A. Michelin, F. Pinna and G. Strukul, *Inorg. Chem.*, 1989, **28**, 1648–1653.

92 M. K. Cybulski, M. F. Mahon, J. E. Nicholls, J. P. Lowe and M. K. Whittlesey, *Organometallics*, 2017, **36**, 2308–2316.

93 M. T. Honaker, B. J. Sandefur, J. L. Hargett, A. L. McDaniel and R. N. Salvatore, *Tet. Lett.*, 2003, **44**, 8373–8377.

94 E. N. Tsvetkov, N. A. Bondarenko, I. G. Malakhova and M. I. Kabachnik, *Synthesis (Stuttg).*, 1986, **1986**, 198–208.

95 A. K. King, A. Buchard, M. F. Mahon and R. L. Webster, *Chem. Eur. J.*, 2015, **21**, 15960–15963.

96 S. K. Edulji and S. T. Nguyen, *Organometallics*, 2003, 3374–3381.

97 P. G. Cozzi, *Chem. Soc. Rev.*, 2004, **33**, 410–421.

98 A. Hille, I. Ott, A. Kitanovic, I. Kitanovic, H. Alborzinia, E. Lederer, S. Wölfl, N. Metzler-Nolte, S. Schäfer, W. S. Sheldrick, C. Bischof, U. Schatzschneider and R. Gust, *J. Biol. Inorg. Chem.*, 2009, **14**, 711–725.

99 A. W. Addison, T. N. Rao, J. Reedijk, J. van Rijn and G. C. Verschoor, *J. Chem. Soc., Dalton Trans.*, 1984, 1349.

100 A. I. Nguyen, R. G. Hadt, E. I. Solomon and T. D. Tilley, *Chem. Sci.*, 2014, **5**, 2874–2878.

101 W. P. Schaefer, R. Waltzman and B. T. Huie, *J. Am. Chem. Soc.*, 1978, **100**, 5063–5067.

102 A. Jozwiuk, A. L. Ingram, D. R. Powell, B. Moubaraki, N. F. Chilton, K. S. Murray and R. P. Houser, *Dalton Trans.*, 2014, **43**, 9740–9753.

103 E. N. Jacobsen, W. Zhang, A. R. Muci, J. R. Ecker and L. Deng, *J. Am. Chem. Soc.*, 1991, **113**, 7063–7064.

104 C. Scriban, I. Kovacik and D. S. Glueck, *Organometallics*, 2005, **24**, 4871–4874.

105 M. R. Douglass, C. L. Stern and T. J. Marks, *J. Am. Chem. Soc.*, 2001, **123**, 10221–10238.

106 M. R. Douglass, M. Ogasawara, S. Hong, M. V. Metz and T. J. Marks, *Organometallics*, 2002, **21**, 283–292.

107 A. D. Sadow, I. Haller, L. Fadini and A. Togni, *J. Am. Chem. Soc.*, 2004, **126**, 14704–14705.

108 W. Malisch, B. Klüpfel, D. Schumacher and M. Nieger, *J. Organomet. Chem.*, 2002, **661**, 95–110.

109 B. D. Vineyard, W. S. Knowles, M. J. Sabacky, G. L. Bachman and D. J. Weinkauff, *J. Am. Chem. Soc.*, 1977, **99**, 5946–5952.

110 E. Duñach and H. B. Kagan, *Tet. Lett.*, 1985, **26**, 2649–2652.

111 O. I. Kolodiazhnyi, *Phosphorus Chemistry I*, Springer International Publishing, Cham, 2015, vol. 360.

112 A. Leyva-Pérez, J. A. Vidal-Moya, J. R. Cabrero-Antonino, S. S. Al-Deyab, S. I. Al-Resayes and A. Corma, *J. Organomet. Chem.*, 2011, **696**, 362–367.